This article was downloaded by:
On: *17 January 2011*
Access details: *Access Details: Free Access*
Publisher *Taylor & Francis*
Informa Ltd Registered in England and Wales Registered Number: 1072954 Registered office: Mortimer House, 37-41 Mortimer Street, London W1T 3JH, UK

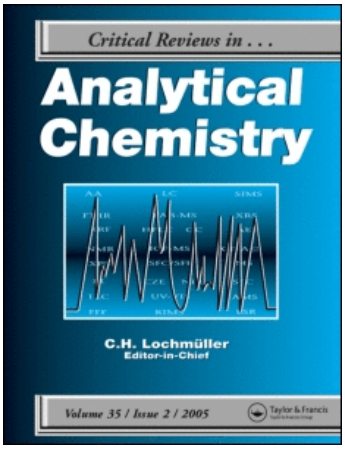

Critical Reviews in Analytical Chemistry
Publication details, including instructions for authors and subscription information:
http://www.informaworld.com/smpp/title~content=t713400837

High-speed countercurrent chromatography

Yoichiro Ito; Walter D. Conway

To cite this Article Ito, Yoichiro and Conway, Walter D.(1986) 'High-speed countercurrent chromatography', Critical Reviews in Analytical Chemistry, 17: 1, 65 — 143
To link to this Article: DOI: 10.1080/10408348608542792
URL: http://dx.doi.org/10.1080/10408348608542792

PLEASE SCROLL DOWN FOR ARTICLE

Full terms and conditions of use: http://www.informaworld.com/terms-and-conditions-of-access.pdf

This article may be used for research, teaching and private study purposes. Any substantial or systematic reproduction, re-distribution, re-selling, loan or sub-licensing, systematic supply or distribution in any form to anyone is expressly forbidden.

The publisher does not give any warranty express or implied or make any representation that the contents will be complete or accurate or up to date. The accuracy of any instructions, formulae and drug doses should be independently verified with primary sources. The publisher shall not be liable for any loss, actions, claims, proceedings, demand or costs or damages whatsoever or howsoever caused arising directly or indirectly in connection with or arising out of the use of this material.

HIGH-SPEED COUNTERCURRENT CHROMATOGRAPHY

Author: **Yoichiro Ito**
Laboratory of Technical Development
National Heart, Lung, and Blood Institute
Bethesda, Maryland

Referee: Walter D. Conway
Department of Pharmaceutics and Medical Chemistry
State University of New York at Buffalo
Amherst, New York

Downloaded At: 15:26 17 January 2011

I. INTRODUCTION

During the past 20 years countercurrent chromatography (CCC) has been steadily improved in both partition efficiency and separation times.[1-15] The original helix CCC and the successively developed nonhelix preparative-scale CCC schemes, such as droplet CCC[16,17] and locular CCC,[17] required relatively long separating times; sizeable separation usually exceeded 24 hr. During the last decade, development of various flow-through centrifuge schemes, such as the flow-through coil planet centrifuge[18,19] (CPC), angle rotor CPC,[20] elution centrifuge,[21] horizontal flow-through CPC,[22-26] toroidal CPC,[27,28] and nonsynchronous flow-through CPC,[29-31] has substantially shortened the separation times so that efficient separations became possible with overnight runs.

Recently, an epoch-making advance in CCC technology has been brought forth by a discovery of a unique hydrodynamic phenomenon which led to the development of high-speed CCC.[13,32,33] This new CCC method is characterized by high partition efficiency and large retention capability of the stationary phase under a high flow rate of the mobile phase, yielding highly efficient separations in a few hours. The method also allows a dual countercurrent flow of two phases through a coiled column which opens a rich domain of future applications such as foam separations,[34] continuous extraction,[35,36] and dual CCC.

In this review article, this most advanced form of CCC was viewed from various aspects to elucidate the characteristic features of the method. Although there remain many unsolved problems for future investigations, the high-speed CCC technology will provide many useful applications at the present stage of development.

II. PRINCIPLE AND DEVELOPMENT OF HIGH-SPEED CCC

A. Two Basic CCC Systems[5]

A variety of existing CCC schemes may be classified into two forms, i.e., hydrostatic equilibrium system (HSES) and hydrodynamic equilibrium system (HDES). The mechanism of the basic model for each system is illustrated in Figure 1.

The hydrostatic system (left) uses a stationary coiled tube. The coil is first filled with the stationary phase and the mobile phase is introduced at one end of the coil. The mobile phase then starts to percolate through the stationary phase segments on one side of the coil, leaving nearly half the volume of the stationary phase in the coil. Consequently, solutes introduced locally at the inlet of the coil are subjected to a continuous partition process between two phases and separated according to their partition coefficients in a manner analogous to liquid chromatography but in the absence of solid support.

Partition efficiency of the hydrostatic system is improved by rotation of the coiled tube around its own axis (right). This motion creates an Archimedean screw force to move all

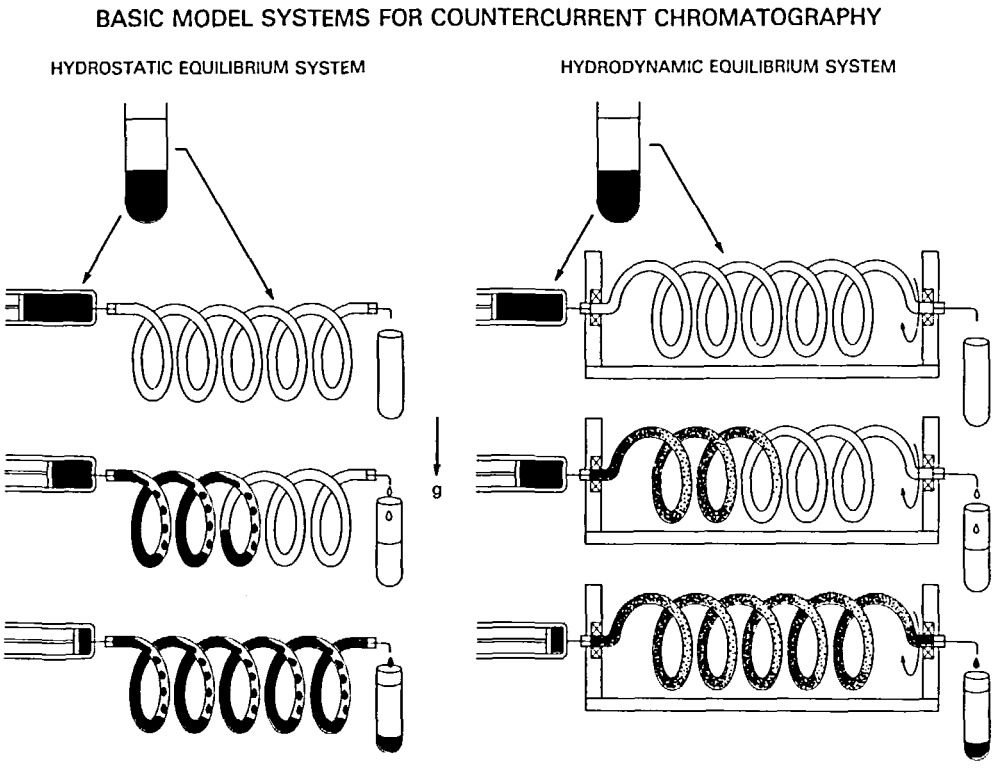

FIGURE 1. Basic model systems for countercurrent chromatography (CCC).

objects in the coil toward one end of the coil. This end is called the "head" and the other end the "tail". Under slow rotation of the coil, the mobile phase introduced at the head of the coil is mixed with the stationary phase to establish a hydrodynamic equilibrium where nearly half the volume of the stationary phase is permanently retained in the coil while continuously mixed with the mobile phase. Consequently, the hydrodynamic system yields a more efficient partition process by additional mixing induced by rotation of the coil. This basic hydrodynamic system was further improved by a discovery of the unilateral hydrodynamic system which led to the development of high-speed CCC.

B. Unilateral HDES[11,13,35]

The principle of the unilateral HDES is elucidated in Figure 2. In this figure, a rotating coil at the top contains nearly equal volumes of two immiscible solvent phases. The rest of the coils are schematically drawn uncoiled to illustrate the relative volume distribution of the two phases along the length of the coil from the head to the tail.

In the basic HDES described earlier (left), slow rotation of the coil evenly distributes the two phases in the coil. In the closed coil, each phase occupies nearly half the space of the coil and any excess of either phase (not shown in the figure), if present, remains at the tail of the coil. Elution of either phase through the head toward the tail results in further decrease of the other phase from the coil. The higher the flow rate of the mobile phase, the less the amount of the stationary phase remaining in the coil. This low retention of the stationary phase limits the application of a high flow rate of the mobile phase in the basic HDES. This problem has been solved by the unilateral HDES.

When the rotational speed of the coil is increased to the critical range (right), the two solvent phases become completely separated in the coil in such a way that one phase (head phase) entirely occupies the head side and the other phase (tail phase) occupies the tail side

Downloaded At: 15:26 17 January 2011

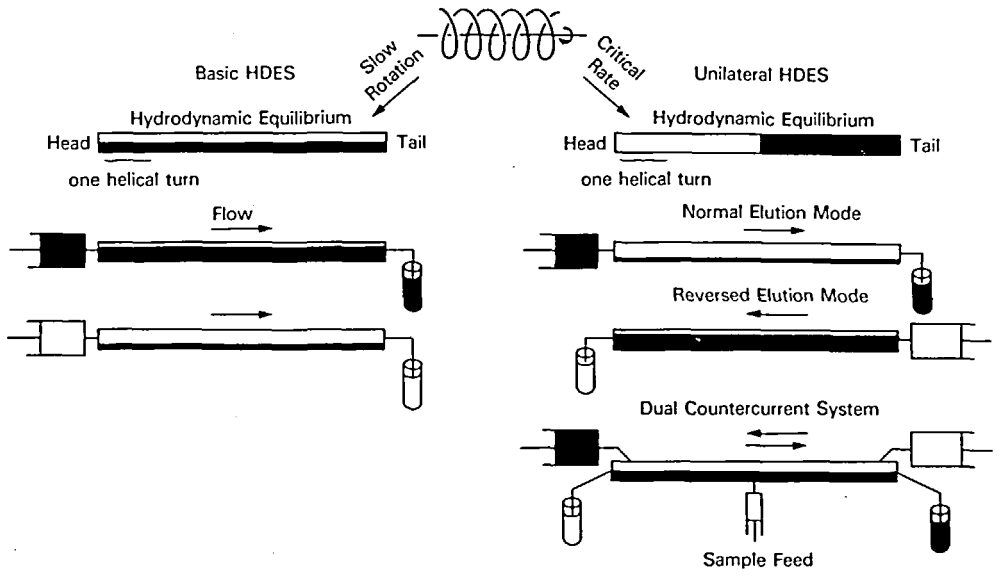

FIGURE 2. Principle of unilateral hydrodynamic equilibrium system.

Downloaded At: 15:26 17 January 2011

of the coil. This unilateral hydrodynamic equilibrium condition clearly indicates that the tail phase, if introduced at the head, would move through the head phase toward the tail and similarly the head phase, if introduced at the tail, would move through the tail phase toward the head. Consequently, this system can be efficiently utilized for performing CCC in the following two different ways: the coil is first entirely filled with the head phase and the tail phase is pumped through the head end. Alternatively, the coil is entirely filled with the tail phase and the head phase is pumped through the tail end. In either case the system can maintain a high retention level of the stationary phase in the coil.

The present system also allows simultaneous elution of the two phases through the respective ends of the coil. This requires an additional flow tube at each end of the coil to collect the effluent and, if desired, the sample feed port is made at the middle portion of the coil. Recently, this dual CCC system has been successfully applied to foam separation as described later in this article.

Hydrodynamic distribution of the two solvent phases in the rotating coil has been studied with a simple rotary device using a two-phase solvent system composed of chloroform, acetic acid, and 0.1 N hydrochloric acid at a 2:2:1 volume ratio.[37] Figure 3 shows the results obtained from 5.5 mm i.d. tubes with three different helical diameters. In each diagram volume percentage of the upper and the lower phases distributed at the head side of the coil is plotted against the applied rotational speed ranging from 0 to 400 rpm. All three coils produced unilateral phase distribution where the lower nonaqueous phase entirely occupied the head of the coil at the critical rotational speeds between 50 and 120 rpm. As expected from this unilateral phase distribution mode, test runs have produced the best peak resolution of DNP (dinitrophenyl) amino acid samples with maximum retention of the stationary phase at the critical rotational speeds.

While this simple CCC method renders many advantages over other CCC schemes, it has an inherent limitation in that the stationary phase is sustained within the coil solely by the unit gravitational force against the flow of the mobile phase. During elution the stationary phase is retained in the coil under a subtle balance between the two forces, i.e., an Archi-

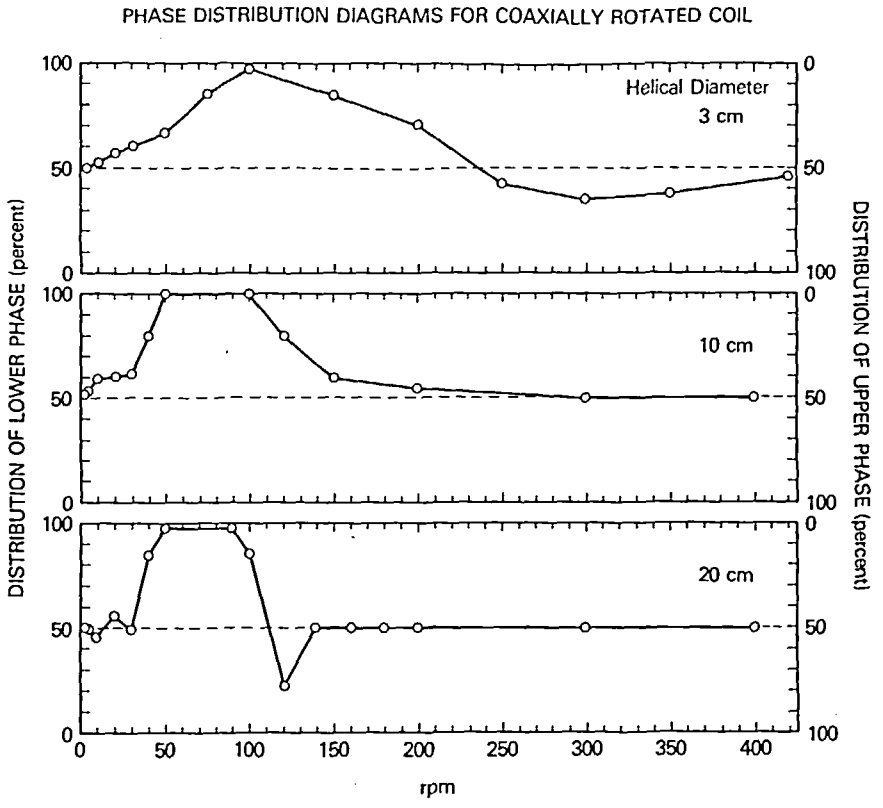

FIGURE 3. Phase distribution diagrams for coaxially rotated coils with three different helical diameters.

Downloaded At: 15:26 17 January 2011

medean screw force which sends the stationary phase toward the inlet of the coil and the flowing mobile phase which carries the stationary phase toward the outlet of the coil. Consequently, application of a high flow rate of the mobile phase would sharply decrease the retention capacity of the coil, thus resulting in loss of the peak resolution and decreased sample-loading capacity. In order to improve the speed and partition efficiency of the method, it became necessary to utilize a centrifugal force field.

C. Flow-Through Centrifuge Schemes Free of Rotary Seals[5]

Figure 4 illustrates various types of flow-through centrifuge schemes developed for performing CCC. All these schemes permit continuous elution without the use of rotary seals. Elimination of the conventional rotary seal device provides two major advantages: (1) the system ensures leak-free elution under high pressure and (2) the system permits the use of multiple flow channels as required for the dual CCC. Consequently, these centrifuge systems provide ideal means for performing CCC.

All centrifuge schemes are divided into three classes, synchronous, nonplanetary, and nonsynchronous, according to their modes of planetary motion. The synchronous schemes numbered I through IV produce a synchronous planetary motion of the holder in such a way that the holder rotates about its own axis once per one revolution around the central axis of the centrifuge. Search for the desired centrifuge scheme to produce the ideal unilateral hydrodynamic distribution of the two solvent phases for high-speed CCC has been successfully made among these synchronous schemes. In Scheme I, the cylindrical column holder counterrotates about its own axis while revolving around the central axis of the centrifuge. This counterrotation of the holder steadily unwinds the twist of the flow tubes

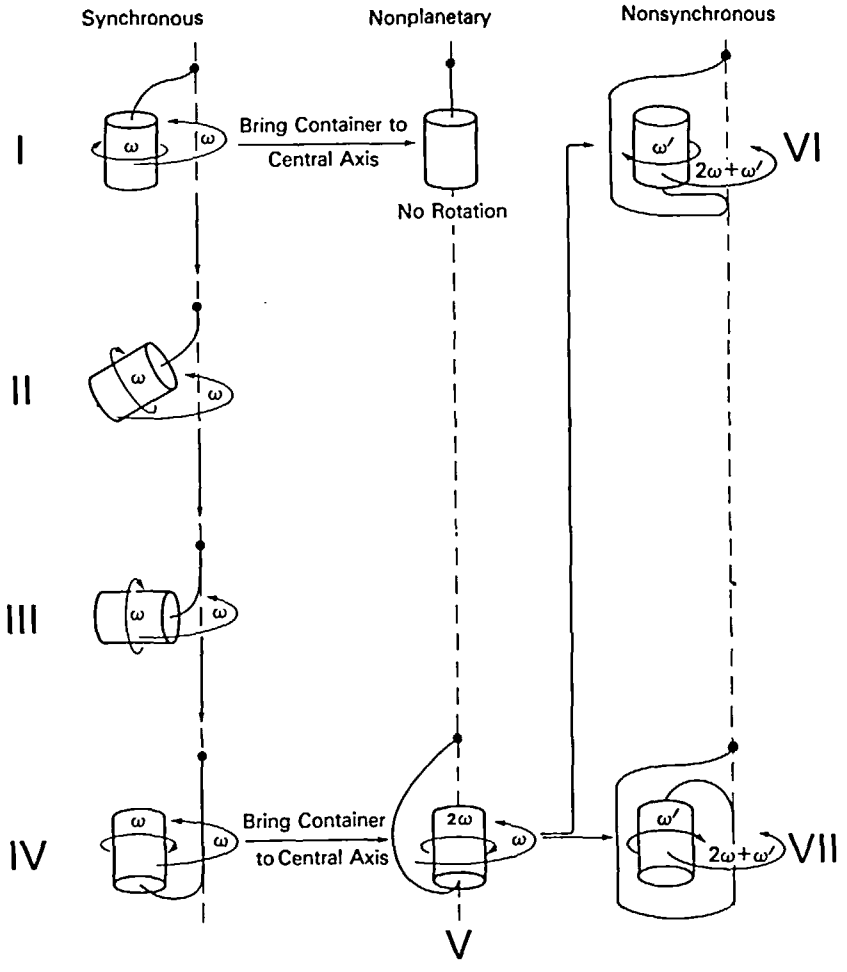

FIGURE 4. Various types of seal-free flow-through centrifuge schemes and their mutual relationship.

caused by revolution, thus eliminating the need for the rotary seal device for continuous elution. This principle can be equally applied to other synchronous schemes of tilted (Scheme II), horizontal (Scheme III), or even inverted (Scheme IV) orientation of the holder. Shifting the position of the Scheme IV holder toward the central axis of the apparatus forms the nonplanetary scheme, Scheme V, which in turn serves as the base of nonsynchronous Schemes VI and VII.

Using the two simplest forms of synchronous planetary motions, Schemes I and IV, a series of experiments has been performed to study hydrodynamic distribution of the two solvent phases in a coiled tube mounted on the holder in various orientations. Figure 5 summarizes the successful search for the unilateral hydrodynamic system ideal for performing high-speed CCC.[11] As mentioned earlier, simple rotation can produce the unilateral phase distribution in the coil but a unit gravity fails to hold a large amount of the stationary phase in the coil against a high flow rate of the mobile phase. In order to enhance the gravity, planetary motion was applied to the coil. The Scheme I synchronous planetary motion was first tested but it produced even distribution of the two phases in the coil as in the basic HDES regardless of the orientation of the coil on the holder. Then, the Scheme IV synchronous planetary motion was examined with various orientation of the coil on the holder

Downloaded At: 15:26 17 January 2011

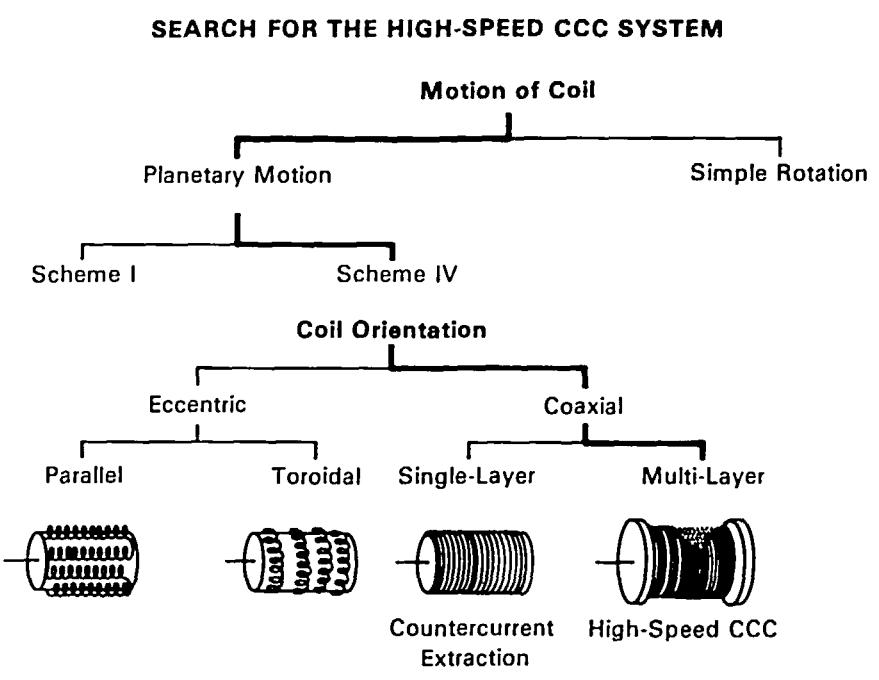

FIGURE 5. Search for the high-speed CCC system.

as illustrated in Figure 5. The eccentric coil orientation to the holder axis, either parallel or toroidal form, produced alternating segments of the two solvent phases in the coil as in the basic HSES. Finally, when the coil was coaxially mounted around the holder, the ideal unilateral distribution of the two solvent phases was observed. Furthermore, the system produced excellent partition efficiency and stationary phase retention under a high flow rate of the mobile phase. The system has been successfully applied to countercurrent extraction with a short coil and to high-speed CCC with a long multilayer coil.

III. THEORY AND EXPERIMENTAL OBSERVATION ON HYDRODYNAMICS

A. Mathematical Analysis on Two Typical Synchronous Planetary Motions[5,23]

A simple mathematical analysis has been applied to two typical synchronous planetary motions, that is, Schemes I and IV illustrated in Figure 4. Figure 6 shows the schematic diagram of each scheme (Figure 6A), the coordinate system for analysis of acceleration (Figure 6B), the orbits of arbitrary points on the holder (Figure 6C), and centrifugal force vectors at various locations on the holder (Figure 6D).

In Scheme I, the column holder revolves around the central axis (center of revolution) and simultaneously counterrotates around its own axis (center of rotation), both at the same angular velocity ω (Figure 6A, left). For analysis of acceleration, the coordinate system is chosen in such a way that the center of revolution is located at the center of the coordinate system and the center of rotation is on the x axis at time 0 (Figure 6B, left). An arbitrary point initially located at P_o forms angle θ_o with the x axis; then after time t, location of the point, P(x,y), is expressed by

$$x = R\cos\theta + r\cos\theta_o \quad (1)$$

$$y = R\sin\theta + r\sin\theta_o \quad (2)$$

Downloaded At: 15:26 17 January 2011

Downloaded At: 15:26 17 January 2011

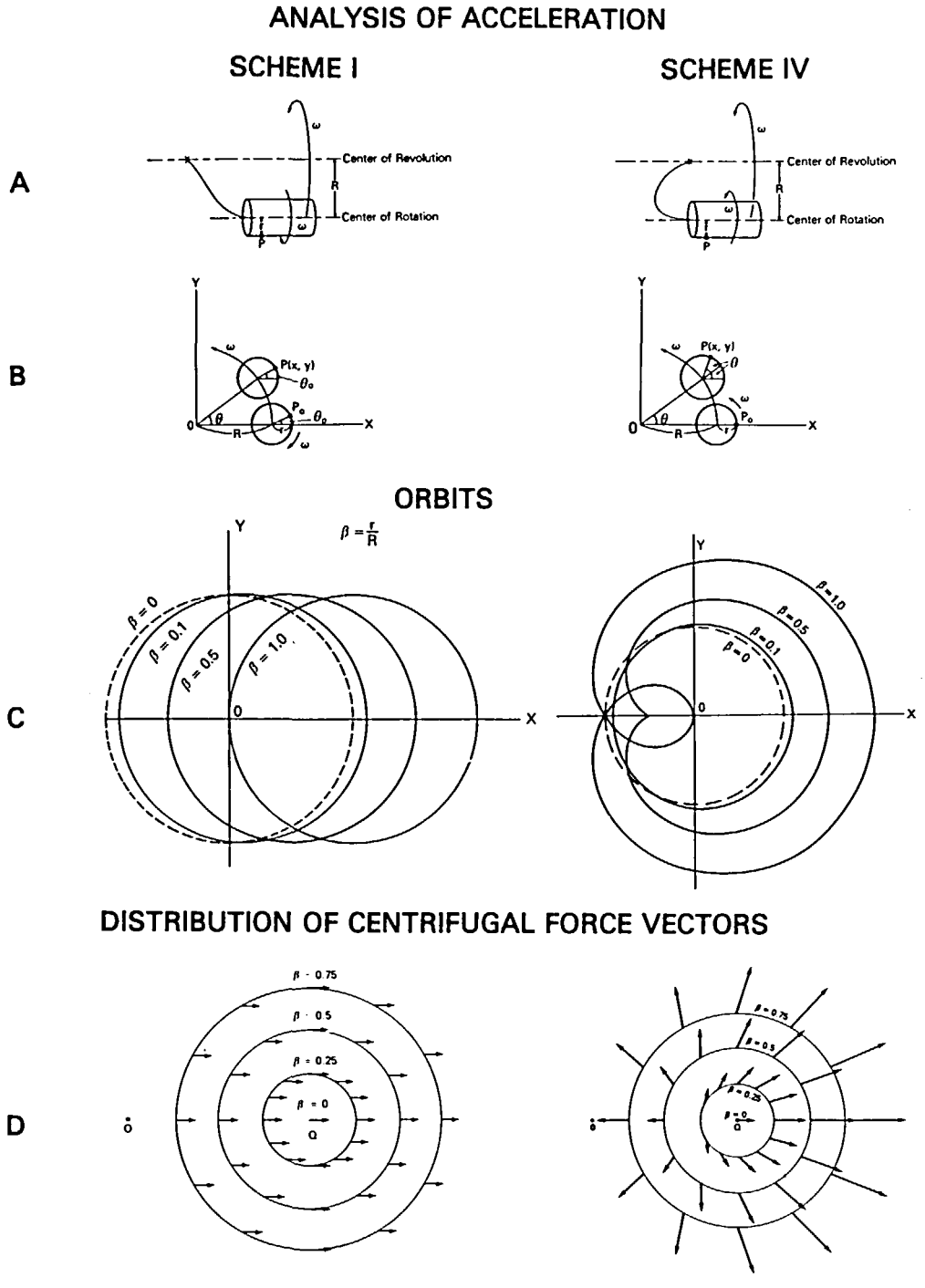

FIGURE 6. Analysis of acceleration for Scheme I and IV synchronous planetary motions.

From these equations, the orbit of the arbitrary point is easily obtained by eliminating the variable, θ, and

$$(x - r\cos\theta_0)^2 + (y - r\sin\theta_0)^2 = R^2 \qquad (3)$$

This represents a circle with radius R centered at point ($r\cos\theta_o$, $r\sin\theta_o$). The fact that radius of the circle, R, is independent of both θ_o and r indicates that every point located on the holder has a circular orbit with radius R (Figure 6C, left).

The net magnitude of acceleration, α, and its acting angle formed from the x axis, γ, at the arbitrary point on the holder are further computed from the second derivatives of Equations 1 and 2, and

$$\alpha = [(d^2x/dt^2)^2 + (d^2y/dt^2)^2]^{1/2} = R\omega^2 \tag{4}$$

$$\gamma - \pi = \tan^{-1}[(d^2y/dt^2)/(d^2x/dt^2)] = \omega t = \theta \tag{5}$$

This shows that the points are subjected to a constant magnitude of acceleration, $R\omega^2$, which rotates around each point at a uniform rate of ω. The acceleration is found to be free of r and θ_o, both of which determine the location of the point on the holder. This indicates that at any given moment every point on the holder is subjected to the identical centrifugal force field acting in a plane perpendicular to the axis of the holder (Figure 6D, left).

The acceleration analysis is similarly carried out on the planetary motion produced by Scheme IV (Figure 6, right). In Figure 6A (right), the holder revolves around the central axis of the apparatus (center of revolution) and simultaneously rotates about its own axis (center of rotation) at the same angular velocity in the same direction. In order to simplify the analysis, the coordinate system is selected so that the center of revolution is located at the central point O, whereas both the center of rotation and the arbitrary point are initially located on the x axis (Figure 6B, right). After the lapse of time t, the center of rotation circles around the point O by $\theta = \omega t$, and the location of the arbitrary point, P(x,y), is given by

$$x = R\cos\theta + r\cos 2\theta \tag{6}$$

$$y = R\sin\theta + r\sin 2\theta \tag{7}$$

The orbit of the point computed from Equations 6 and 7 displays a great variety in shape, depending on the locations of the point on the holder, which are conveniently expressed by the ratio of the radius of rotation, r, to the radius of revolution, R, or $\beta = r/R$ (Figure 6C, right). When $\beta < 0.25$, the orbit is a single circular loop. As β increases, it becomes heart shaped ($\beta = 0.5$) and then forms a double loop ($\beta = 1.0$) which gradually approaches a double circle with greater β values. These results suggest that the acceleration field also fluctuates periodically during each revolutional cycle of the holder.

The acceleration acting on the arbitrary point is further calculated from the second derivatives of Equations 6 and 7 as

$$\alpha = [(d^2x/dt^2)^2 + (d^2y/dt^2)^2]^{1/2} = R\omega^2(1 + 16\beta^2 + 8\beta\cos\theta)^{1/2} \tag{8}$$

acting at the angle γ_x, relative to the x axis, that is,

$$\gamma_x = \pi + \tan^{-1}[(d^2y/dt^2)/(d^2x/dt^2)]$$

$$= \pi + \tan^{-1}\frac{(\sin\theta + 4\beta\sin 2\theta)}{(\cos\theta + 4\beta\cos 2\theta)} \tag{9}$$

where $\beta = r/R$, provided that $R \neq 0$.

From Equations 8 and 9, the relative centrifugal force vectors acting at various locations on the holder are obtained. In Figure 6D (right) three circles centered at Q correspond to β

Downloaded At: 15:26 17 January 2011

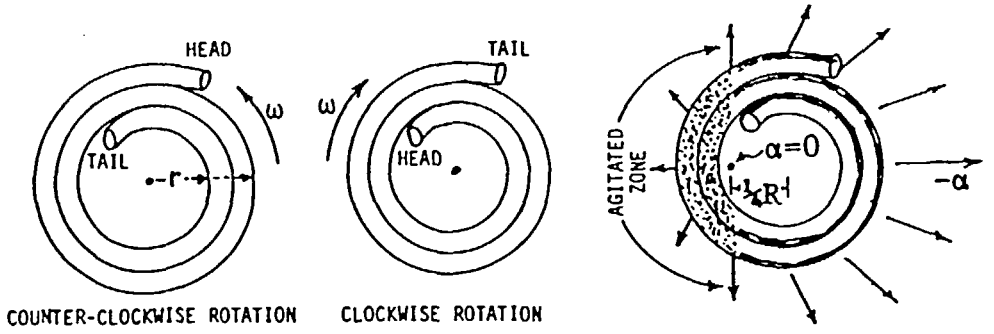

FIGURE 7. Head and tail relationships and centrifugal force fields (-α) for a spiral coil.

values of 0.25, 0.5, and 0.75, as labeled, while point Q, the center of rotation, is at β = 0. A set of arrows around each circle indicates the distribution pattern of the centrifugal force field at a given moment. It is important to note that the arbitrary point on the holder experiences these vectors in sequence during each revolutional cycle. As clearly shown in Figure 6D (right), when β > 0.25, the vector is always directed outward from the circle. The vector also undulates in its relative magnitude and direction according to the location on the holder at given β values. As the β value increases, the magnitude of the relative centrifugal force vector becomes greater while the amplitude of angular oscillation around the axis of rotation decreases.

The results of the above analyses clearly illustrate a great contrast between the two types of synchronous planetary motions. In Scheme I, a uniform acceleration field rotates around the point regardless of the location on the holder. Scheme IV, on the other hand, gives a heterogeneous acceleration field which varies in both magnitude and direction according to the location of the point on the holder.

In short, Scheme IV produces a more complex pattern of acceleration, but it promises greater versatility in application to CCC by allowing one the choice of the orientation and location of the coil on the holder to obtain the desirable hydrodynamic distribution of the two solvent phases in the coil.

Downloaded At: 15:26 17 January 2011

B. Stroboscopic Observation on Hydrodynamics

A series of experiments has been performed by Conway and Ito[38] to study hydrodynamic motion of the two immiscible solvents in the rotating column. Using a specially designed Scheme IV coil planet centrifuge with a 10 cm revolutional radius, phase distribution and mixing of the chloroform/acetic acid/water (2:2:1) system in a single-layer spiral and a multilayer helical coil was observed and photographically recorded under stroboscopic illumination.

The columns (Figure 7), mounted concentric with the axis of the column holder, were driven in either direction to reverse the head and tail relationship of the peripheral and central ends of the coil. The centrifugal field (−α), shown for β = 0.5, is unsymmetrical in intensity and direction, where β is the ratio of the coil radius, r, to the orbital radius, R, of the column holder. All vectors radiate from a common point, β = 0.25 and α = 0.

The single-layer spiral column consisted of about 3.5 m of 2.6 mm i.d. PTFE tubing, volume 20.9 mℓ, with 10 coils from 11.5 cm (β = 0.57) to 18 cm (β = 0.9) in diameter. The multilayer helical coil consisted of about 17 m of the same tubing, volume 102 mℓ, 5 rows wide, 10 helical layers ranging from 10 cm (β = 0.5) to 17 cm (β = 0.85) in diameter. The column was first filled with stationary phase and mobile phase pumped at 240 mℓ/hr into either end while rotating the apparatus at 800 rpm. A stroboscope was magnetically synchronized for observation and photography of the phases dyed yellow and red.

Table 1
STATIONARY PHASE RETENTION FOR THE $CHCl_3$:HOAc:H_2O;2:2:1;V:V:V SYSTEM

		Single-layer spiral, S_F(%)		Multi-layer coil, S_F(%)	
		Mobile phase			
Rotation	Flow	Light	Heavy	Light	Heavy
CW	Hc → Tp	a, 5	A, 82	—	A, 78, 78
CW	Hc ← Tp	b, 84, 82	B, 3, 0.5	b, 70, 70	—
CCW	Hp → Tc	c, 12	C, 77	—	—
CCW	Hp ← Tc	d, 78, 72	D, 2, 0.5	—	—

Phase volume equilibrium was quickly established immediately behind the mobile phase front. Stationary phase retention (S_F = fraction of column volume occupied by stationary phase, tabulated as percentage) for various conditions is summarized in Table 1. Flow direction is symbolized by the arrow between H (head) and T (tail), located at the coil center (c) or periphery (p). The best retention is obtained with the column head at the center and heavier phase pumped from H to T (conditon A) or lighter phase pumped from T to H (condition b). However, only slightly lower retention is obtained in the single-layer spiral with reverse rotation (conditions C and d).

Under conditions with good retention and with the heavier phase mobile (A and C), the column was divided into an agitated zone, to the left of the vertical line through = 0, in which good mixing was observed (Figure 7), and the quiescent zone in the remainder of the column where heavier phase migrated along the periphery of each coil with little apparent mixing. With a mobile lighter phase, mixing was also observed in the left part of the column (conditions b and d) but it was not as uniform, and additional agitated zones were observed in the right side of the coil. Two zones of apparent column flooding were observed with the light mobile phase in the multilayer coil (condition b), one of which was associated with the passage of tubing from the end row of coils to the adjacent inner row.

More recently, Sutherland and Heywood-Waddington[39] have extended the above study with a similar type of the CPC with a spiral column covering a lower range of β values from 0.35 to 0.82. The results showed, in addition to the hydrodynamic trends previously reported, that the reversed volume distribution of the two phases at the inner portion of the spiral column with small β values. The above finding is consistent with the results of hydrodynamic studies described in the following section.

These results clearly demonstrate a unique hydrodynamic behavior of the two solvent phases in the present system as schematically illustrated in Figure 8. The top diagram illustrates successive positions of the spiral column during one complete revolution around the central axis of the centrifuge. The mixing zone is always located near the center of the centrifuge while the spiral column rotates about its own axis twice during one revolutional cycle. At the bottom, uncoiled columns numbered I through IV correspond to the column position in the top diagram and show movement of the mixing zone through the spiral column. Each mixing zone is traveling toward the head of the spiral column at a rate equal to the revolutional speed of the column. This indicates an extremely interesting fact that the two solvent phases at any portion of the column are subjected to a typical partition process of repetitive mixing and settling at an enormously high rate of over 13 times per second while the mobile phase is steadily passing through the stationary phase. Consequently, this finding promises a high partition efficiency of the present scheme under a high flow rate of the mobile phase.

While the stroboscopic observation above described can shed light on the hydrodynamic

Downloaded At: 15:26 17 January 2011

DROPLET ZONE MOTION IN THE CONCENTRIC COIL PLANET CENTRIFUGE

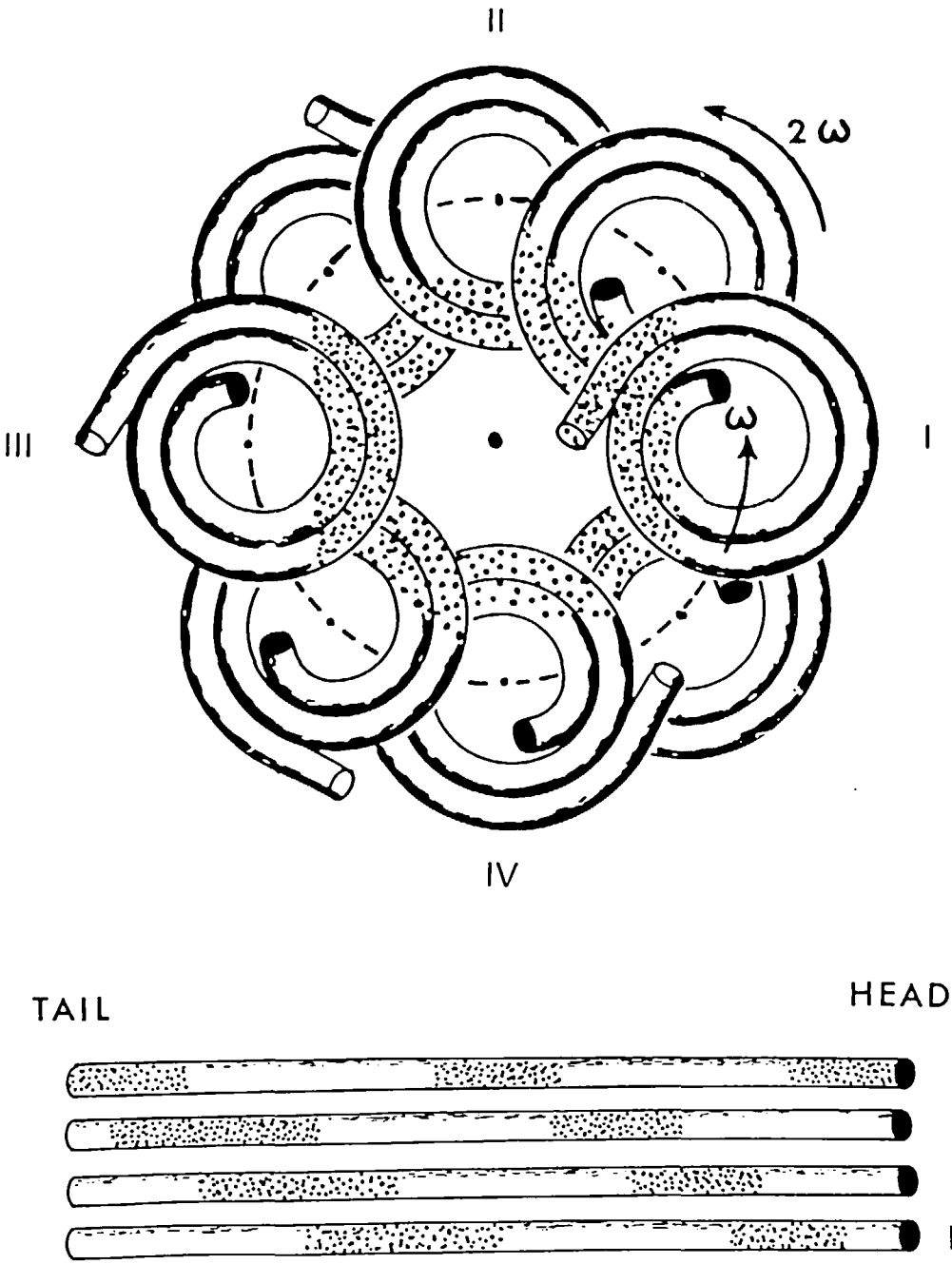

FIGURE 8. Formation and motion of mixing zones through a spiral coil in the concentric coil planet centrifuge.

Downloaded At: 15:26 17 January 2011

interaction of the two solvent phases taking place in the column, it leaves a number of questions to be answered in the future. Some examples are (1) how the mixing and settling zones are formed, (2) why two solvent phases are unilaterally distributed, and (3) which phase becomes the head phase and how it is determined. Although the unique distribution of the centrifugal force vectors described earlier (Figure 6D, right) seems to provide some rationale to the formation of the mixing and settling zones, further studies are required to establish the theory.

It is most likely that the hydrodynamic interaction of the two solvent phases in the rotating column is caused and affected by a number of physical factors involved in the present system. If this is the case, it becomes necessary to investigate the effects of these physical factors on the hydrodynamic distribution of the two solvent phases in the present system.

C. Phase Distribution Diagrams

In order to further develop the theory and application of high-speed CCC, a series of systematic studies has been performed on the hydrodynamic distribution of various two-phase solvent systems in the rotating helical column.

1. Phase Distribution Diagrams Obtained by Two Typical Synchronous Planetary Motions[40]

In the first series of the experiments, a set of phase distribution diagrams was obtained from each of the two typical synchronous planetary motions, Schemes I and IV, using a combined horizontal flow-through coil planet centrifuge. The apparatus holds a pair of column holders in the symmetrical positions at 20 cm from the central axis of the centrifuge. The pulley-driven holder produces the Scheme I planetary motion and the gear-driven holder, the Scheme IV planetary motion. The detailed design of the apparatus is described in Section IV. A and Figure 23.

Experiments were performed with helical columns, 5 m × 1.6 mm i.d. PTFE tubing wound around a 10 cm diameter column holder mounted on each side. For the present study, nine different types of volatile two-phase solvent systems, covering a broad spectrum in hydrophobicity, were selected. They include hexane/water, hexane/methanol, ethyl acetate/water, ethyl acetate/acetic acid/water (4:1:4), chloroform/water, chloroform/acetic acid/water (2:2:1), *n*-butanol/water, *n*-butanol/acetic acid/water (4:1:5), and sec.-butanol/water. Each solvent system was prepared by equilibrating the solvent mixture in a separatory funnel at room temperature and separated before use.

For each measurement, the column was first entirely filled with the stationary phase. Then the apparatus was run at a desired revolutional speed while the mobile phase was pumped through the column at a given flow rate. The effluent from the outlet of the column was collected in a graduated cylinder to measure the volume of the stationary phase eluted from the column as well as the total volume of the mobile phase eluted. From the data obtained from the above experiments, phase distribution diagrams were produced. The volume of the stationary phase retained in the column was first calculated from the volume of the stationary phase eluted from the column and expressed as a percentage of the total column capacity according to the expression $100\ (V_c + V_f - V_s)/V_c$, where V_c denotes total column capacity; V_f, the volume of the flow tubes; and V_s, the volume of the stationary phase eluted from the column. The hydrodynamic distribution of the two solvent phases in the column was summarized by a phase distribution diagram constructed by plotting the percentage retention of stationary phase as a function of revolutional speed for a particular mobile-phase flow rate. A group of retention curves produced by different elution modes but otherwise identical experimental conditions can be illustrated in the same distribution diagram with a set of symbolic designs (Table 2A).

The experimental data are summarized in Figure 9. Nine different solvent systems were examined by using each phase as the mobile phase at a flow rate of 120 mℓ/hr except for

Downloaded At: 15:26 17 January 2011

Table 2
SYMBOLIC DESIGN OF THE RETENTION CURVES IN THE PHASE DISTRIBUTION DIAGRAM FOR HELICAL AND SPIRAL COLUMNS

	Elution mode		Retention curve
(A) Helical column	H → T		Solid line
	H ← T		Broken line
	Elution mode		
	Upper phase mobile	**Lower phase mobile**	**Retention curve**
(B) Spiral column	EH→ IT	IH → ET	Thick solid line
	IH → ET	EH → IT	Thin solid line
	IH ← ET	EH ← IT	Thick broken line
	EH ← IT	IH ← ET	Thin broken line

Note: H = head; T = tail; I = internal; E = external.

Downloaded At: 15:26 17 January 2011

the butanol phase systems in which, because of its high viscosity, the flow rate was reduced at 60 mℓ/hr. Other important experimental conditions, such as the column i.d., R, r, and β values, and the revolutional speeds, etc., are indicated in Figure 9. Two retention curves are drawn in each diagram, the solid line for head to tail elution, and the broken line for tail to head elution. These phase distribution diagrams are arranged, from left to right, in the order of hydrophobicity of the major organic solvent, i.e., hexane, ethyl acetate, chloroform, and butanol. Within each organic solvent group, the phase composition is modified by addition of mutually miscible solvent to moderate the interfacial tension of the solvent system.

The phase distribution diagram of the hexane/water system obtained by the Scheme IV planetary motion, upper left diagram in Figure 9, will serve to illustrate the interpretation of these diagrams. In the upper diagram, plotting lower-phase retention on the ordinate implies that the upper phase is mobile. The retention of the lower phase sharply increases with revolutional speed, reaching over 90% at 800 rpm with the tail to head elution mode (broken line), while no retention occurs in the head to tail elution mode (solid line). This retention behavior can be described as unilateral, to indicate that the upper phase has a strong hydrodynamic tendency to move to the head and lower phase to the tail of the column. Thus with tail to head elution of the upper phase, the lower phase is well retained and the flowing upper phase quickly moves through it. On the other hand, with head to tail elution of the upper phase, the natural tendency of the lower phase to move to the tail is enhanced and the lower phase is simply washed out of the column. In the diagram second from the top, where the lower phase is mobile, high stationary phase retention results from the head to tail elution mode (solid line) because the natural tendency of the upper phase to flow toward the head is opposed by the mobile-phase flow. Again, poor retention of the upper phase is obtained if the lower phase is pumped from tail to head. These findings agree with the previous observation[35] that the hexane/water system, if confined in a similar column, establishes a unilateral hydrodynamic distribution where the two phases are completely separated in the direction of the column axis, with the upper phase entirely occupying the head side and the lower phase, the tail side of the column. This unilateral hydrodynamic distribution of the two phases is ideal for performing CCC, because high retention of the stationary phases is attainable with either phase used as the mobile phase by selecting the proper mode of elution.

Downloaded At: 15:26 17 January 2011

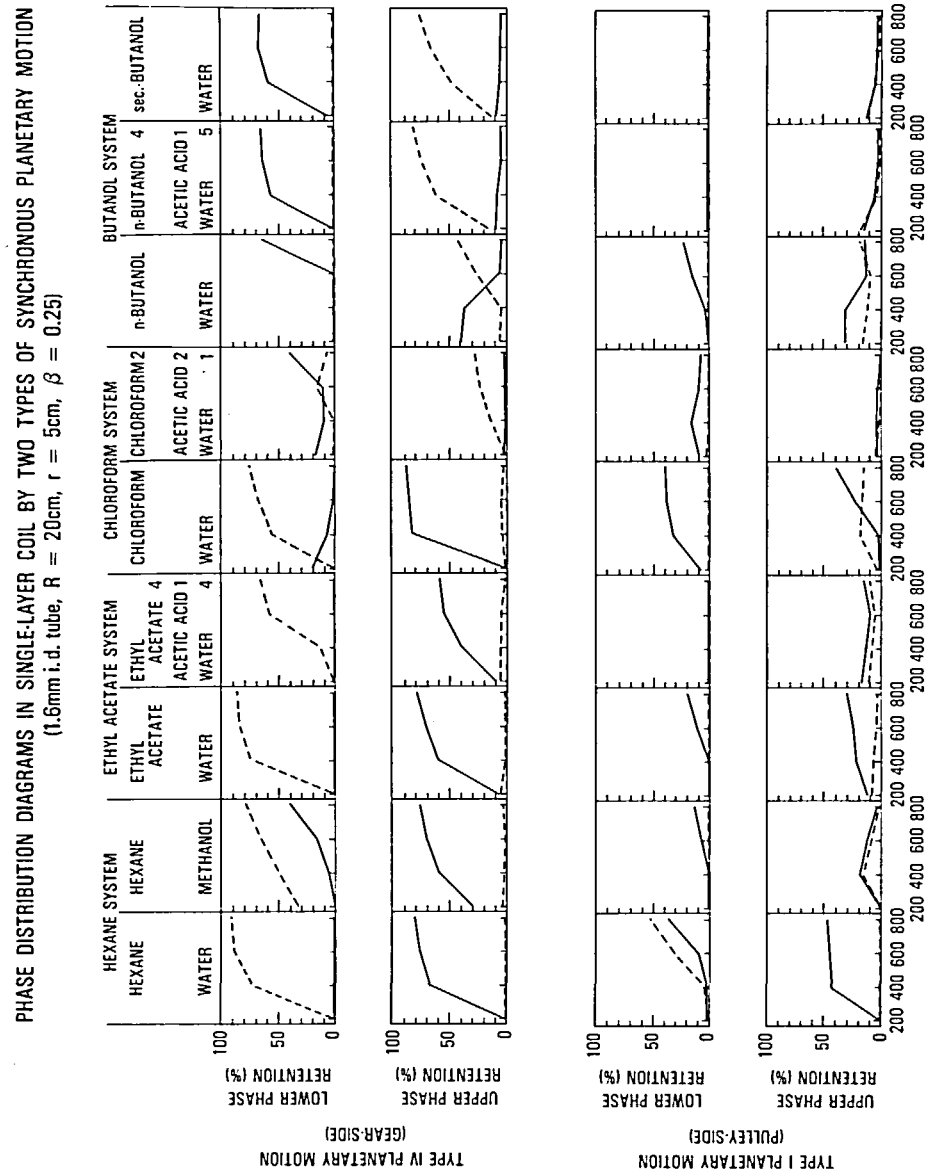

FIGURE 9. Phase distribution diagrams in single-layer coil by two types of synchronous planetary motion.

Two other solvent systems, ethyl acetate/water and chloroform/water, also exhibit the ideal retention curves similar to those of hexane/water, when subjected to the Scheme IV planetary motion. These three solvent systems are characterized by high interfacial tension and a strongly hydrophobic organic phase.

Ideal retention curves, but with completely reversed hydrodynamic trends, are observed in the two butanol solvent systems, *n*-butanol/acetic acid/water (4:1:5) and sec.-butanol/water. Both organic phases are very hydrophilic and possess high viscosity and low interfacial tension to the aqueous phase. As seen from the retention curves, these solvent systems display a reversed unilateral hydrodynamic motion in the column; the upper phase moves toward the tail and the lower phase, toward the head. If the two phases are confined in the column without introduction of external flow, they establish a unilateral hydrodynamic distribution or complete separation along the axis of the column with the upper phase on the tail side and the lower phase on the head side.

The remaining solvent systems in the Scheme IV group show phase distributions intermediate between those of the above two extreme groups. These intermediate solvent systems are usually prepared by adding methanol or acetic acid to a hydrophobic solvent system to moderate the interfacial tension and hydrophobicity of the organic phase. The relatively hydrophilic *n*-butanol/water also falls in this intermediate group. All solvent systems treated with the Scheme IV planetary motion display a trend of the unilateral hydrodynamic distribution in which one phase moves toward the head and the other phase, toward the tail of the column, though some are similar to hexane/water while others resemble the reversed hydrodynamic equilibrium of sec.-butanol/water.

Downloaded At: 15:26 17 January 2011

Phase distribution diagrams obtained from the Scheme I planetary motion under the otherwise identical experimental conditions are illustrated in the lower half of Figure 9. As these phase distribution diagrams clearly indicate, the Scheme I planetary motion fails to yield a satisfactory retention level of the stationary phase in all solvent systems. The fact that the solid curve is generally higher than the broken curve indicates that higher retention levels are attained by the head to tail elution mode regardless of which phase is used as the mobile phase. These findings strongly suggest that the two solvent phases establish a basic hydrodynamic equilibrium in the column in which each phase occupies nearly equal volume on the head side as previously demonstrated in the coiled column with much smaller helical diameters.[19] Under this basic hydrodynamic equilibrium, the head to tail elution mode always favors the retention of the stationary phase regardless of the choice of the mobile phase, and the maximum attainable retention is usually less than 50% of the total column capacity. The reversed mode of elution from the tail toward the head of the column in these circumstances is usually not feasible because of poor stationary phase retention and steady carryover of the stationary phase resulting in loss of peak resolution.

Comparison of the phase distribution diagrams for the two different types of the synchronous planetary motion clearly reveals that the Scheme IV planetary motion produces much higher stationary phase retention for all solvent systems under otherwise identical experimental conditions. This surprising contrast between the retention capability of these two schemes must be attributed to the difference in the centrifugal force field produced by their planetary motions illustrated in Figure 6D. As stated earlier, the Scheme I planetary motion produces a homogeneous centrifugal force field which synchronously rotates with the high revolutional rate of the column. This steadily rotating force field would introduce constant and vigorous agitation of the two solvent phases in a coiled column especially with large internal diameters.

In the Scheme IV synchronous planetary motion, the centrifugal force vectors always directed outwardly from the holder provide a force component which steadily acts perpendicularly to the coiled tube. Under these circumstances the two solvent phases are separated to form two layers along the helical flow path with the heavier phase in the outer portion

and the lighter phase in the inner portion except for one local mixing zone for each helical turn as observed under the stroboscopic illumination (Figures 7 and 8).[38] Thus, the Scheme IV planetary motion provides a suitable condition for the two solvent phases to flow smoothly against each other with no risk of emulsification.

2. Phase Distribution Diagrams for Helical Columns Under Scheme IV Planetary Motion[41]

The second series of experiments was conducted to investigate the effects of various physical factors on the phase distribution diagrams produced by the helical column under the Scheme IV planetary motion. Two Scheme IV coil planet centrifuges were employed: the apparatus with a 20 cm revolutional radius used in the previous studies and a new apparatus with a 10 cm revolutional radius (Figure 18). In addition to the nine volatile solvent systems previously tested, six different types of butanol solvent systems were newly examined.

Figure 10A illustrates a set of phase distribution diagrams obtained from the nine volatile solvent systems using the 1.6 mm i.d. helical column at three different β values mounted at a 20 cm revolutional radius. Both upper and lower phases were used as the mobile phase at a flow rate of 120 mℓ/hr except for the viscous butanol systems which were eluted at a reduced flow rate of 60 mℓ/hr. The upper block of diagrams was obtained with an upper mobile phase and the lower block, with a lower mobile phase. The middle rows of diagrams shown in each block were obtained using a 10 cm diameter holder ($\beta = 0.25$) and are the same data illustrated in Figure 9 (upper half).

Overall results clearly indicate that phase distribution curves display diverse patterns according to the hydrophobicity of the solvent systems and that within each solvent system the distribution pattern significantly changes with β values. As earlier described, these solvent systems may be classified into three groups according to their characteristic retention profile in the phase distribution diagram.

The hydrophobic solvent group including hexane/water, ethyl acetate/water, and chloroform/water, displays high retention of the stationary phase if the upper phase is eluted in the tail to head mode (broken line) or the lower phase is eluted in the head to tail mode (solid line). The reversed elution modes result in almost no retention except for chloroform/water which produces 20 to 30% retention at a small β value of 0.125. This retention profile of the solvent group indicates that the upper phase has a strong hydrodynamic tendency to move toward the head and the lower phase toward the tail of the helical column regardless of the β values within the range investigated.

The hydrophilic solvent group represented by *n*-butanol/acetic acid/water (4:1:5) and sec.-butanol/water displays a retention profile contrasting with that of the hydrophobic solvent group. These solvent systems yield high retention of the stationary phase when eluting with the upper phase in the head to tail mode (solid line) or the lower phase in the tail to head mode (broken line), while no retention occurs with the reversed modes of elution. This retention profile of the hydrophilic solvent systems implies a reversed hydrodynamic tendency with the lower phase moving toward the head and the upper phase toward the tail within the range of β values studied.

The rest of the solvent systems belong to the intermediate solvent group which is characterized by moderate hydrophobicity of the organic phase. These solvent systems exhibit a very complex retention profile which is sensitively affected by a change of the β value. At a small β value of 0.125, better retention of the lower phase is obtained under conditions represented by the solid curve while the broken curve indicates better retention of the upper phases. This pattern is analogous to that observed in the hydrophilic solvent group and indicates that the upper phase moves toward the tail and the lower phase toward the head under these conditions. At a larger β value of 0.375, this retention profile is completely reversed, i.e., the broken curve shows greater lower-phase retention and the solid curve

Downloaded At: 15:26 17 January 2011

Downloaded At: 15:26 17 January 2011

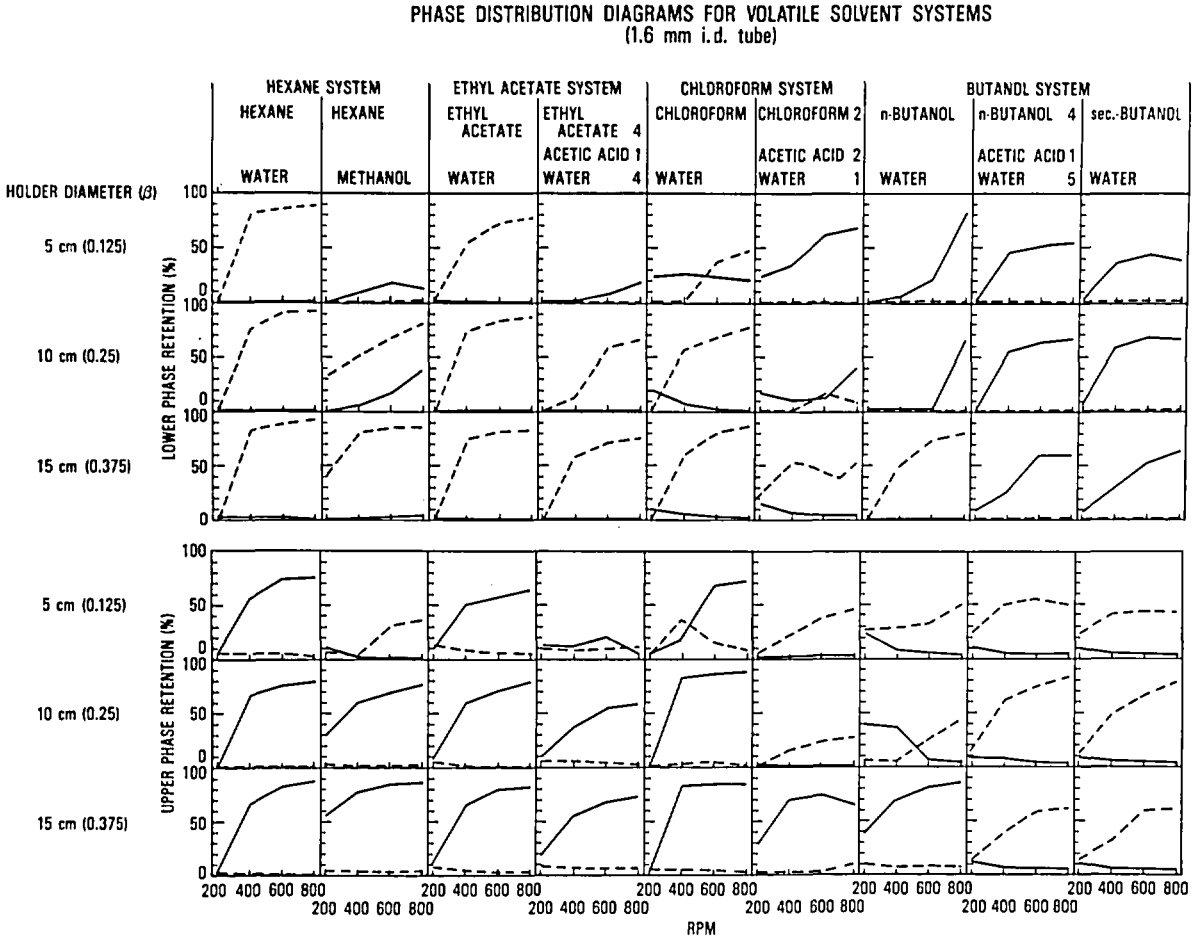

FIGURE 10A. Phase distribution diagrams for volatile solvent system in helical columns obtained with a 20 cm revolutional radius.

Downloaded At: 15:26 17 January 2011

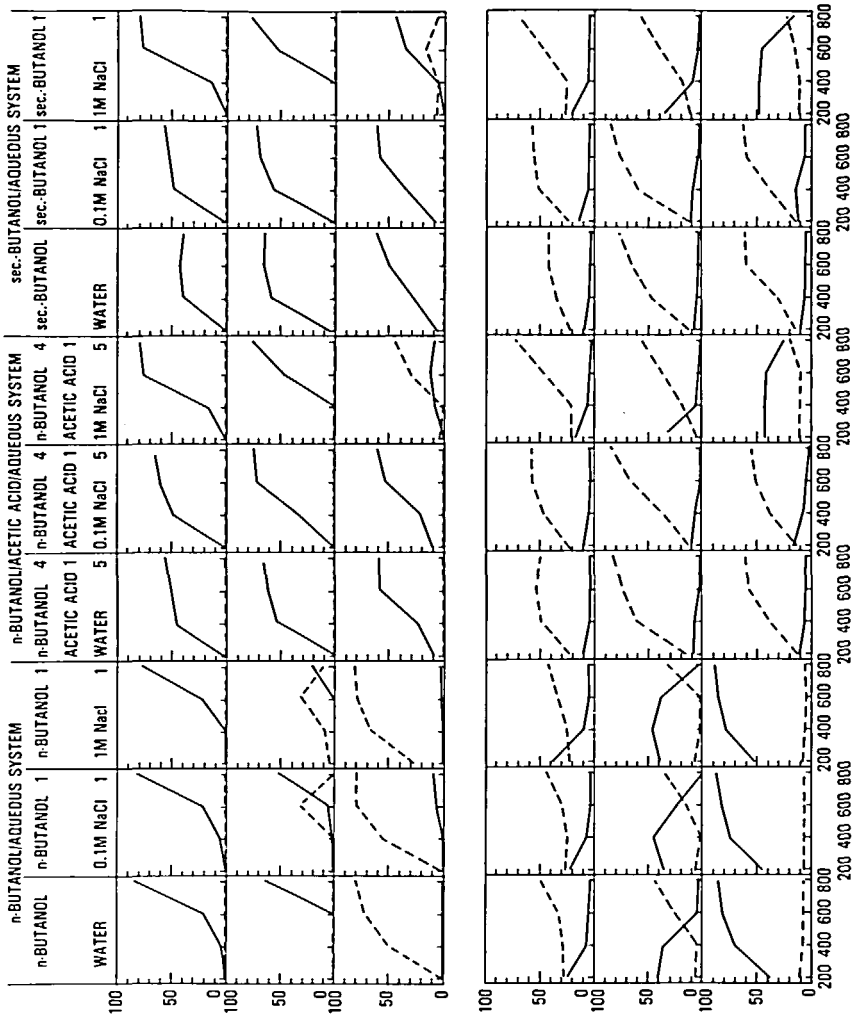

FIGURE 10B. Phase distribution diagrams for butanol solvent systems in helical columns obtained with a 20 cm revolutional radius.

shows greater upper-phase retention analogous to the hydrophobic solvent group indicating that the upper phase moves toward the head and the lower phase toward the tail. In brief, the hydrodynamic motion and resulting retention profiles of the intermediate solvent group approach those of the hydrophilic solvent group at a small β value and become quite similar to those of the hydrophobic solvent group at a large β value.

The butanol solvent systems were further modified by adding sodium chloride to study the effects of salt concentration on the retention curves under otherwise identical experimental conditions. The results of the experiments are summarized in Figure 10B in a similar fashion. The phase distribution diagrams of *n*-butanol/water, *n*-butanol/acetic acid/water (4:1:5), and sec.-butanol/water which appeared on Figure 10A are repeated in Figure 10B for comparison. Addition of 0.1 *M* NaCl to the solvent system produces no significant effect on the retention curves in all solvent systems, However, at the 1 *M* NaCl concentration some interesting changes appear in the retention curves of the hydrophilic solvent systems. In both *n*-butanol/acetic acid/1 *M* NaCl (4:1:5) and sec.-butanol/1 *M* NaCl (1:1), increase in β value tends to depress the solid curve for the lower phase retention (top) and the broken curve for the upper phase retention (bottom) as if the whole curves are shifted toward the right. At $\beta = 0.375$, the other curves start to rise suggesting that, as the β value and/or the salt concentration are further increased, the retention profile of these solvent systems would become similar to those in the *n*-butanol/aqueous systems given at $\beta = 0.375$.

The studies on the effects of the β values were continued with the same set of helical columns using the second apparatus which produces the Scheme IV planetary motion with a smaller revolutional radius of 10 cm hence doubling the β value for each column. In order to compensate for the reduced revolutional radius, the experiments were peformed at higher revolutional speeds ranging between 400 rpm and 1000 rpm while other operational conditions were unaltered. The phase distribution diagrams obtained from this series of experiments are illustrated in Figure 11A and B using the same format as in Figure 10A and B to facilitate comparison.

Figure 11A shows the phase distribution diagrams for the set of nine volatile solvent systems obtained from the helical columns rotated at a 10 cm revolutional radius. Compared with a 20 cm revolutional radius (Figure 10A), both hydrophobic and intermediate solvent groups show substantial improvement in stationary phase retention, especially for the systems, chloroform/acetic acid/water (2:2:1) and *n*-butanol/water. In these two solvent systems, the relative heights of the two retention curves in each diagram become reversed at the 10 cm helical diameter ($\beta = 0.5$), while a similar reversal of the two curves occurred at the 15 cm helical diameter ($\beta = 0.375$) with the 20 cm revolutional radius. In the hydrophilic solvent group, the retention of both *n*-butanol/acetic acid/water (4:1:5) and sec.-butanol/water was improved at the 5 cm helical diameter but it declined at the 10 to 15 cm helical diameter compared with the data obtained at the 20 cm revolutional radius. Although there is no reversal of the two retention curves observed in the hydrophilic solvent group, the retention diagrams of the upper phase obtained at 15 cm holder diameter ($\beta = 0.75$) show substantial rise of the solid curve which indicates that the reversal of the two curves might occur at a larger helical diameter.

Figure 11B shows a similar set of diagrams for the butanol solvent systems obtained at the 10 cm revolutional radius. Here again, the retention data of *n*-butanol/water, *n*-butanol/acetic acid/water (4:1:5), and sec.-butanol/water illustrated in Figure 11A are repeated in Figure 11B for comparison. Comparison of Figures 10B and 11B shows some important effects of the altered revolutional radius on the retention curves in all solvent groups. In the relatively hydrophobic *n*-butanol/aqueous systems, a 10 cm holder diameter at the 10 cm revolutional radius gives the highest retention for all NaCl concentrations and reversal of the retention curves generally occurs in the region of β values between 0.25 and 0.375. In the hydrophilic solvent group of *n*-butanol/acetic acid/aqueous solution (4:1:5) and sec.-

Downloaded At: 15:26 17 January 2011

Downloaded At: 15:26 17 January 2011

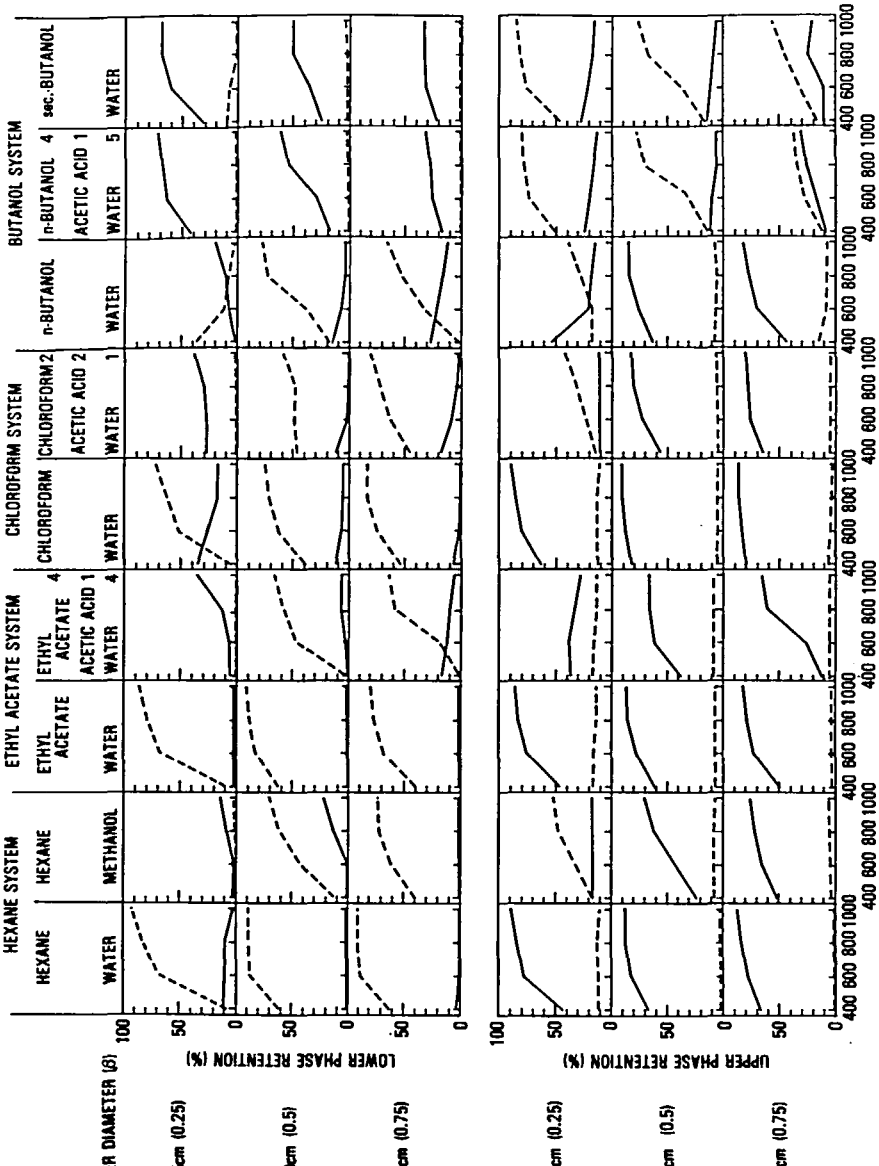

FIGURE 11A. Phase distribution diagrams for volatile solvent systems in helical columns obtained with a 10 cm revolutional radius.

Downloaded At: 15:26 17 January 2011

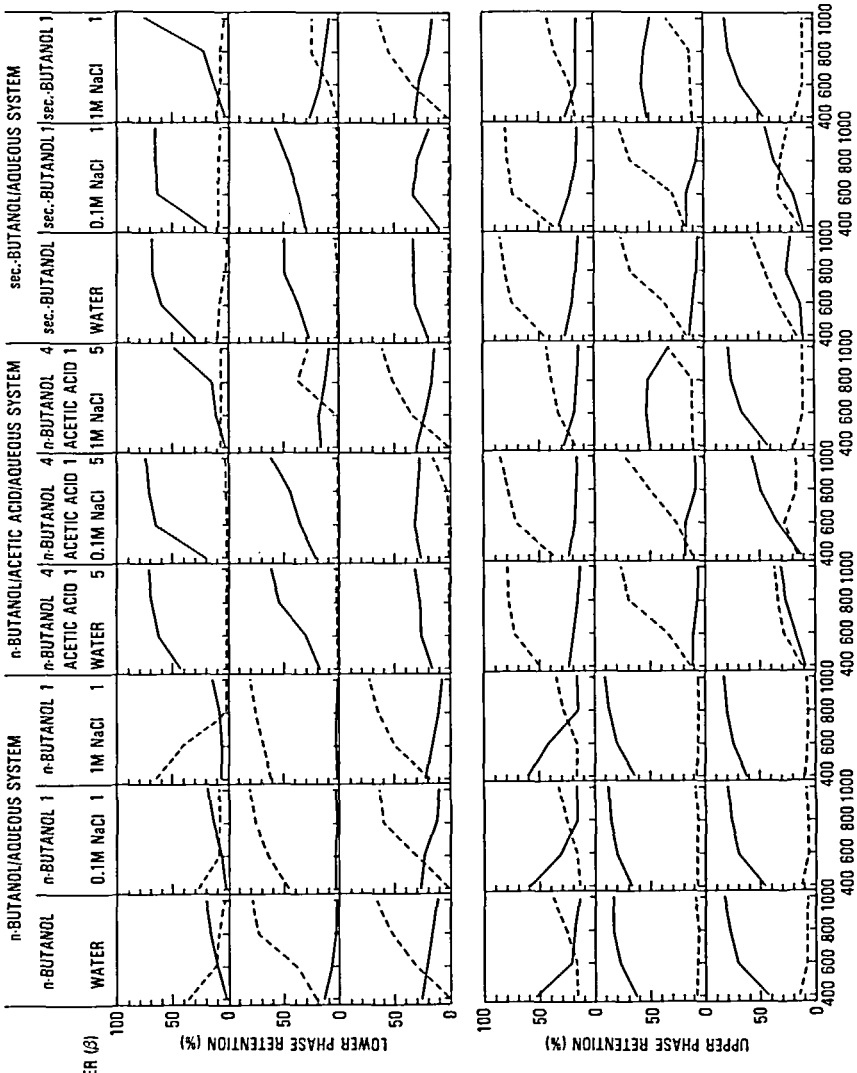

FIGURE 11B. Phase distribution diagrams for butanol solvent systems in helical columns obtained with a 10 cm revolutional radius.

butanol/aqueous solution (1:1), 1 *M* NaCl concentration produces a complete reversal of the retention curves between 5 and 10 cm helical diameters and at the 15 cm helical diameter the retention profile becomes similar to those of the *n*-butanol/aqueous systems.

Phase distribution diagrams obtained from the helical columns under various experimental conditions (Figures 10 and 11) show complex patterns of the retention curves which are, at present, unpredictable on a theoretical basis. The retention profile of the two-phase solvent systems is certainly based on the hydrodynamic interaction of the two solvent phases in the rotating coiled column. As described earlier, for Scheme IV planetary motion the two solvent phases exhibit unilateral distribution along the axis of the coiled column in such a way that one phase entirely occupies the head side and the other phase occupies the tail side. Which phase is directed toward the head of the column is determined by the combined effects of various factors characteristic of the particular experimental condition. Overall results of the present studies suggest that conditions favoring the upper phase movement toward the head and the lower phase toward the tail include: (1) increase in hydrophobicity of the nonaqueous phase; (2) increase in interfacial tension between the two solvent phases; (3) decrease in viscosity of the solvent phases; (4) increase in the density difference between the solvent phases; (5) increase in β value; (6) decrease in revolutional radius; and (7) increase in the helical diameter of the column.

The effects produced by the physical properties of the solvent system, (1 to 4), are intermingled and difficult to isolate from each other and, in addition, the effects of solvent-wall interaction should be further investigated with a column which provides a hydrophilic surface. The effects of the column factors (5 to 7) are also complex, but the β value may be the most sensitive parameter of the three. The revolutional speed produces highly complex effects on the interaction of the two solvent phases, often causing a reversal of the unilateral hydrodynamic motion of the two phases which occurs at the crossing point of the two retention curves in the phase distribution diagram. In most cases, increasing the revolutional speed tends to direct the upper phase toward the head of the coiled column, i.e., for lower phase retention, the broken curve crosses upward over the solid curve and for upper phase retention, the solid curve crosses over the broken curve. However, reversal of the retention curves is also occasionally observed with butanol solvent systems. Although the flow rate of the mobile phase is an important factor affecting the retention of the stationary phase, it is not likely to cause reversal of the unilateral hydrodynamic motion.

Among the various factors mentioned above, the β value may play a universal role in the unilateral hydrodynamic distribution of the two solvent phases. The phase distribution diagrams obtained at various β values strongly suggest that further increase of the β value by the use of a larger diameter holder would eventually reverse the direction of the unilateral hydrodynamic separation of the hydrophilic solvent systems. The decrease of the β value by the use of a smaller diameter holder may reverse the unilateral hydrodynamic motion of the hydrophobic solvent systems, as illustrated by the retention curves of chloroform/water at $\beta = 0.125$ in Figure 10A.

3. Phase Distribution Diagrams for Spiral Columns Under Scheme IV Planetary Motion[41]

The third series of experiments has been performed to study the phase distribution in the spiral columns subjected to the Scheme IV synchronous planetary motion. In the spiral column, retention of the stationary phase is affected by two forces: one is the Archimedean screw force governed by the head-tail relationship as in the helical column and the other, the centrifugal force field gradient created by the spiral pitch of the column. The separate effects of these two forces are graphically presented in the phase distribution diagrams by the choice of symbols for drawing the retention curves as indicated in Table 2B. Effects of the Archimedean screw are shown by the difference between the solid and broken curves as in the previous diagrams for the helical column while the effects of centrifugal force

Downloaded At: 15:26 17 January 2011

gradient are indicated by the difference between the thick and thin curves. For simplification, the choice of stationary and mobile phases giving the greater stationary phase retention as a result of the force gradient is shown by the thick line and the reversed elution mode by the thin line so that the thick curve always appears higher in the diagram regardless of the choice of the lower or upper layer as the mobile phase.

The phase distribution diagrams for the nine volatile solvent systems for single-layer spiral columns mounted at a 10 cm revolutional radius are illustrated in Figure 12A, where the top two rows show the data for the 1.6 mm i.d. column and the bottom two rows, the data for the 2.6 mm i.d. column. In order to provide similar linear flow velocity of the mobile phase in each of the two columns, the flow rate for the 2.6 mm i.d. column was made double that of the smaller column, i.e., 240 mℓ/hr for the hexane, ethyl acetate, and chloroform systems and 120 mℓ/hr for the butanol systems.

The effects of the centrifugal force gradient in the spiral column on the retention curves are quite different in each solvent group. In the hydrophobic solvent group including hexane/water, ethyl acetate/water, and chloroform/water, the force gradient contributes little effect in either the 1.6 mm or 2.6 mm i.d. column as indicated by the small difference in retention level between the thick and thin curves for each pair of the solid and broken curves. In the intermediate solvent group, including hexane/methanol, ethyl acetate/acetic acid/water (4:1:4), chloroform/acetic acid/water (2:2:1), and n-butanol/water, the effects of the force gradient becomes significant especially in the 2.6 mm i.d. column where much wider gaps were formed between the thick and thin curves. In the hydrophilic solvent group of *n*-butanol/acetic acid/water (4:1:5) and sec.-butanol/water, the force gradient effects become further enhanced and except for the top diagrams (lower phase retention in the 1.6 mm i.d. column) both thick curves are higher than the pair of thin curves indicating that the force gradient plays a more important role in retention than the head-tail relationship. In the 2.6 mm i.d. column, both hydrophilic solvent systems show a radical change in retention curves at the revolutional speeds between 700 and 900 rpm where the two thick curves cross each other indicating that at higher revolutional speeds, the upper phase is directed toward the head and the lower phase toward the tail in the spiral column as is the case with other solvent groups.

Downloaded At: 15:26 17 January 2011

Figure 12B shows sets of phase distribution diagrams of butanol solvent systems obtained from the 1.6 mm i.d. and 2.6 mm i.d. spiral columns. Addition of NaCl to *n*-butanol/water produces no significant change in the stationary phase retention profile regardless of the internal diameter of the column. However, the retention curves for the *n*-butanol/acetic acid/water (4:1:5) and sec.-butanol/water are significantly altered at the 1 *M* NaCl concentration where the phase distribution profile becomes similar to those for the *n*-butanol/water and other intermediate solvent systems.

Performance of the spiral columns has also been examined with the third type of the coil planet centrifuge which provides greater β values by further reducing the revolutional radius and/or increasing the holder diameter. The retention data were obtained from a 1.6 mm i.d. spiral column wound around a 15 cm diameter holder which was placed at 10 cm or 5 cm from the central axis of the centrifuge, providing the β values of 0.75 to 0.95 or 1.5 to 1.9, respectively. Figure 13 shows a set of phase distribution diagrams obtained from four different solvent pairs with a 5 cm revolutional radius (top two rows) and a 10 cm revolutional radius (bottom two rows).

The retention data in Figure 13 (bottom two rows) may be compared with those in Figure 12A (the corresponding solvent systems in the top two rows) to observe the effects of increasing the holder-hub diameter from 10 to 15 cm at the same revolutional radius of 10 cm. The increase of the holder-hub diameter substantially widens the gaps between the thick and the thin curves in intermediate solvent systems, indicating the enhanced force gradient effects on the retention of the stationary phase.

Downloaded At: 15:26 17 January 2011

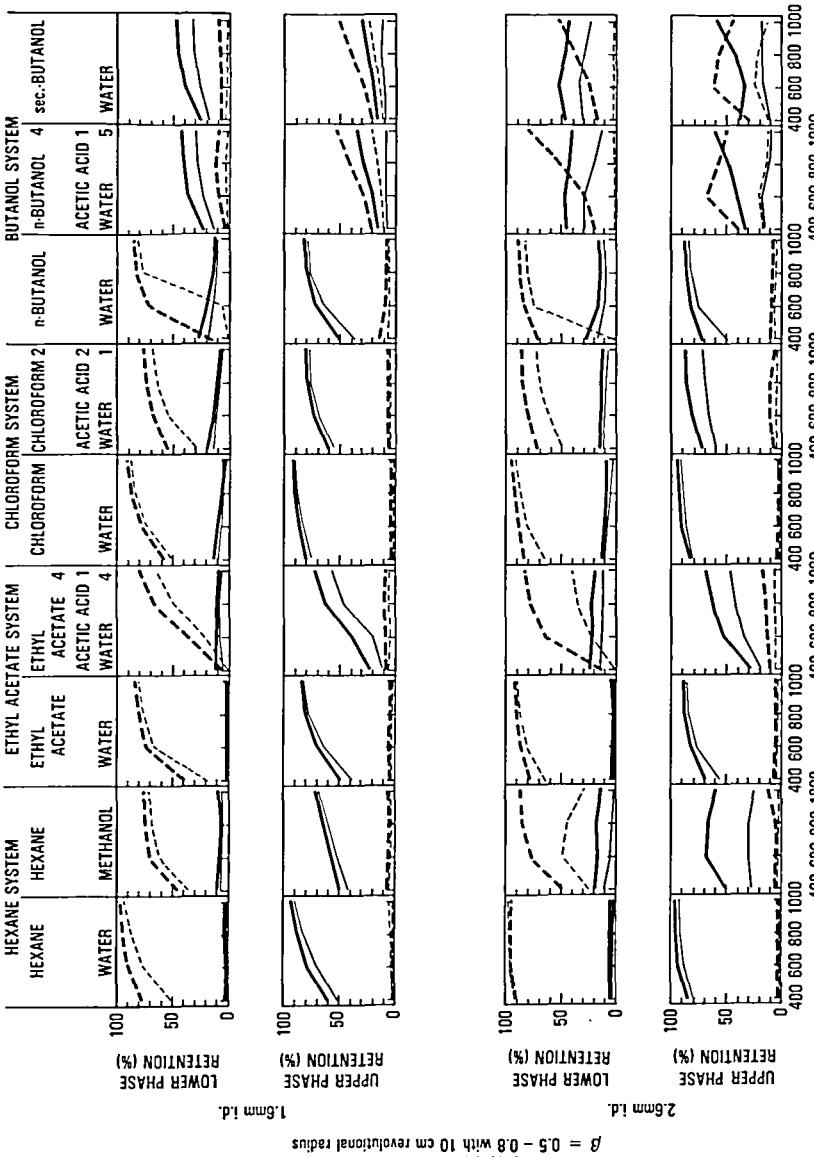

FIGURE 12A. Phase distribution diagrams for volatile solvent systems in spiral columns obtained with a 10 cm revolutional radius.

Downloaded At: 15:26 17 January 2011

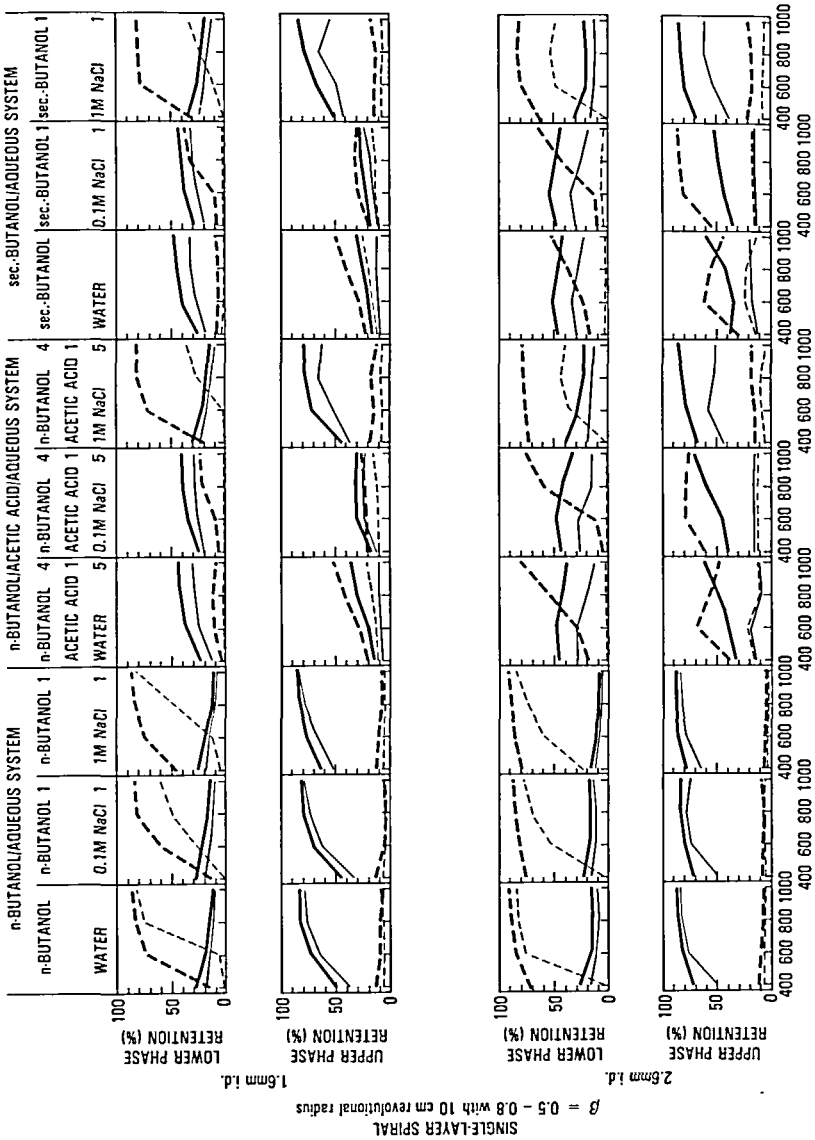

FIGURE 12B. Phase distribution diagrams for butanol solvent systems in spiral columns obtained with a 10 cm revolutional radius.

Comparison between the two top and the two bottom rows of the phase distribution diagrams in Figure 13 shows the effects of reducing the revolutional radius from 10 to 5 cm in the same spiral column on the 15 cm diameter holder. This reduction of the revolutional radius not only causes an increase of β values but also halves the net centrifugal force field at a given revolutional speed. The results clearly show that the retention levels are further decreased especially in the intermediate solvent systems, although, widened gaps between the thick and thin curves in both hydrophobic and intermediate solvent systems indicate the enhanced effects of the force gradient on the retention of the stationary phase in the spiral column. The hydrophilic solvent system of *n*-butanol/acetic acid/water (4:1:5) shows no significant change when the revolutional radius is reduced. Overall results indicate that the large β values in the spiral column obtained by increasing the holder-hub diameter and decreasing the revolutional radius, produces substantial enhancement of the force gradient effects but fails to improve the retention of the stationary phase apparently due to the loss of the Archimedean screw effects produced by the head-tail hydrodynamic interaction of the two solvent phases.

D. Physical Properties of Solvent Systems and Settling Times[42]

Studies on phase distribution diagrams previously described have demonstrated that the two-phase solvent systems display characteristic behavior related to the hydrophobicity of the nonaqueous phases. The hydrophobic solvent systems exhibit a strong hydrodynamic trend in the coiled column where the two solvent phases are unilaterally distributed in such a way that the upper phase is always directed toward the head and the lower phase toward the tail. The hydrophilic solvent systems show the opposite hydrodynamic tendency, with the upper phase being directed toward the tail and the lower phase toward the head. In the solvent systems with moderate hydrophobicity intermediate between the above two extremes, the hydrodynamic tendency is sensitive to the centrifugal conditions. In a system having a column of small helical diameter with a large radius of revolution, the hydrodynamics of the intermediate solvent group approaches that of the hydrophilic solvent group while with the reversed conditions (large helical diameter and small radius of revolution) the hydrodynamics becomes quite similar to that of the hydrophobic solvent group.

In the present studies, efforts were made to correlate the hydrodynamics of the two-phase solvent systems with three major physical properties: interfacial tension, viscosity, and the difference in density between the two phases. Measurement of the settling time of the two-phase solvent systems under unit gravity gave a parameter which provided a reliable numerical index which correlated with the hydrodynamics observed for the solvent systems in a centrifugal force field.

1. Measurement of Physical Properties of the Two-Phase Solvent System

Major physical properties of the solvent systems including density, viscosity, and interfacial tension were measured using conventional methods as decribed below. The densities of the upper and the lower phases in each solvent system were measured using a set of hydrometers (Fisher Scientific Company, Pittsburgh, PA) and the density difference between the two phases was calculated. The viscosity of each solvent phase was measured using a falling ball type viscometer (VWR Scientific Inc., Baltimore, MD). A modified Wilhelmy balance was used to determine the surface tension of each solvent phase against air, using water (73 dyne/cm) and hexane (18.4 dyne/cm) for standardization of the instrument for aqueous and organic phases, respectively. The interfacial tension was calculated as the difference in surface tension between the upper and the lower phases of each solvent pair. All measurements above were performed at room temperature of 22 ± 1°C. The results are summarized in Table 3. Among three physical properties measured for the solvent system, interfacial tension ($\Delta\gamma$) shows extremely high correlation with both the hydrophobicity and

Downloaded At: 15:26 17 January 2011

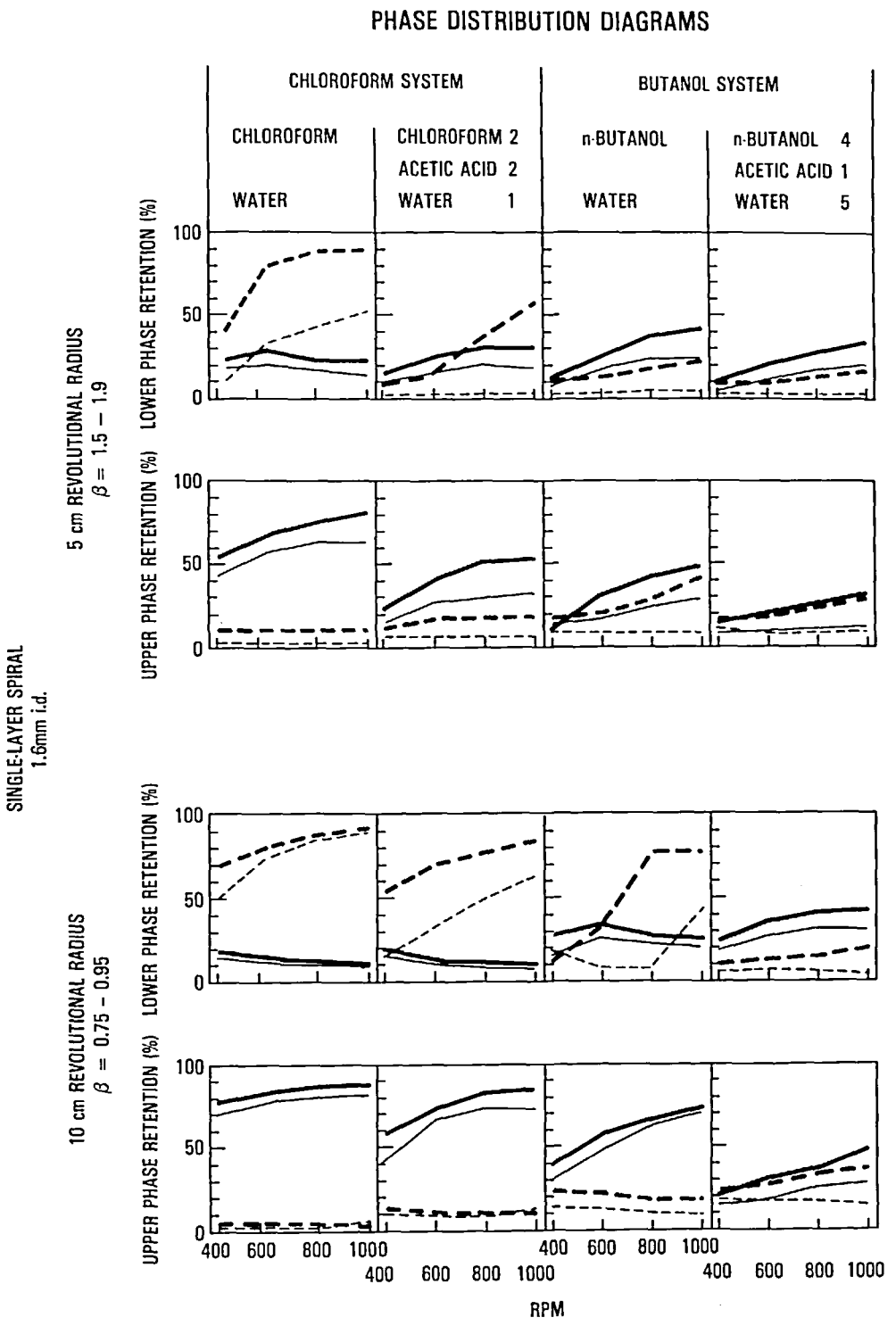

FIGURE 13. Phase distribution diagrams for chloroform and butanol solvent systems in spiral columns with large β values.

Downloaded At: 15:26 17 January 2011

Downloaded At: 15:26 17 January 2011

Table 3
PHYSICAL PROPERTIES OF THE TWO-PHASE SOLVENT SYSTEM

Solvent group	Two-phase solvent system (volume ratio)	Interfacial tension (dyne/cm)	Viscosity (c.p.)		Density (g/cm³)		Settling time (sec)	
		$\Delta\gamma$	$\eta U/\eta L$	$\bar{\eta}$	$\rho U/\rho L$	$\Delta\rho$	T	T′
Hydrophobic	Hexane-water	52	0.41/0.95	0.68	0.66/1.00	0.34	< 1	8
	Ethyl acetate-water	31	0.47/0.89	0.68	0.92/0.99	0.07	15.5	21
	Chloroform-water	42	0.95/0.57	0.76	1.00/1.50	0.50	3.5	5.5
Intermediate	Hexane-methanol	4	0.50/0.68	0.59	0.67/0.74	0.07	5.5	6
	Ethyl acetate-acetic acid water (4:1:4,v/v/v)	16	0.76/0.81	0.79	0.94/1.01	0.07	15	16
	Chloroform-acetic acid-water (2:2:1,v/v/v)	12	1.16/0.77	0.97	1.12/1.35	0.24	29	27.5
	n-Butanol-water	3	1.72/1.06	1.40	0.85/0.99	0.14	18	14
	n-Butanol-0.1 *M* NaCl (1:1,v/v)	4	1.66/1.04	1.35	0.85/0.99	0.15	16	14.5
	n-Butanol-1 *M* NaCl (1:1,v/v)	5	1.75/1.04	1.40	0.84/1.04	0.20	23.5	21.5
Hydrophilic	*n*-Butanol-acetic acid-water (4:1:5, v/v/v)	<1	1.63/1.40	1.52	0.90/0.95	0.05	38.5	37.5
	n-Butanol-acetic acid-0.1 *M* NaCl (4:1:5, v/v/v)	<1	1.68/1.25	1.47	0.89/1.01	0.11	32	30.5
	n-Butanol-acetic acid-1 *M* NaCl (4:1:5, v/v/v)	1	1.69/1.26	1.48	0.88/1.05	0.16	26.5	24.5
	sec.-Butanol-water	<1	2.7/1.67	2.19	0.87/0.97	0.10	57	58
	sec.-Butanol-0.1 *M* NaCl (1:1, v/v)	<1	1.96/1.26	1.61	0.86/0.98	0.12	46.5	49.5
	sec.-Butanol-1 *M* NaCl (1:1, v/v)	3	1.91/1.29	1.60	0.84/1.03	0.19	34	33.5

Note: $\eta U/\eta L$ = Upper phase/lower phase; $\bar{\eta}$ = mean viscosity of the two phases; $\rho U/\rho L$ = upper phase/lower phase; $\Delta\rho$ = density difference between the two phases; T = settling time after gentle mixing, T′ = settling time after vigorous shaking.

the hydrodynamic behavior of the solvent system in that the value is highest for the hydrophobic solvent group and lowest for the hydrophilic solvent group. The viscosity of each phase (η_U and η_L) or the mean viscosity of both phases ($\bar{\eta}$), are also very well correlated with the solvent group, being lowest in the hydrophobic solvent systems and highest in the hydrophilic solvent systems. The density difference between the upper and the lower phases ($\Delta\rho$) appears to be less well correlated with the solvent groups. Although the value is generally high in the hydrophobic solvent group and low in the hydrophilic solvent group, a discrepancy is presented by ethyl acetate/water in the hydrophobic solvent group which shows the second lowest value among all solvent systems. Thus, all three physical properties examined have some significant relationship to the stationary phase retention profile and the hydrodynamic behavior of the solvent systems in high-speed CCC.

2. Settling Time for the Two-Phase Solvent Systems

In order to correlate the hydrodynamic phase distribution in the rotating coiled column to the physical properties of the solvent system, simple tests were performed to measure the settling time of the two solvent phases, i.e., the time required for the solvent mixture to be completely separated into two layers in a unit gravitational field. Each two-phase solvent system was first equilibrated in a separatory funnel at room temperature and separated into two phases. A 2 mℓ aliquot of each phase, total volume 4 mℓ, was delivered to a 5-mℓ graduated cylinder which was then sealed with a glass stopper. The solvents in the cylinder were gently mixed by inverting the cylinder 5 times and the cylinder was immediately placed on a flat table in an upright position and the time required for the two phases to settle was measured. The measurement was repeated several times to obtain a mean value. A second set of tests were performed in a similar manner except that the cylinder was vigorously shaken 5 times to see the tendency for emulsification. The test was again repeated several times to obtain a mean value for each solvent system.

The settling times of the two-phase solvent systems are also shown in Table 3 where T indicates the settling time after gentle mixing by inverting the cylinder 5 times and T′, after vigorous shaking of the cylinder 5 times. The results clearly show a close correlation between the settling times in a unit gravitational field and the hydrodynamic behavior of the solvent phases observed in a centrifugal field. The settling times of the hydrophobic solvent systems are shortest ranging from 5 to 16 sec while those of the hydrophilic solvent systems are longest ranging from 38 to 59 sec. The intermediate solvent systems gave moderate values ranging from 15 to 29 sec with the exception of the nonaqueous system hexane/methanol which had short settling time of 5.5 sec. The difference between T and T′ for each solvent system was found to be quite small in both the intermediate and hydrophilic solvent systems. However, in the hydrophobic solvent group, T′ becomes much greater than T especially in hexane/water.

Because of the parallel trend observed with the hydrophobicity of the solvent group, the settling time may serve as a useful parameter for correlating the physical properties of the solvent system with the hydrodynamic behavior of the solvent systems in a centrifugal force field.

The values for $\Delta\gamma$, $\Delta\rho$, and $\bar{\eta}$ (mean viscosity of the upper and the lower phases) in Table 3 are, respectively, plotted against the settling time (T) of the solvent system in Figures 14A through C where the open circle represents the hydrophobic solvent system; the solid circle, the hydrophilic solvent system; and the semisolid circle, the intermediate solvent system. The correlation coefficient (r) for each plot of physical property with settling time (T) was computed for the set of 15 solvent systems. The density difference ($\Delta\rho$) gave a weak negative correlation ($r = -0.45$) (Figure 14A) and the interfacial tension ($\Delta\gamma$), a moderate negative correlation ($r = -0.65$) (Figure 14B). A strong positive correlation ($r = +0.88$) was observed between the settling time and the mean viscosity ($\bar{\eta}$) as illustrated

Downloaded At: 15:26 17 January 2011

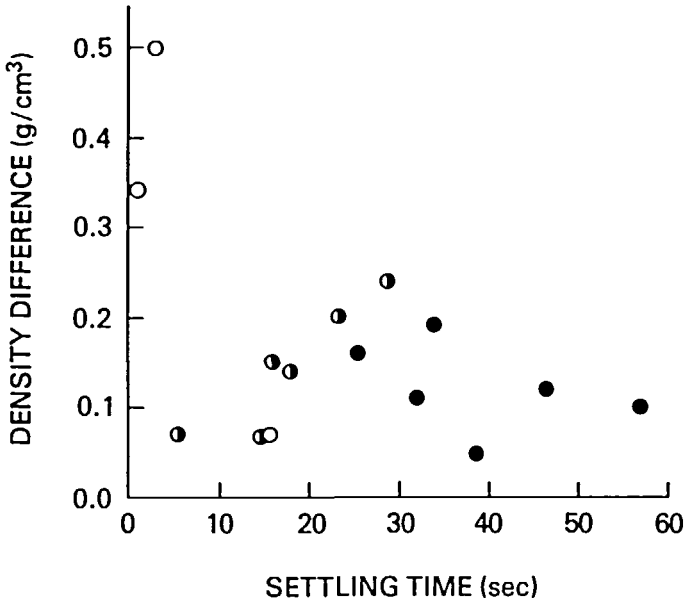

A

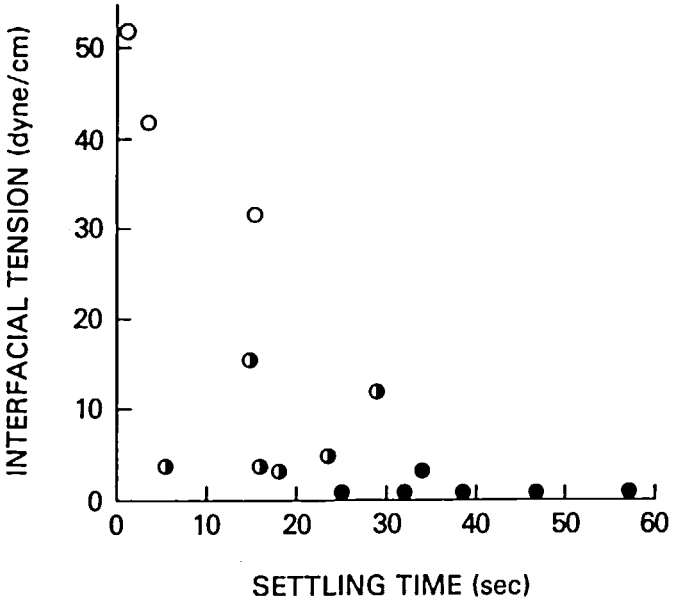

B

FIGURE 14. Correlation between the settling time and three major physical properties of the two-phase solvent system. (A-C) Open circle indicates the hydrophobic solvent system; semisolid circle, the intermediate solvent system; and solid circle, the hydrophilic solvent system. (A) Density difference of the two phases vs. settling time ($r = -0.45$). (B) Interfacial tension vs. settling time ($r = -0.65$). (C) Mean viscosity vs. settling time ($r = +0.88$). (D) Correlation between the settling time and viscosity of each solvent phase. Open circle: viscosity of nonaqueous phase vs. settling time ($r = +0.83$). Solid circle: viscosity of aqueous phase including the lower phase of hexane-methanol vs. settling time ($r = +0.89$).

Downloaded At: 15:26 17 January 2011

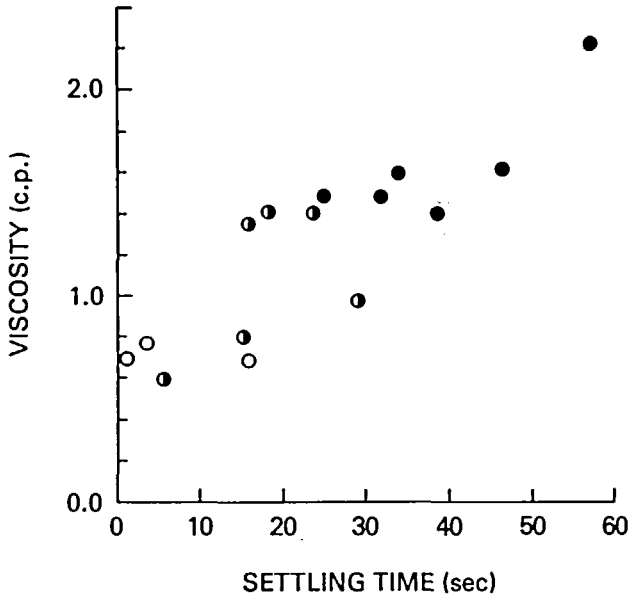

FIGURE 14C.

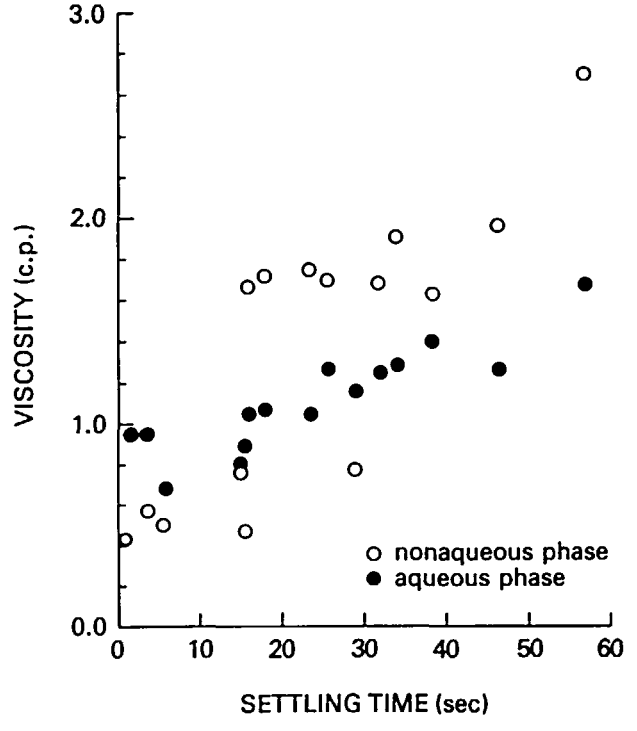

FIGURE 14D.

in Figure 14C. When the correlation coefficient between the viscosity and the settling time is computed individually for each phase, the aqueous phase including the lower phase of hexane/methanol (solid circle) gave the highest value of 0.89 and the nonaqueous phase (open circle), a lower value of 0.83 (Figure 14D).

Downloaded At: 15:26 17 January 2011

The above findings suggest that among various physical properties of the solvent system viscosity may play a major role in retention of the stationary phase. The less viscous the solvent system, the higher level of retention to be expected. Although the interfacial tension and density difference between the two phases appear to be less important factors than the viscosity, they would exert a strong influence on the settling times near the plait point of the solvent as described later in detail.

3. Effects of the Temperature on the Settling Time

As described earlier, hydrophilic solvent systems such as *n*-butanol/acetic acid/water (4:1:5) and sec.-butanol/water exhibit unique hydrodynamic behavior; the upper phase is distributed toward the tail and the lower phase toward the head. Therefore, the reversed elution mode is required to obtain retention of the stationary phase in the helical column. These solvent systems are characterized by high viscosity and low interfacial tension associated with the longest settling times among all solvent systems examined. The highly significant correlation found between viscosity and settling times of various solvent systems strongly suggests that the above unique hydrodynamic behavior of the hydrophilic solvent systems may be attributed to their high viscosity and that reduction of the viscosity by raising the temperature of these solvent systems would reduce their settling times to the range observed for other solvent systems, thus converting their reversed hydrodynamic mode to the normal mode. This reversal of the hydrodynamic behavior of the butanol solvent systems will provide an obvious advantage in performing high-speed CCC in that all conventional solvent systems could then be eluted with the normal mode with high flow rates of the mobile phase.

Downloaded At: 15:26 17 January 2011

In order to demonstrate the feasibility of this hydrodynamic reversal, settling times of the butanol solvent systems were measured at various temperatures ranging from room temperature to around 80°C. Figure 15 shows the effects of temperature on the settling times of *n*-butanol/water and sec.-butanol/water. The settling time of the sec.-butanol/water system sharply declines to less than 20 sec on increasing the temperature to 50°C. The settling time of the less viscous *n*-butanol/water system exhibits a similar trend, dropping to less than 10 sec at 50°C. As judged from the settling times, it is expected that at a temperature of 50°C these solvent systems would produce phase distribution diagrams similar to those of the intermediate and hydrophobic solvent systems which allow high retention levels of the stationary phase with the normal elution mode. It is interesting to note that the curves of the settling time vs. temperature for these binary butanol systems (Figure 15A) are quite similar to that of the viscosity vs. temperature plot for n-butanol (Figure 15B) which is consistent with the high positive correlation between the settling time and viscosity described earlier.

Figure 16 shows the effects of temperature on the settling times of the ternary butanol systems. In *n*-butanol/acetic acid/water (4:1:5) the settling times decline with an increase in temperature to 50°C reaching a minimum of 23 sec. An increase in the temperature further results in an increase of the settling times up to 65°C where the system forms a single phase. The increase of the settling times near the plait point is apparently caused by the extremely low interfacial tension and the small difference in density between the two phases. This anomaly can be corrected by reducing the amount of acetic acid in the solvent system as shown in the settling time curve obtained for *n*-butanol/acetic acid/water (9:1:10) which decreases to about 10 sec at 50°C.

Alternatively, the above problem may be solved by the addition of a salt in the aqueous solution. Figure 16B illustrates effects of salt concentration on the settling time vs. temperature curve in *n*-butanol/acetic acid/aqueous solution (4:1:5). At 0.1 *M* NaCl concentration, the solvent system still retains the anomalous zone although it has shifted about 15° toward the right on the temperature axis. Increase of the NaCl concentration to 1 *M* normalizes the settling time curve which declines to 15 sec at 50°C.

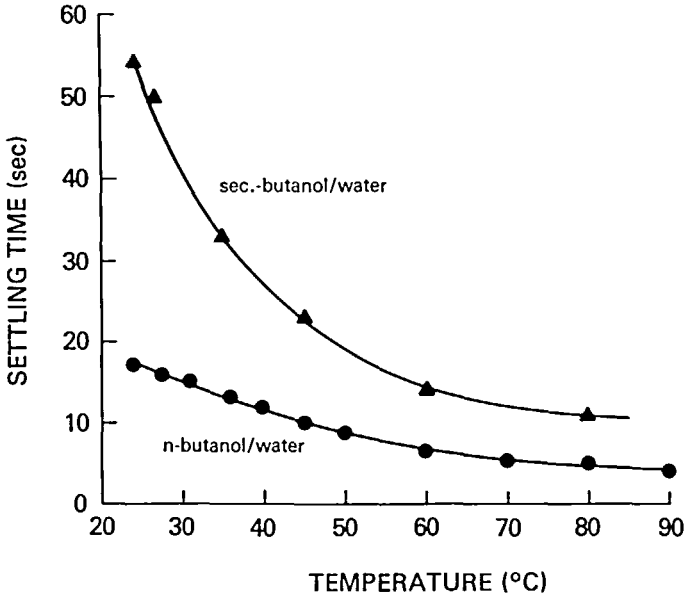

A

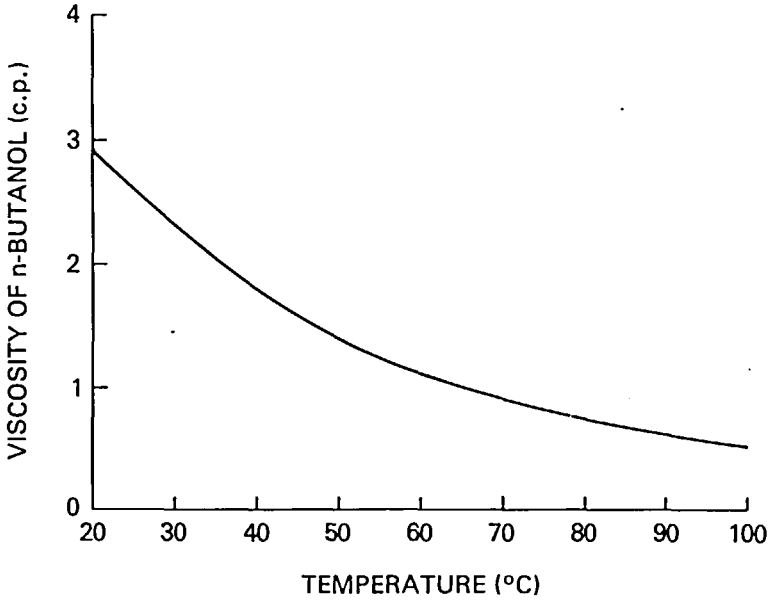

B

FIGURE 15. (A) Effects of temperature on the settling time of binary butanol systems. Circles for *n*-butanol/water and triangles for *sec.*-butanol/water. (B) Effects of temperature on the viscosity of *n*-butanol.

The above findings clearly indicate that at a higher temperature the hydrophilic solvent systems may display the normal hydrodynamic behavior observed in the hydrophobic and intermediate solvent systems, provided that the phase composition is kept away from the vicinity of the plait point. Raising the temperature slightly above room temperature may

Downloaded At: 15:26 17 January 2011

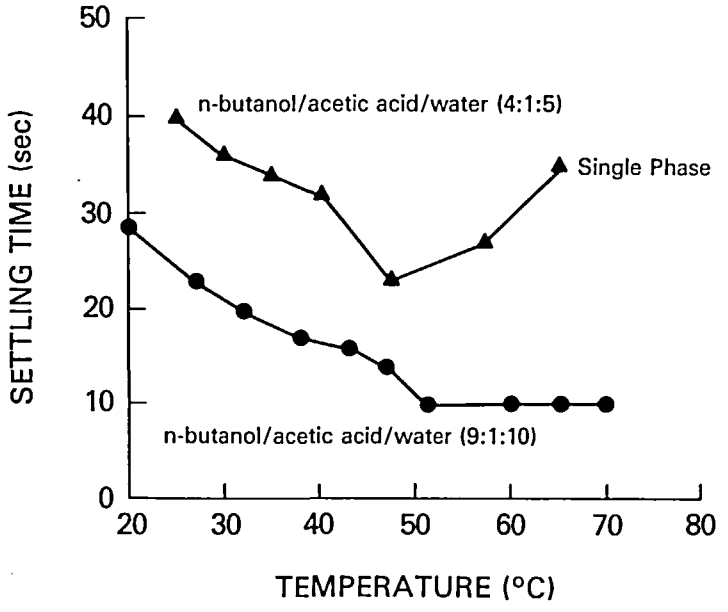

A

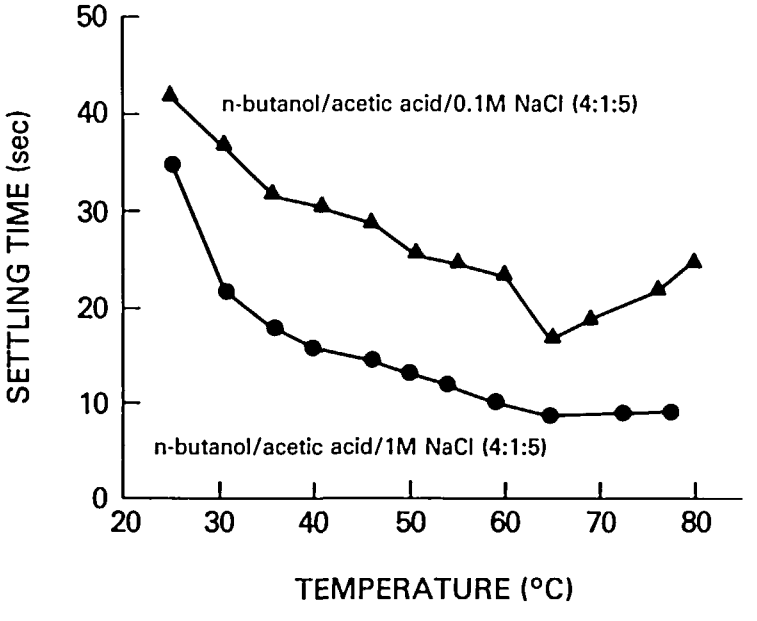

B

FIGURE 16. (A) Effects of temperature on the settling time of ternary *n*-butanol systems. Circles for *n*-butanol/acetic acid/water (9:1:10) and triangles for *n*-butanol/acetic acid/water (4:1:5). (B) Effects of temperature on the settling time of quadruple *n*-butanol systems containing NaCl. Circles for *n*-butanol/acetic acid/1 *M* NaCl (4:1:5) and triangles for *n*-butanol/acetic acid/0.1 *M* NaCl (4:1:5).

Downloaded At: 15:26 17 January 2011

also reduce the settling time of the intermediate solvent systems and therefore would improve the retention of stationary phase and increase partition efficiency during the separation.

Performing CCC at an elevated temperature will provide a number of beneficial effects including: (1) conversion of the hydrodynamic behavior of the hydrophilic solvent systems to the normal mode, (2) improved retention of the stationary phase resulting in higher peak resolution, (3) higher partition efficiency due to reduction of mass transfer resistance, (4) increased sample loading capacity due to higher solubility, (5) prevention of altered hydrodynamics at the column inlet when a highly concentrated sample is introduced with resultant loss of the stationary phase as described in the following section.

These expectations have been confirmed recently using a high-speed CCC apparatus equipped with a temperature-control system which has been constructed in our laboratory.

IV. APPARATUS AND APPLICATION

A. Design of the Apparatus

As described earlier in Section II, high-speed CCC is based on the Scheme IV synchronous planetary motion illustrated in Figure 4-IV. Figure 17A shows the design principle of the coil planet centrifuge for high-speed CCC in which the orientation of the centrifuge axis is horizontal. A large cylindrical coil holder coaxially holds a planetary gear which is coupled to an identical stationary sun gear (shaded) mounted on the central axis of the centrifuge. This gear arrangement produces a synchronous planetary motion to the coil holder; the holder revolves about the central axis of the apparatus and simultaneously rotates about its own axis at the same angular velocity in the same direction. In doing so, the holder maintains its position parallel to and at distance R from the central axis of the apparatus. This synchronous planetary motion of the holder prevents twisting the flow tubes as illustrated by successive positions of the planetary and sun gears during one complete revolution (Figure 17B).[23]

Downloaded At: 15:26 17 January 2011

The column is prepared by winding a piece of flexible plastic tubing, typically PTFE, around the holder. The column design may be classified into three categories: the single layer or short coil for extraction purposes, the long multilayer coil for high-speed CCC, and the column equipped with five flow channels for dual countercurrent operation.

Figure 18 shows a cross-sectional view of the coil planet centrifuge for countercurrent extraction.[35,36] The motor (Electro-Craft) drives the rotary frame around the horizontal stationary pipe (shaded) mounted on the axis of the centrifuge. The rotary frame consists of a pair of aluminum discs rigidly bridged together with multiple links (not shown in the figure) and holds a pair of rotary column holders in the symmetrical positions 10 cm away from the central axis of the centrifuge. The bottom holder has a diameter of 15 cm ($\beta = 0.75$) and the top holder of 10 cm ($\beta = 0.5$). The shaft of each holder is equipped with a plastic planetary gear which is coupled to an identical sun gear (shaded) mounted around the central stationary pipe. In order to provide mechanical stability, a short coupling pipe is coaxially mounted to the free end (right side) of the rotary frame while the other end of the coupling pipe is supported by a stationary wall member of the centrifuge through a ball bearing. The coiled column was made by winding the desired length of PTFE tube around one of the holders while a counterweight is applied on the other holder to balance the centrifuge. A pair of flow tubes from the coiled column is first passed through the center hole of the holder shaft and led through the side hole of the short coupling pipe to reach the opening of the central stationary pipe. These flow tubes are thoroughly lubricated with silicone grease and protected with a piece of plastic tubing at each supported portion to prevent direct contact with metal parts. The revolutional speed can be regulated up to 1000 rpm. The apparatus is a compact table-top model whose dimensions are about 16 × 16 × 17 in.

Figure 19 shows the original multilayer coil planet centrifuge modified from the above

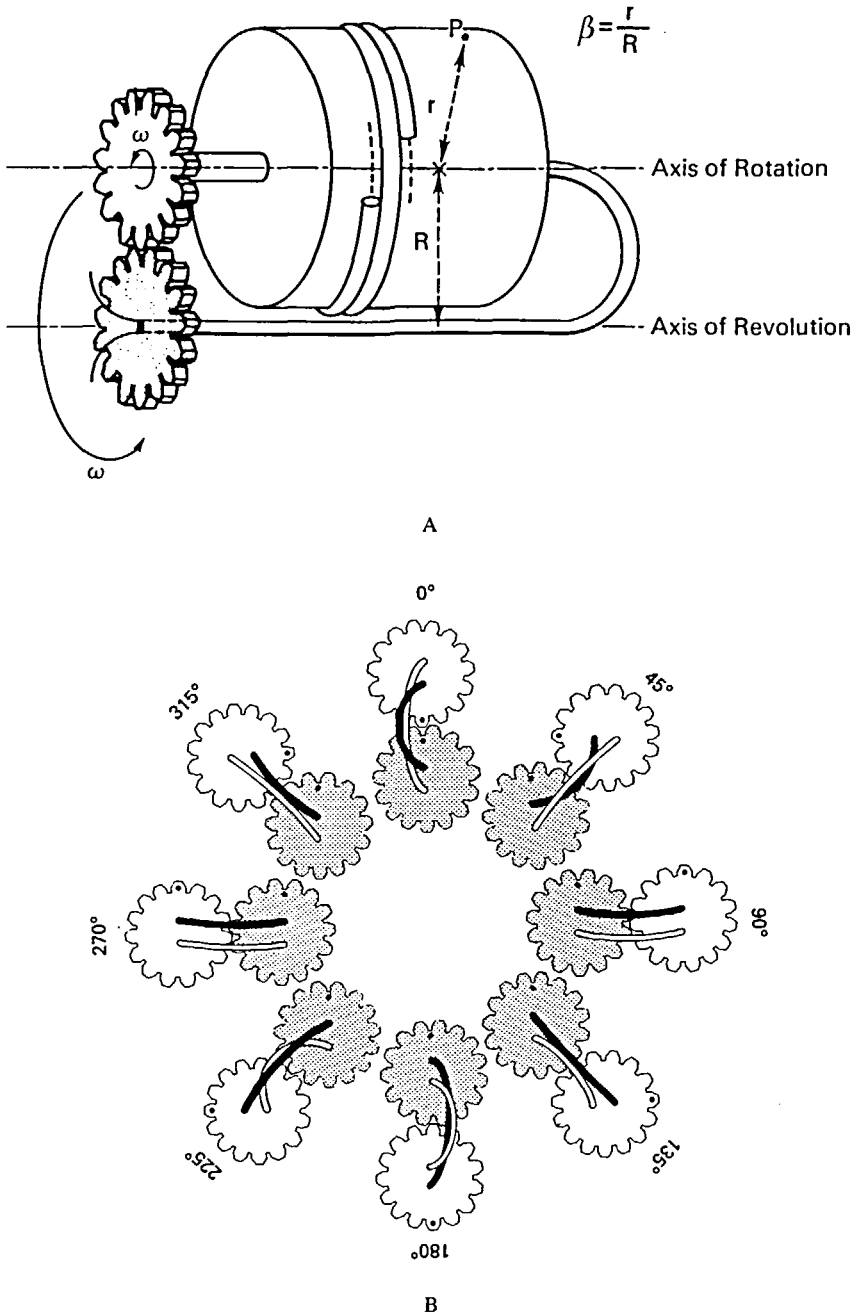

FIGURE 17. Design principle of the coil planet centrifuge for high-speed CCC. (A) Overall view of the design. (B) Successive gear positions during one revolution showing a twist-free mechanism.

model used for countercurrent extraction. In order to accomodate a long coiled column, a pair of flanges was mounted around the smaller holder to support multiple layers of coil. This apparatus has produced a rapid chromatographic separation of DNP amino acid samples.[32]

The partition efficiency of high-speed CCC was further increased by mounting a longer multilayer coil around a large spool-shaped holder as shown in Figure 20.[33] In order to facilitate the column preparation, the column holder was made removable from the rotary

Downloaded At: 15:26 17 January 2011

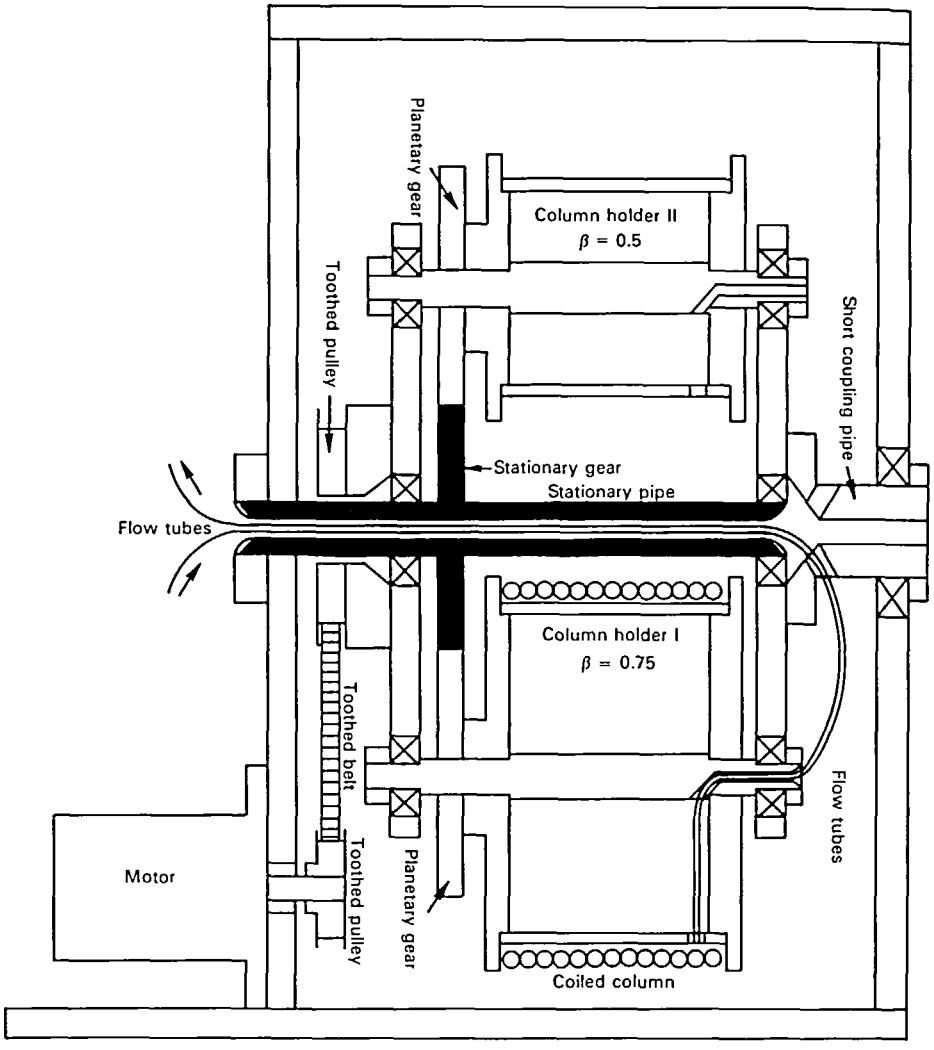

FIGURE 18. Cross-sectional view of a coil planet centrifuge for continuous extraction.

frame simply by loosening a pair of screws on each bearing block. Figure 21 shows the multilayer coil planet centrifuges constructed in our laboratory. A compact table top model of the coil planet centrifuge shown in Figure 21A has a multilayer coil consisting of a 130 m long, 1.6 mm i.d. PTFE tube with a total capacity of about 280 mℓ. Several hundred milligrams of samples can be loaded in each separation. Recently, a similar multilayer coil planet centrifuge became commercially available through P.C. Inc., Potomac, MD and also from Pharma-Tech Research Corp., Baltimore, MD. Figure 21B shows a bench top model of the coil planet centrifuge with 5.5 mm i.d. multilayer coil for large-scale preparative separations.[43]

Preparation of the multilayer coil requires caution to prevent dislocation of the column on the holder during the run. Because the holder is constantly subjected to a planetary motion, the resulting acceleration tends to rotate the column around the holder. This problem becomes serious when a large column is subjected to a high revolutional speed. In our laboratory the multilayer coil is prepared in the following manner with a satisfactory result: a sheet of emery cloth is glued around the holder core and the PTFE tubing is tightly wound over it between the two large flanges which provide boundaries for multilayer configuration.

Downloaded At: 15:26 17 January 2011

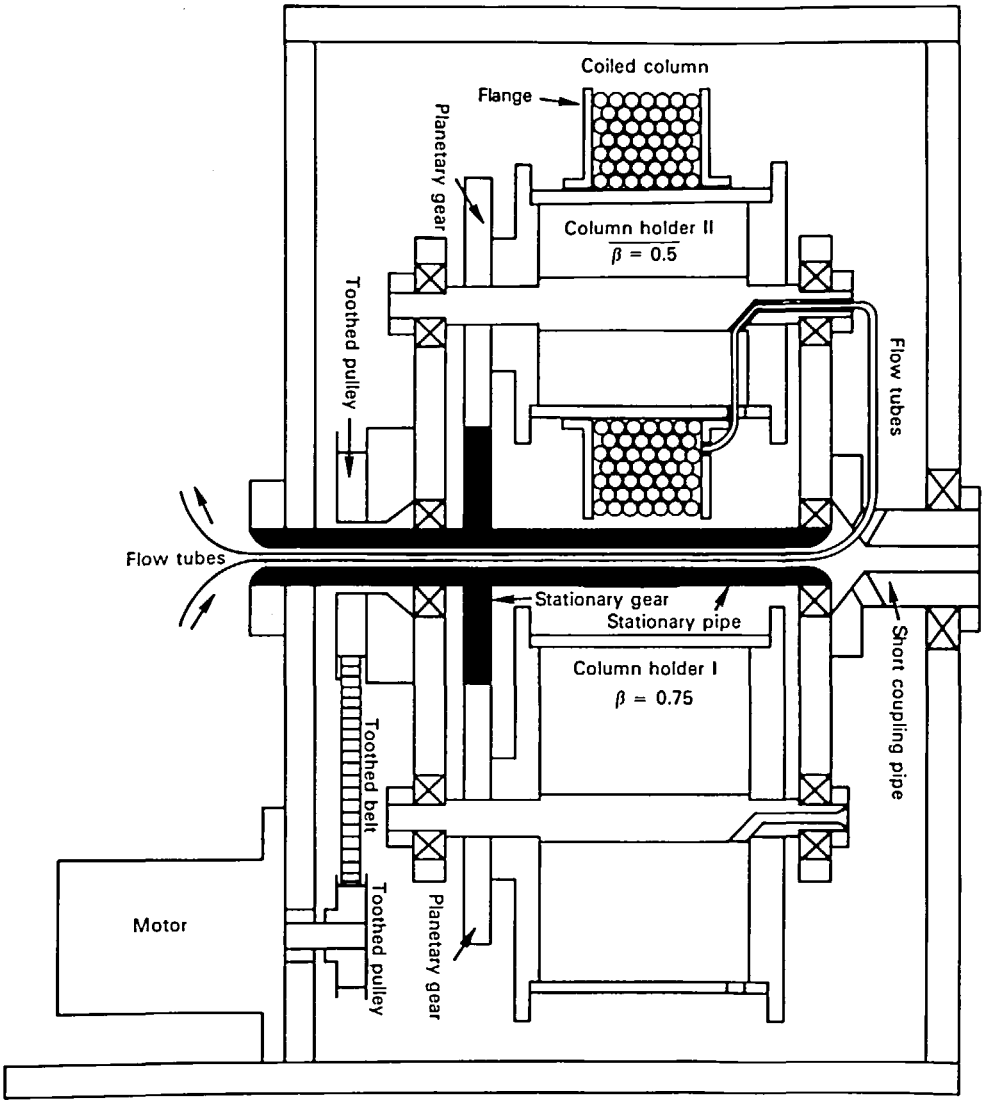

FIGURE 19. Cross-sectional view of a coil planet centrifuge with the original multilayer coil.

To prevent the movement of the column with respect to the holder, each layer of coil is attached to the flanges with a piece of fiberglass reinforced adhesive tape across the width of the coil. To further enhance greater stability, the same fiberglass tape is wrapped around the circumference of the coil. Around this layer of tape is wound a single piece of wire in which the ends are anchored to each flange. Around this wire another single layer of tape is wrapped, in effect, sandwiching the wire between the two layers of tape. This arrangement firmly anchors the multilayer coil to the holder.[44]

In addition to the above Scheme IV coil planet centrifuges, various studies have been performed with a combined horizontal flow-through coil planet centrifuge[24-26,45] which produces two different types of synchronous planetary motions, Schemes I and IV. The design principle of this centrifuge is illustrated in Figure 22. The top diagram labeled I to IV are identical to those in Figure 4 except that the centrifuge axis is placed in the horizontal position. Because of the symmetrical orientation of the column holders, Schemes I and IV can be conveniently paired in one apparatus as shown in the bottom diagram, while still

Downloaded At: 15:26 17 January 2011

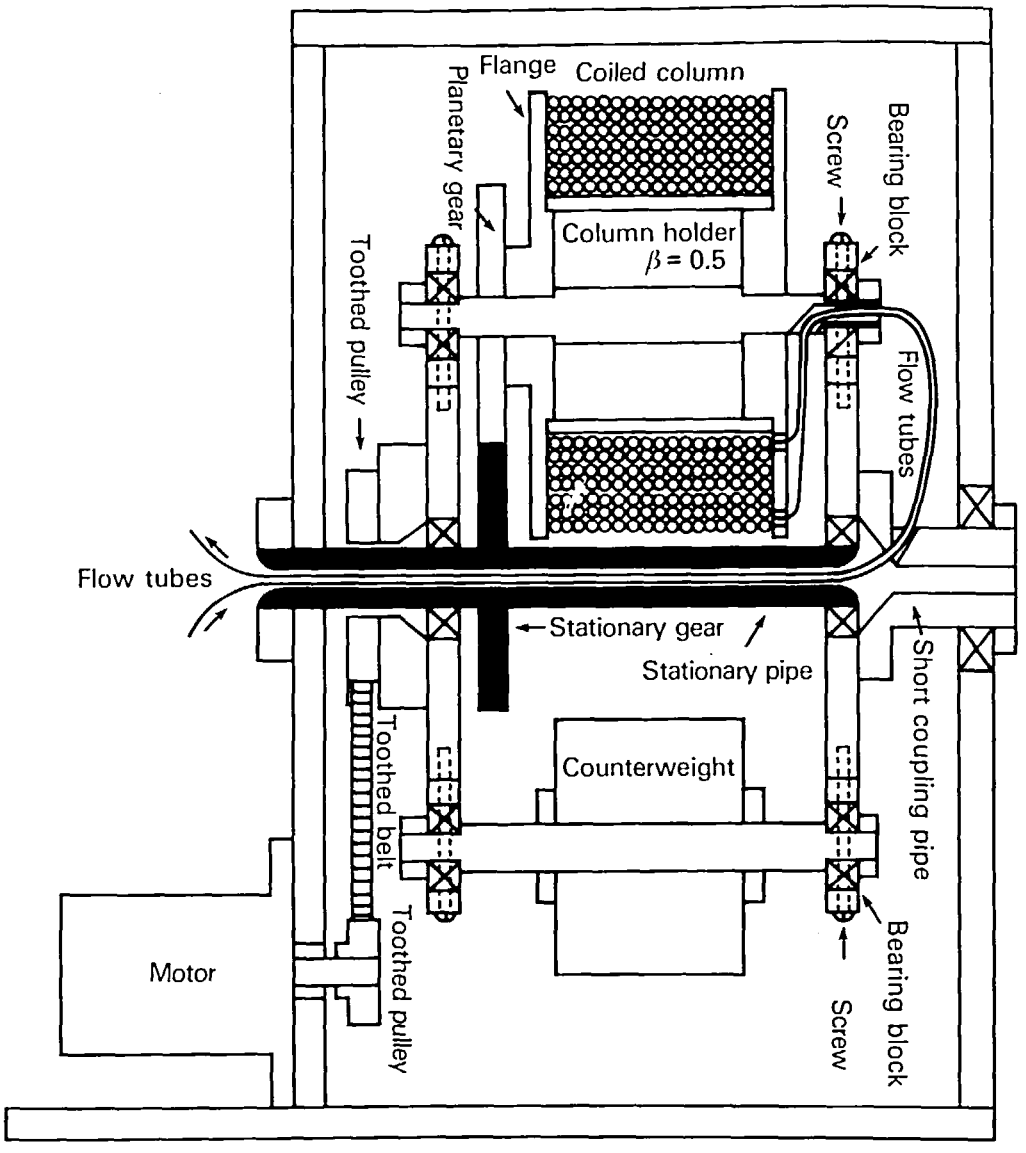

FIGURE 20. Cross-sectional view of a coil planet centrifuge with a large multilayer coil.

maintaining the antitwisting feature. The Scheme I synchronous planetary motion is produced by driving a timing pulley on the column holder with a toothed belt coupled to an identical stationary pulley on the central axis of the centrifuge. The Scheme IV synchronous planetary motion is produced by coupling a planetary gear on the column holder with an identical stationary sun gear on the central axis of the centrifuge. In the actual design, the use of countershafts provides a large revolutional radius without increasing the size of the gears.

Figure 23 illustrates a cross-sectional view through the central axis of the combined horizontal flow-through coil planet centrifuge. The motor (Bodine Electric Co., Chicago, IL) drives the rotary frame around the central stationary pipe (shaded) by a pair of toothed pulleys coupled with a toothed belt. To stabilize the centrifuge system, the other end of the rotary frame is coaxially connected to a short coupling pipe which is in turn supported by a ball bearing mounted in a stationary wall member of the centrifuge. The rotary frame

Downloaded At: 15:26 17 January 2011

Downloaded At: 15:26 17 January 2011

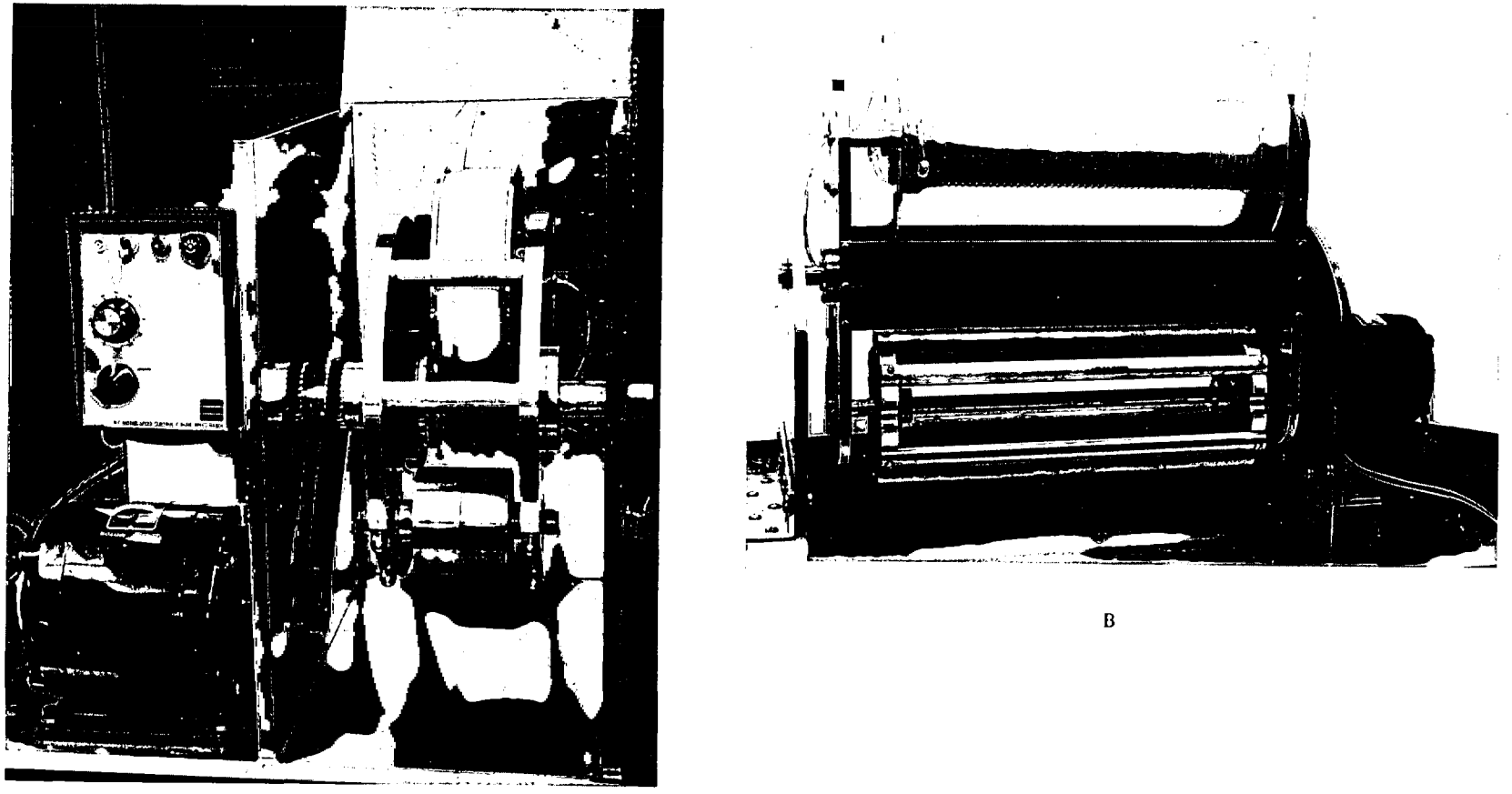

A B

FIGURE 21. Photograph of the apparatus. (A) Prototype of the coil planet centrifuge for high-speed CCC. (B) Coil planet centrifuge for large-scale preparative separations.

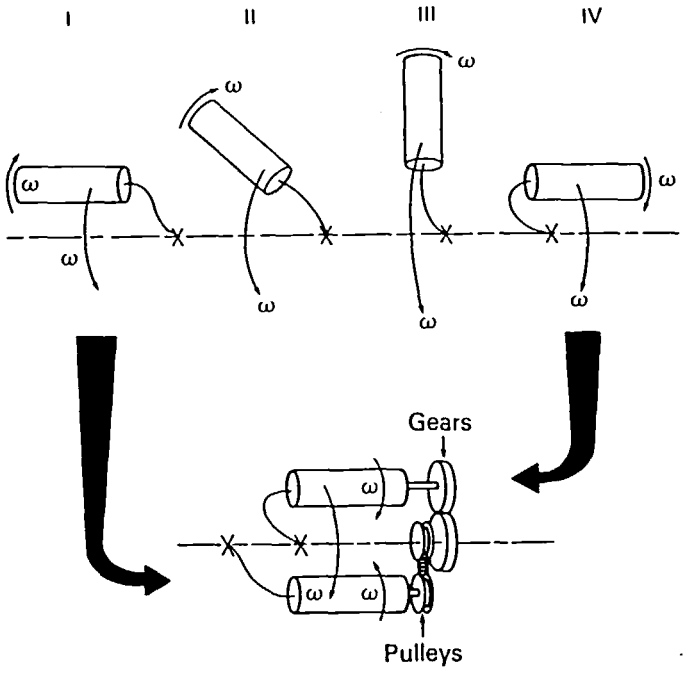

FIGURE 22. Design principle of the combined horizontal flow-through coil planet centrifuge.

holds column holders and countershafts on each side in symmetrical positions. On the lower side of the rotary frame (pulley-drive), a toothed pulley mounted on the central stationary pipe is coupled with a toothed belt to an identical pulley on the countershaft. This coupling produces synchronous counterrotation of the countershaft with respect to the rotary frame. This motion is conveyed to the column holder by a belt coupling a pair of identical toothed pulleys, one mounted on the countershaft and the other on the column holder shaft. Consequently, the column holder undergoes synchronous planetary motion identical to that of Scheme I illustrated in Figure 22. On the upper side of the rotary frame (gear-drive), the stationary gear mounted around the central stationary pipe is coupled to an identical gear on the countershaft to produce synchronous rotation of the countershaft with respect to the rotating frame. This motion is similarly conveyed to the holder by a belt and a pair of identical timing pulleys. The gear-driven column holder, then, rotates with respect to the rotary frame once about its own axis per each revolution of the rotary frame around the central axis of the centrifuge as in Scheme IV illustrated in Figure 22.

The column holder on each side is removable from the rotary frame and may be positioned at 15 or 20 cm from the axis of the centrifuge by selecting the respective bearing holes on the pair of bearing blocks. For each position of the holder the β value can be varied by changing the holder diameter up to a maximum β value of 0.5, as limited by the presence of the countershaft on each side of the rotary frame. The helical column was prepared by winding a piece of PTFE tubing directly onto the holder making multiple helical turns of uniform diameter. The flow tubes from the pulley-driven column holder (bottom) are first passed through the center hole of the holder shaft and then led through a side hole of the short coupling pipe to reach the stationary tube support as illustrated. The flow tubes from the gear-driven column holder (top) are similarly passed through the center hole of the holder shaft and then led through another side hole of the short coupling pipe to enter the opening of the central stationary pipe. Each pair of flow tubes is lubricated with silicone grease and

Downloaded At: 15:26 17 January 2011

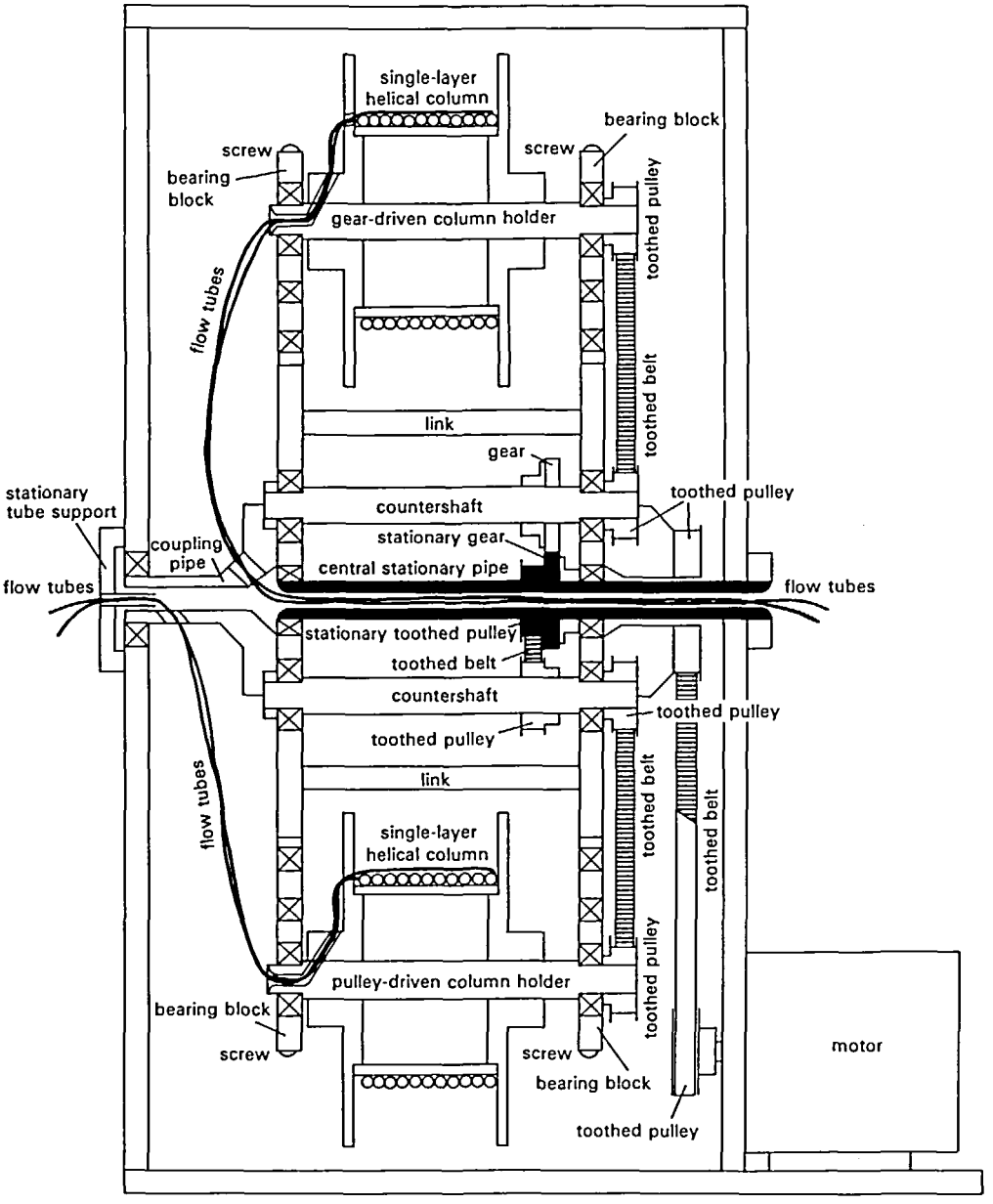

FIGURE 23. Cross-sectional view of the combined horizontal flow-through coil planet centrifuge.

the portions rotating with the frame are protected by a flexible plastic sheath to prevent abrasion by direct contact with metal parts. The revolutional speed of the apparatus is continuously adjustable up to 1000 rpm with a speed control unit.

B. Continuous Extraction

The unique capability of the present scheme to retain a large volume of the stationary phase in the column under efficient mixing with the mobile phase provides an ideal condition for performing continuous extraction. Because no solid support is used in the column, a minute amount of the sample can be recovered with minimum adsorption loss onto the liquid-solid interface.

Downloaded At: 15:26 17 January 2011

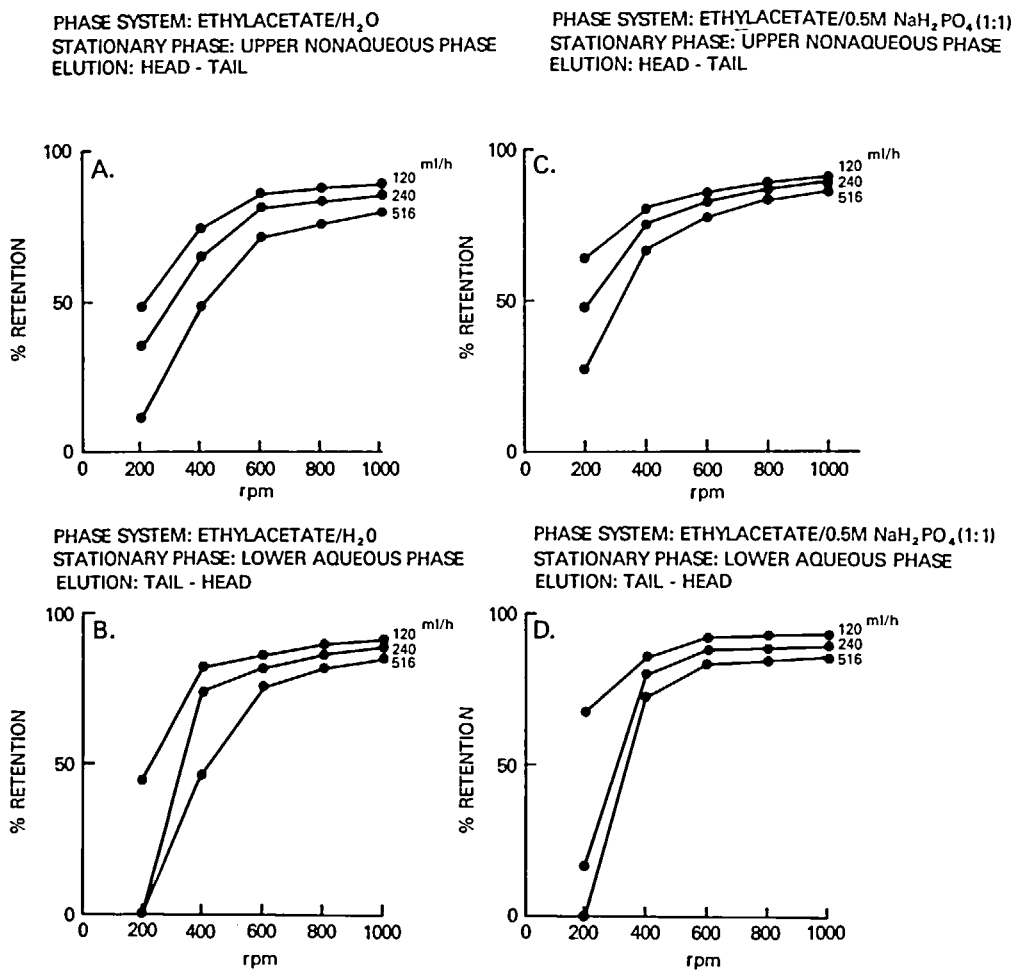

FIGURE 24. Phase distribution diagrams of ethyl acetate/aqueous systems in a helical column for continuous extraction.

1. Preliminary Studies[35]

a. Retention of the Stationary Phase

In the first series of experiments, the capability of the present scheme in retaining a large amount of stationary phase was demonstrated with a coiled column prepared from 2.5 m long, 2.6 mm i.d. PTFE tube which was coiled around the larger holder of the coil planet centrifuge illustrated in Figure 18. The column consisted of five helical turns at $\beta = 0.75$ and had a total capacity of about 15 mℓ. Typical two-phase solvent systems composed of ethyl acetate/water and ethyl acetate/0.5 *M* sodium phosphate (pH 4.4) at a volume ratio of 1:1 were selected.

In each operation, the coiled column and the free space in the flow path were entirely filled with the stationary phase and the mobile phase was pumped into the column in the proper direction (head-tail elution for the aqueous phase and tail-head elution for the nonaqueous phase) while the apparatus was run at a given revolutional speed. The eluate through the outlet of the column was pooled in a graduated cylinder to measure the volume of the stationary phase retained in the column. The experiments were performed under various revolutional speeds and flow rates using both nonaqueous and aqueous phases as the stationary phase.

The results of the retention studies are summarized in Figure 24 where the percentage

Downloaded At: 15:26 17 January 2011

retention of the stationary phase was plotted against the applied revolutional speeds. The three lines drawn in each diagram indicate the effects of the different flow rates applied. The flow rate of 516 mℓ/hr is the maximum rate available with the Beckman Accu-Flo Pump employed. The ideal retention level for extraction may be considered to be over 70% at or near the plateau of the curve, although much lower retention levels can be applied for extraction unless carryover of the stationary phase occurs. Figure 24A and B show the retention curves of the solvent system composed of ethyl acetate and water, where both nonaqueous (A) and aqueous (B) phases were used as the stationary phase. In both cases, the ideal retention levels are provided at the revolutional speed of over 600 rpm at all flow rates applied. Figure 24C and D show similar retention curves for the phase system composed of ethyl acetate/0.5 *M* NaH_2PO_4 (1:1). In both C and D, retention levels show much improvement over the previous phase system. Addition of salt to the phase system results in a greater density difference which promotes countercurrent movement of the two phases in the coil. The overall results indicate that the system provides excellent retention under a broad range of operational conditions for both aqueous and nonaqueous stationary phases. The results also suggest that much higher flow rates are applicable with high revolutional speeds.

Downloaded At: 15:26 17 January 2011

b. Continuous Extraction

The second series of experiments has been performed to demonstrate the capability of the present scheme to extract a solute present in a large volume of the mobile phase into a small volume of the stationary phase retained in the coiled column. This requires a set of conditions such that the solute must favor partition to the stationary phase. With commonly used extraction media such as an ethyl acetate/aqueous system, partition coefficients of various biological materials can be conveniently adjusted by modifying the pH and/or ionic strength of the aqueous phase to meet the above requirement. For the present studies, a pair of DNP-amino acids, N-DNP-L-leucine (DNP-leu) and delta-N-DNP-L-ornithine (DNP-orn), were selected as samples because they are readily observed through the column wall during the extraction process under stroboscopic illumination and also provide suitable partition coefficients for this present solvent system. The experiments were performed with the coiled column used in the previous retention studies. The overall experimental conditions in the following studies are summarized in Table 4.

A typical extraction procedure may be divided into three steps, i.e., extraction, cleaning, and collection. In each operation, the column was filled with the stationary phase and the mobile phase containing the sample was eluted through the column in the proper direction while the apparatus was run at 600 rpm. The extraction process was continued until 400 mℓ of the mobile phase was eluted. Then the mobile phase was replaced by the same phase but free of solute to wash the column contents. This cleaning process was continued until the additional 100 mℓ of the mobile phase was eluted. This would elute out all impurities having partition coefficients of 0.1 or greater. The sample extracted into the stationary phase in the coiled column was collected by eluting with the mobile phase in the opposite direction. This was done by switching the feed and return flow lines either by simply disconnecting the flow lines or the use of a four-way slide valve. The sample still remaining in the column was then washed out by eluting the column with the other phase originally used as the stationary phase.

The results were summarized in Table 4. In experiments 1 through 3 in Table 4, DNP-leu was dissolved in 400 mℓ of the aqueous phase at various concentrations and extracted into the nonaqueous phase retained in the column. The extracted sample was then cleaned by eluting the column with 100 mℓ of the clean aqueous phase and then collected from the column. The harvested stationary phase volume measured about 10 mℓ, containing over 90% of the original sample. A small amount of the sample still remaining in the column,

Downloaded At: 15:26 17 January 2011

Table 4
EXPERIMENTAL CONDITIONS AND RESULTS OF EXTRACTION

Exp. no	Solvent system	Mobile phase	Stationary phase	Sample (P.C.)*	Sample conc. in mobile phase	Extracted mobile phase vol.	Flow rate (direction)	RPM	Collected stationary phase vol.	Sample recovery
1	Ethylacetate 1 0.5 *M* NaH_2PO_4 2	Aqueous	Nonaqueous	DNP-leu (<0.01)	4 mg%	400 mℓ	516 mℓ/hr (head-tail)	600	10.5 mℓ	94%
2	Ethylacetate 1 0.5 *M* NaH_2PO_4 2	Aqueous	Nonaqueous	DNP-leu (<0.01)	0.4 mg%	400 mℓ	516 mℓ/hr (head-tail)	600	10.0 mℓ	97%
3	Ethylacetate 1 0.5 *M* NaH_2PO_4 2	Aqueous	Nonaqueous	DNP-leu (<0.01)	0.04 mg%	400 mℓ	516 mℓ/hr (head-tail)	600	10.4 mℓ	100%
4	Ethylacetate 2 0.5 *M* NaH_2PO_4 1	Nonaqueous	Aqueous	DNP-orn (<0.01)	0.4 mg%	400 mℓ	516 mℓ/hr (tail-head)	600	11.8 mℓ	97%
5	Ethylacetate 2 0.5 *M* NaH_2PO_4 1	Nonaqueous	Aqueous	DNP-orn (<0.01)	0.04 mg%	400 mℓ	516 mℓ/hr (tail-head)	600	11.8 mℓ	100%
6	Nonequilibrium system	5% Ethylacetate in 0.5 *M* NaH_2PO_4	Ethylacetate	DNP-leu (<0.01)	0.4 mg%	400 mℓ	516 mℓ/hr (head-tail)	600	6.1 mℓ	99%

* Partition coefficient is defined as solute concentration in the mobile phase divided by that in the stationary phase.

usually a few percent of the total, was conveniently recovered by eluting the column with several milliliters of the nonaqueous phase. The total sample recovery is always well over 90%, as shown in the table. The reduction of the sample concentration from 4 to 0.04 mg% somewhat improved the recovery rate, indicating that no significant sample loss occurs due to the adsorption effects and that further reduction of the sample concentration is feasible with high levels of recovery. The mode of elution that uses the nonaqueous phase as the stationary phase renders a great advantage in practical extraction in that the collected solvent is highly volatile and free of salts, facilitating further concentration. It also permits the stepwise or gradient elution of the sample by eluting the column with a modified aqueous phase to achieve further purification.

In experiments 4 and 5 in Table 4, the DNP-orn sample was dissolved in 400 mℓ of the mobile nonaqueous phase and extracted into the stationary aqueous phase by eluting the column from the tail toward the head. The retained aqueous phase in the column was then similarly cleaned with 100 mℓ of nonaqueous phase free of sample. The collected stationary aqueous phase measured about 12 mℓ in volume. This exceeds the volumes in experiments 1 through 3, as expected from the results of the retention studies. The sample still remaining in the column was eluted out with several milliliters of the aqueous phase. The sample recovery ranged over 95% with an improved figure at the reduced sample concentration as observed in the previous experiments.

Downloaded At: 15:26 17 January 2011

In practice, application of the method to aqueous crude extracts or physiological fluids requires a preliminary adjustment of the solvent composition to provide a suitable partition coefficient of the desired material for the applied pair of solvents. In this case preequilibration of the two phases is not essential. Experiment 6 in Table 4 shows an example of operation with such nonequilibrated solvents. The sample DNP-leu was first dissolved in 400 mℓ of 0.5 *M* NaH_2PO_4 aqueous solution containing ethyl acetate at 5%, which is slightly below the saturation level of about 7%. The column was filled with ethyl acetate followed by elution with the above sample solution. Both extraction and cleaning processes were performed as in other experiments. The sample solution collected from the column measured slightly over 6 mℓ. This depletion of the stationary phase apparently resulted from the use of the nonequilibrated solvent pair but without any effect on the sample recovery.

The overall results indicate a potential usefulness of the present method in processing a large amount of crude extracts or biological fluids in research laboratories. A small amount of the sample present in several hundred milliliters of the original solution can be enriched in 10 mℓ of the nonaqueous phase free of salt in 1 hr at a high recovery rate.

2. *Continuous Extraction of Urinary Drug Metabolites*[36]

In spite of the great potential of the present method demonstrated in the above preliminary studies, the application data so far published are limited to extraction of urinary metabolites of two anthracycline antitumor drugs, adriamycin (ADR), and daunorubicin (DNR) by Nakazawa et al.

a. Extraction Medium

Partition coefficients, defined as the ratio of the concetration of drug in the nonaqueous phase to that in the aqueous phase, were determined for ADR and DNR in biphasic solvent systems. Chloroform-isopropanol (3:1) mixture, ethyl acetate, and *n*-butanol were individually tested against 1.0 *M* solutions of various salts. Equal volumes of organic and aqueous phases were placed in a test tube, 100 nmol of drugs were added, and the tube was vigorously mixed for 30 sec. Quantities of drug in each phase were measured by fluorometry (SPF 125, American Instrument, excitation, 470 nm; emission, 585 nm).

The results are summarized in Tables 5A and 5B for ADR and DNR, respectively. In nearly all cases, partitioning of anthracyclines into *n*-butanol was greater than into either of

Table 5A
PARTITION COEFFICIENTS FOR ADRIAMYCIN

Salt	*n*-Butanol-water (1:1)	Chloroform-isopropanol-water (3:1:2)	Ethyl acetate-water (1:1)
None	2.1	2.3	0.1
$(NH_4)_2SO_4$	2.2	0.4	0.1
NaH_2PO_4	4.3	0.3	0.4
NH_4Cl	7.6	1.1	0.1
KCl	12.3	2.4	0.8
LiCl	10.0	1.8	0.7
CH_3COONH_4	10.1	4.1	0.4
NaCl	11.7	1.8	0.9
Na_2SO_4	10.8	7.7	0.1
Na_2HPO_4	> 40.0	—	> 1.2

Note: Adriamycin (100 nmol) was added to each 4.0-mℓ phase system. The concentration of aqueous salt solution was 1.0 *M* in all cases. The systems were vigorously mixed and allowed to equilibrate. Concentration of drug in each phase was measured by fluorometry, and partition coefficients were calculated as the ratio of the concentration in the nonaqueous phase to that in the aqueous phase. Insoluble salt crystals were noted in mixing 1.0 *M* Na_2HPO_4 with all nonaqueous phases, and no coefficient could be determined for the chloroform-isopropanol-Na_2HPO_4 system.

Table 5B
PARTITION COEFFICIENTS FOR DAUNORUBICIN

Salt	*n*-Butanol-water (1:1)	Chloroform-isopropanol-water (3:1:2)	Ethyl acetate-water (1:1)
None	2.7	3.2	0.1
$(NH_4)_2SO_4$	5.9	1.6	0.1
NaH_2PO_4	12.4	0.6	0.2
NH_4Cl	16.8	2.3	0.3
KCl	27.3	4.7	0.4
LiCl	20.9	4.4	0.3
CH_3COONH_4	21.6	12.1	1.3
NaCl	24.4	4.6	0.3
Na_2SO_4	36.3	12.5	0.6
Na_2HPO_4	> 85.5	—	> 6.9

Note: Experimental conditions were as described in Table 5A. Daunorubicin (100 nmol) was added to each system. Insoluble crystals of Na_2HPO_4 were encountered with all nonaqueous phases, and no coefficient could be determined for the chloroform-isopropanol-Na_2HPO_4 system.

the other two systems. Partition coefficients were higher for DNR compared to ADR in nearly every biphasic system tested, because ADR is more polar than DNR. The highest coefficients were obtained for the *n*-butanol/Na_2HPO_4 system at the 1.0 *M* Na_2HPO_4 concentration, although precipitation of salt crystals was noted. Partition coefficients for a range of Na_2HPO_4 concentrations were measured and a plateau was observed for concentrations greater than 0.4 *M*, while no crystal formation occurred at Na_2HPO_4 concentrations less than 0.4 *M*. Therefore, further studies utilized the *n*-butanol/0.3 *M* Na_2HPO_4 system. At this Na_2HPO_4 concentration, partition coefficients for ADR and DNR were 31 and 78, respectively.

Downloaded At: 15:26 17 January 2011

b. Extraction of Drug Metabolites

Extraction experiments were performed with a table top model of the coil planet centrifuge (Figure 18) equipped with a 60 mℓ-capacity column consisting of 18 helical turns of a 10 m long, 2.6 mm i.d. PTFE tube mounted around the 15 cm diameter holder ($\beta = 0.75$).

The column was filled with *n*-butanol (stationary phase), and was subjected to the Scheme IV planetary motion. The revolutional speed was 650 rpm. Disodium hydrogen phosphate (Na_2HPO_4) solution, 0.3 *M*, saturated with *n*-butanol, was pumped through the moving column to establish equilibrium conditions at 650 rpm. The stationary (butanol) phase volume was 32 mℓ. Prepared urine samples, 1-2 *l* in volume, were then pumped through the column at flow rates of 500 to 700 mℓ/hr, employing a metering pump.

Urine was collected from patients or normal volunteers for 24 hr during control periods, and patients for the first 24 to 48 hr following anthracycline chemotherapy. Sufficient Na_2HPO_4 to yield a concentration of 0.3 *M* was added to several liters of urine. Salted urines were filtered to remove precipitated material, and then saturated with *n*-butanol to prevent leaching of the column's stationary phase. In some cases, filtration of the urine after butanol saturation was necessary. To test the efficiency of the countercurrent centrifuge extraction, known quantities of ADR and DNR were added to control urines. These spiked samples were processed in an identical fashion to post therapy urines. After each sample was chromatographed, the column was cleaned by elution with 100 mℓ of aqueous, *n*-butanol-saturated 0.3 *M* Na_2HPO_4. The *n*-butanol phase was drained from the column; several milliliters of *n*-butanol were passed through the column to recover any remaining sample. The *n*-butanol extracts were combined and evaporated to dryness by flash evaporation. The deep-red residue remaining after drying was redissolved in methanol. Aliquots of prechromatography urine, column eluate (mobile phase), and the final extract from the column in methanol were analyzed for anthracycline content by fluorescence. A small volume of the aliquot was added to 2 mℓ of 1.8 *M* hydrochloric acid-ethanol (1:3), and concentration determined against known ADR standards in an Aminco-Bowman® spectrophotofluorometer.

Figure 25 shows the experimental results of DNR extraction. The top chromatogram (A) was obtained from a reversed phase HPLC analysis of the urine from a cancer patient who has received DNR. Only two anthracycline species, D_1 and D_2, were detected. The bottom chromatogram (B) was similarly obtained from HPLC analysis of the same urine sample after extraction with the coil planet centrifuge method. It shows enriched D_1 and D_2 peaks and three previously undetectable metabolite peaks, dD_3, demethyl-dD_3 and 4-*O*-glucuronide. Figure 26 shows a similar enrichment obtained for ADR and its metabolites, where relatively greater amounts of interfering materials were recovered due to the higher polarity of ADR.

Comparative studies revealed that the standard method with an XAD-2-resin yielded more efficient extraction of ADR than did the coil planet centrifuge, from spiked samples, but the methods were equivalent in their recoveries of the less polar DNR. The reverse was seen in the case of treated patients' urine, with about 50% improvement in recovery of ADR and metabolites using the coil planet centrifuge. This difference may have been due to altered partitioning of drug metabolites between the two phases, compared to parent drug. In particular, aglycone metabolites would be expected to distribute well into the *n*-butanol phase. Both TLC and reversed-phase HPLC confirmed that the coil planet centrifuge allowed recovery of relatively greater quantities of aglycones from urine than the XAD-2 column for ADR (60% aglycones with coil planet centrifuge vs. 12% with XAD-2 column) and DNR (48% aglycones vs. 6%).

C. Preparative CCC

Among a variety of existing CCC methods, a high-speed CCC produces the most efficient preparative separations which are comparable to those achieved by preparative-scale HPLC.

Downloaded At: 15:26 17 January 2011

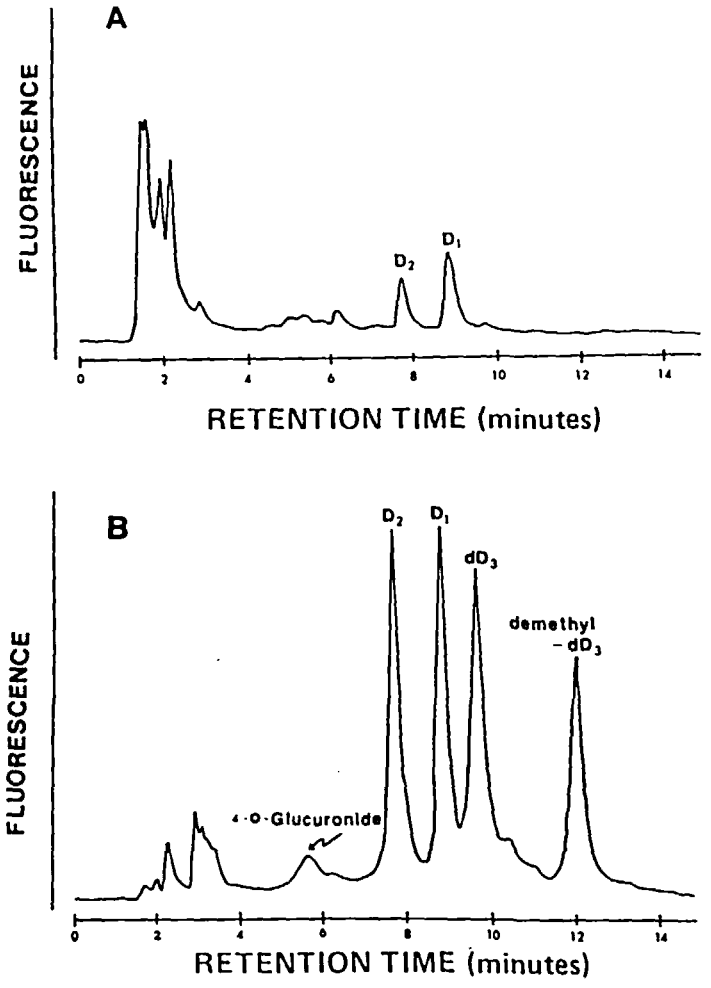

FIGURE 25. Daunorubicin extraction from urine. (A) HPLC analysis of the urine sample before extraction. The early eluate contained considerable amount of interfering materials. Only two anthracycline species, DNR (D_1) and 13-OH-DNR (D_2), were identifiable. (B) HPLC analysis of the same urine sample after extraction with the coil planet centrifuge. The early interfering materials were largely excluded from the extract. Sharp, enriched peaks for D_1 and D_2 were evident, and three previously undetectable metabolites of DNR-1 conjugated species and two aglycones, dD_3 and demethyl-D_3, were made apparent.

1. Two-Phase Solvent System

As in other chromatographic methods, selection of a suitable solvent system is the key to the successful separation in high-speed CCC. The selection of the solvent system in high-speed CCC should be focused on the following points:

1. No decomposition or denaturation of the sample
2. Sufficient sample solubility
3. Suitable partition coefficient values
4. Satisfactory retention of the stationary phase

a. Partition Coefficient

The partition coefficient (PC) is defined here as solute concentration in the stationary

Downloaded At: 15:26 17 January 2011

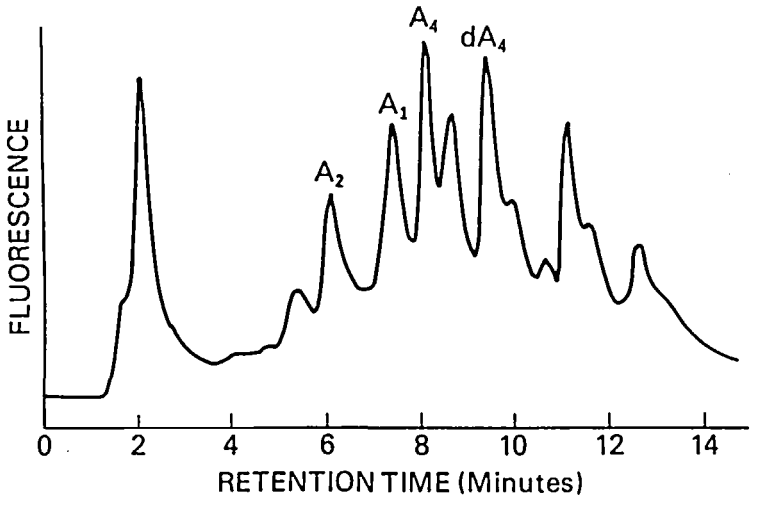

FIGURE 26. Adriamycin extraction from urine by the coil planet centrifuge. HPLC analysis showed enriched adriamycin (A_1) and three metabolites (A_2, A_4, and dA_4).

Downloaded At: 15:26 17 January 2011

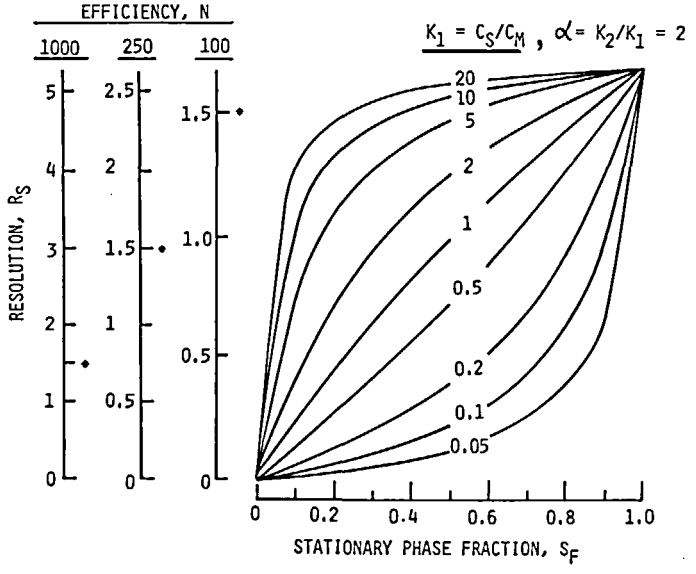

FIGURE 27. Predicted resolution as a function of stationary phase fraction, S_F, the partition coefficient of the first-eluted solute, K_1, and a constant separation factor, α, of 2, for columns containing 100, 250, or 1000 theoretical plates, N. Baseline resolution, R_s = 1.5, is indicated by an asterisk. K is expressed as concentration in stationary phase divided by concentration in mobile phase. The diagram was derived from the equation:

$$R_S = {}^1/_2\sqrt{N}\,(\alpha\text{-}1)/[(\alpha + 1) + 2(1\text{-}S_F)/K_1S_F].$$

phase (Cs) divided by that in the mobile phase (Cm) or K = Cs/Cm. The PC value is accurately determined by a simple test-tube experiment with a pure compound or the standard.[46] When the standard is not available, the PC of each component in a crude sample mixture can be accurately determined by HPLC analysis on each layer of the two-phase solvent system equilibrated with the sample mixture.[47] As reported elsewhere,[48] the optimum PC values in CCC depend upon the retention of the stationary phase in the column (Figure 27).

When the retention of the stationary phase substantially exceeds 0.5 or 50% of the total column capacity, rapid and efficient separations can be attained by adjusting the PC at between 1 and 0.5. When the stationary phase retention becomes lower than 0.5, the peak resolution is effectively improved by increasing the PC values at a range between 1 and 2. Since the present method usually permits either upper or lower phase to be the mobile phase, the PC values between 2 and 0.5 will produce excellent results.

Once the PC (K) of the solute is determined, the retention volume (R) or the peak location on the chromatogram is predicted from the following equation:

$$R = (V_C - R_{SF})\,K + R_{SF} \tag{10}$$

where V_C is the total column capacity and R_{SF}, the retention volume of the solvent front. From the above equation, it is apparent that the solute with $K = 1$ is always eluted at $R = V_C$ or the elution volume equal to the total column capacity, regardless of the position of the solvent front. The solutes with $K < 1$ and $K > 1$ are eluted earlier and later than V_C, respectively. When no stationary phase is retained in the column ($R_{SF} = V_C$), all components would be eluted together at V_C. The PC value (K) of each component on the chromatogram can also be determined from a modified equation:[49]

$$K = (R - R_{SF})/(V_C - R_{SF}) \tag{11}$$

b. Search for the Solvent System

Various solvent systems which have been successfully used in CCC were listed in Tables 6 to 9. When the nature of the aimed compound is unknown or the previous work on the similar compounds is not found, the search for the suitable solvent systems must rely on a tedious trial and error method. However, one may save a considerable amount of time and labor by making a systematic search such as the following: the search may be initiated with a moderately hydrophobic solvent system such as chloroform/methanol/water (4:4:3) which is extensively used in droplet CCC. If the sample is partially distributed into both phases, the further adjustment of the PC may be effected by changing the amount of methanol or substituting acetic acid for methanol, etc. If the sample is unilaterally distributed to the lower nonaqueous phase, the solvent system requires a higher hydrophobicity. In this case, hexane/ethyl acetate/methanol/water (1:1:1:1) will improve the PC value. The hydrophobicity of this solvent system is conveniently modified by changing the volume ratio between hexane and ethyl acetate while the volumes of methanol and water are unaltered. For example, the above ratio is shifted to 0.8:1.2:1:1, if the sample is excessively partitioned into the lower aqueous phase, and to 1.2:0.8:1:1, if the sample is mostly partitioned to the upper nonaqueous phase. This process may be continued until the desired PC value is attained. When the chloroform system initially distributes the sample almost entirely into the upper aqueous phase, a hydrophilic solvent system such as *n*-butanol/water may be the choice. The adjustment of the PC in this system may be carried out by adding small amounts of acids (acetic acid, dichloroacetic acid, trifluoroacetic acid, etc.) or salts (phosphate buffer, ammonium acetate, sodium chloride, etc.) to the solvent system. These additions usually move polar samples such as peptides from the lower aqueous phase to the upper nonaqueous phase.

Evaluation of each solvent system may be conveniently carried out by the TLC screening test[12] (Figure 28) which has been recommended by Hostettmann for droplet CCC. The method has been found to be useful in selecting solvents for centrifugal CCC separation of synthetic peptides.[50]

In the course of a solvent search, care should be taken to avoid the use of solvent composition at the vicinity of the plait point where the solvent mixture forms a single phase. Such solvent systems possess low interfacial tension and a small difference in density between

Downloaded At: 15:26 17 January 2011

Downloaded At: 15:26 17 January 2011

Table 6
APPLICATIONS OF HIGH-SPEED CCC

Substance*	Solvent system*	Volume ratio	Remarks	Ref.
Insecticides: Demeton O and S	Pen/EtOH/H_2O	6:5:1	S = P-O & O = P-S isomers	54
Herbicides: S-Triazines	Hex/EtOAc/MeOH/H_2O	8:2:5:5	Mass spec analysis	55
Plant hormones: Auxins	Hex/EtOAc/MeOH/H_2O	3:7:5:5		56
IAA & ABA	$CHCl_3$/HOAc/H_2O	2:2:1		56
Antibiotics: Siderocheline A	$CHCl_3$/MeOH/H_2O	7:13:8		57
Efrotomycin	CCl_4/$CHCl_3$/MeOH/H_2O	5:5:6:4		57
Pentalenolactone	$CHCl_3$/MeOH/H_2O	1:1:1		57
Bu 2313 B	Hex/CH_2Cl_2/MeOH/H_2O	5:1:1:1		57
A 201 E	CCl_4/$CHCl_3$/MeOH/H_2O	2:5:5:5		57
Tirandamycin A and B	Hex/EtOAc/MeOH/H_2O	70:30:15:6		57
Steroids: Hydrocortisone	CH_2Cl_2/Hex/MeOH/H_2O	40:10:17:8		58
1,2-Dihydrotriamcinolone	CH_2Cl_2/MeOH/H_2O	40:13:7		58
6-Methylprednisolone derivative	CH_2Cl_2/Bu_3N/HCOOH/H_2O	5000:24:5:1000		58
Acetophenone, *o*-Nitrophenol, *p*-Nitrophenol, & Phenol	$CHCl_3$/MeOH/H_2O	3:1:3	For HSCCC/FT-IR	59
Pigments: Methyl Violet 2B	$CHCl_3$/HOAc/H_2O	2:2:1	Mass spec analysis	60
DNP Amino acids	$CHCl_3$/HOAc/0.1 N HCl	2:2:1	Standard test system	32, 33, 44
Purines & Pyrimidines	*n*-BuOH/1 *M* PO_4 (K,pH 6.5)	1:1		33
Tannins	*n*-BuOH/0.1 *M* NaCl	1:1	Poor resolution with HPLC	61
	n-BuOH/1 m *M* phytic acid in 0.1 *M* NaCl (pH 4.0)	1:1		61
Peptides: Dipeptides	*n*-BuOH/HOAc/H_2O	4:1:5	Reversed elution mode	62
	n-BuOH/DCA/0.1 *M* NH_4CO_2H	100:1:100 → 100:0:100	Gradient elution	33
Gramicidins	$CHCl_3$/Ben/MeOH/H_2O	15:15:23:7		33
Cholecystokinin fragment	*n*-BuOH/0.2 *M* NH_4OAc	1:1	at 50°C	52
Bombesin	*n*-BuOH/DCA/H_2O	100:1:100	at 45° to 50°C	53
Bovine insulin	*sec.*-BuOH/DCA/H_2O	200:1:200	at 50°C	62

*Abbreviations: ABA, abscisic acid; Ben, benzene; Bu_3N, tributylamine; BuOH, butanol; DCA, dichloroacetic acid; EtOAc, ethyl acetate; EtOH, ethanol; Hex, *n*-hexane; HOAc, acetic acid; IAA, indole-3-acetic acid: MeOH, methanol; NH_4OAc, ammonium acetate; Pen, *n*-pentane.

Table 7
COMPOUNDS SEPARATED BY DCCC AND SOLVENT SYSTEMS[63]

Separated compounds	Solvent systems
Saponins (spirostanol glycosides)	$CHCl_3$-MeOH-H_2O (7:13:8)
Saponins (triterpenoid glycosides)	$CHCl_3$-MeOH-H_2O (7:13:8)
	$CHCl_3$-MeOH-H_2O (5:6:4)
	$CHCl_3$-MeOH-*n*-PrOH-H_2O (9:12:1:8)
	$CHCl_3$-C_6H_6-EtOAc-MeOH-H_2O (45:2:3:60:40)
Saponins (ginsenosides)	$CHCl_3$-MeOH-*n*-PrOH-H_2O (45:60:6:40)
	$CHCl_3$-MeOH-iso-PrOH-H_2O (5:6:1:4)
	$CHCl_3$-MeOH-*n*-PrOH-H_2O (4:6:1:4)
Flavonoid glycosides	$CHCl_3$-MeOH-H_2O (7:13:8)
	$CHCl_3$-MeOH-H_2O (5:6:4)
	$CHCl_3$-MeOH-H_2O (4:4:3)
	$CHCl_3$-MeOH-*n*-PrOH-H_2O (5:6:1:4)
	$CHCl_3$-MeOH-*n*-BuOH-H_2O (10:10:1:6)
	n-BuOH-AcOH-H_2O (4:1:5)
Isoflavone glycosides	$CHCl_3$-MeOH-H_2O (7:13:8)
Anthraquinone glycosides	$CHCl_3$-MeOH-H_2O (5:5:3)
	$CHCl_3$-MeOH-*n*-PrOH-H_2O (9:12:1:8)
	n-BuOH-acetone-H_2O (33:10:50)
Chromenes, lignans	$CHCl_3$-MeOH-H_2O (5:6:4)
	$CHCl_3$-MeOH-H_2O (4:4:3)
Xanthones	$CHCl_3$-MeOH-H_2O (13:7:4)
	$CHCl_3$-MeOH-*n*-PrOH-H_2O (9:12:1:8)
Cardenolides	$CHCl_3$-MeOH-H_2O (5:6:4)
	$CHCl_3$-MeOH-H_2O (5:10:6)
	$CHCl_3$-MeOH-H_2O (5:9:7)
Iridoid glycosides	$CHCl_3$-MeOH-H_2O (43:37:20)
	$CHCl_3$-MeOH-H_2O (5:5:3)
Secoiridoid glycosides	$CHCl_3$-MeOH-*n*-PrOH-H_2O (9:12:1:8)
Terpenoids (diterpenes)	$CHCl_3$-MeOH-H_2O (7:13:8)
Terpenoids (gibberellins)	$CHCl_3$-MeOH-H_2O (5:5:3)
Terpenoid glycosides	$CHCl_3$-MeOH-H_2O (7:13:8)
Alkaloids	$CHCl_3$-MeOH-H_2O (13:7:8)
	$CHCl_3$-MeOH-H_2O (5:5:3)
	$CHCl_3$-MeOH-5% HCl (5:5:3)
	C_6H_6-$CHCl_3$-MeOH-H_2O (5:5:7:2)
	$CHCl_3$-MeOH-*n*-PrOH-H_2O (45:60:2:40)

the two phases which would adversely affect the retention of the stationary phase as described in Section III.D.

2. Sample Solution Preparation

Preparation of sample solution requires some considerations on several factors which would affect the partition efficiency. In order to maintain the normal phase composition, samples should be dissolved in the solvents, upper and/or lower phases, to be used for the separation. The maximum concentration of solutes in the sample solution, effectively applied to the column, may be limited by several factors such as solubility, nonlinear isotherm and alteration of the two-phase composition. The nonlinear isotherm produces skewed peaks causing a loss of peak resolution, while the altered phase composition results in decrease

Downloaded At: 15:26 17 January 2011

Downloaded At: 15:26 17 January 2011

Table 8
APPLICATIONS OF CENTRIFUGAL CCC OTHER THAN HSCCC

Substance[a]	Solvent system[b] (volume ratio)	Apparatus[c]
Prostaglandins	$CHCl_3$/HOAc/H_2O (2:2:1)	CHCPC[49]
Catecholamine metabolites	EtOAc/10%HOAc, 5% NaCl (1:1)	ACPC[20]
Urinary VMA & HVA	EtOAC/10%HOAc, 5% NaCl (1:1)	ACPC[20], VCPC[64]
S-Triazines	Hex/EtOAc/MeOH/H_2O (8:2:1:1)	HCPC[56]
Parathion-ethyl & p-Nitrophenol	CCl_4/H_2O	HCPC[65]
Plant hormones		
Indole auxins	Hex/EtOAc/MeOH/H_2O (3:7:5:5)	TCPC[66,58]
Indole auxins & ABA	$CHCl_3$/HOAc/H_2O (2:2:1)	TCPC[66,58] RC[58]
Gibberellins	Et_2O/MeOH/0.5 *M* PO_4 (pH 5.9) (3:1:2)	TCPC[66]
Cytokinins	EtOAc/MeOH/0.5 *M* PO_4 (pH 7) (3:1:3)	TCPC[66]
Antitumor drugs		
Daunorubicin derivatives	$CHCl_3$/DCE/Hex/MeOH/H_2O (2:2:2:7:2)	CHCPC[67]
Diaziquone	DCE/MeOH/10 mM Maleate (Na, pH 6.1) (3:3:1)	CHCPC[68]
	DCE/MeOH/10 m*M* PO_4 (Na, pH 6.1) (3:3:1)	CHCPC[68]
	$CHCl_3$/Ethylene glycol	CHCPC[68]
	Hex/EtOAc/NO_2CH_3/MeOH (8:2:2:3)	CHCPC[68]
Antibiotics		
Candicidin, levorin, trichomycin & hemycin	$CHCl_3$/MeOH/Borate buffer (pH 8.2) (4:4:3)	VCPC[69]
Echinomycin & triostin A	TCE/MeOH/H_2O (7:3:1)	VCPC[70]
Quinomycin C & echinomycin	Hep/EtOAc/ $(CH_3)_2CO$/H_2O (1:1:3:1)	VCPC[70]
Aureomycin & terramycin	*n*-BuOH/0.01*N* HCl (1:1)	HCPC[65]
Tetracycline	CH_3NO_3/$CHCl_3$/Pyridine/0.1 *M* EDTA (pH 7) (20:10:3:33)	HCPC[65]
Trichomycin	$CHCl_3$/MeOH/Borate buffer (4:4:3)	HCPC[65]
Globoroseamycin	$CHCl_3$/MeOH/Borate buffer (4:4:3)	HCPC[65]
Nystatin	$CHCl_3$/MeOH/Borate buffer (2:4:3)	HCPC[65]
Erythromycin	Methyl-isobutyl-ketone/Acetone/ 0.2 *M* Phosphate-citrate buffer (pH 6.5) (20:1:21)	HCPC[65]
Kangdisu & colistin E	*n*-BuOH/2% DCA, 5% NaCl (6:7)	HCPC[65]
Medicinal herbs		
Quercetin & rutin	EtOAc/EtOH/0.07 *M* NaOH (2:1:2)	HCPC[65]

Downloaded At: 15:26 17 January 2011

Squalidine & platyphilline	$CHCl_3$/0.07 *M* PO_4 (pH 6.2) (1:1)	HCPC[65]
Scopolamine, hyoscyamine, & nor-hyoscyamine	$CHCl_3$/0.07 M PO_4 (pH 6.5) (1:1)	HCPC[65]
Scopolamine, anisodine, & 8-isopropyl-scopolamine	$CHCl_3$/0.07 M PO_4 (pH 6.3) (1:1)	HCPC[65]
Saponins	$CHCl_3/C_6H_6$/HOAc/MeOH/H_2O (45:2:3:60:40)	CDCCC[71]
Sugars		
Sucrose, glucose, & fucose	*n*-BuOH/EtOH/H_2O (4:1:4)	CDCCC[71]
Fatty Acids	Hep/MeOH/HOAc (1:1:1)	CDCCC[71]
P-Nitrophenol conjugates	EtOAc/0.5-1.0 *M* KH_2PO_4 (5:1) (EtOAc presaturated with water)	CHCPC[46]
Purines & pyrimidines	*n*-BuOH/1 M PO_4 (K, pH 6.5) (1:1)	ACPC[20]
Heparin	1%HPC in *n*-BuOH/aqueous NaCl gradient	RC[72]
Pigments	IsoAmOH/EtOH/HOAc/H_2O (4:2:1:5)	CPC[73]
DNP amino acids	$CHCl_3$/HOAc/0.1 *N* HCl (2:2:1)	RC[15,37,74,75,76]
		TCPC[25,27,28]
		CHCPC[15,25,45,77,78]
		HCPC[22,23]
		ACPC[20]
		EC[21]
		VCPC[2,18,19]
		TCC[2,17,79]
		CDCCC[71]
Dipeptides	*n*-BuOH/HOAc/H_2O (4:1:5)	VCPC[19], TCPC[28] ACPC[20], HCPC[23] RC[75] CHCPC[15,25,77,78]
	n-BuOH/DCA/NH_4COOH (100:1:100)→(100:0:100) DCA gradient	VCPC[19], ACPC[20]
Gramicidins	$CHCl_3/C_6H_6$/MeOH/H_2O (15:15:23:7)	CHCPC[4,78]
Synthetic peptides		
5,6,9, & 15 amino acid peptides	*n*-BuOH/HOAc/H_2O (4:1:5)	CHCPC[26,77,80]
Des-enkephalin γ-endorphin (12 amino acids)	*n*-BuOH/0.1% TFA (1:1)	CHCPC[81]
Cholecystokinin fragments (4 to 8 amino acids)	*n*-BuOH/HOAc/H_2O (4:1:5)	CHCPC[50]
	n-BuOH/0.2 to 0.5 *M* NH_4OAc (1:1)	CHCPC[50]
Sulfated cholecystokinin fragments	*n*-BuOH/0.1% TFA (1:1)	CHCPC[50]
	n-BuOH/0.2 to 0.5 *M* NH_4OAc (1:1)	CHCPC[50]

Downloaded At: 15:26 17 January 2011

Table 8 (continued)
APPLICATIONS OF CENTRIFUGAL CCC OTHER THAN HSCCC

Substance[a]	Solvent system[b] (volume ratio)	Apparatus[c]
	n-BuOH/EtOH/Hex/HOAc/H_2O (3:1:2:1:5)	CHCPC[50]
	n-BuOH/HOAc/H_2O (4:1:5)	CHCPC[50]
Bovine insulin	sec.-BuOH/DCA/H_2O (100:3:100)	VCPC[3], ACPC[20]

[a] ABA, abscisic acid; DNP, dinitrophenyl; HVA, homovanillic acids; VMA, vanillylmandelic acid.

[b] BuOH, butanol; DCA, *dichloroacetic acid*; EDTA, ethylenediaminetetraacetic acid; Et_2O, diethyl ether; EtOAc, ethyl acetate; EtOH, ethanol; Hep, *n*-heptane; Hex, *n*-hexane; HOAc, acetic acid; HPC, hexadecylpyridinium chloride; isoAmOH, isoamyl alcohol; MeOH, methanol; NH_4OAc, ammonium acetate: TFA, trifluoroacetic acid; TCE, trichloroethane.

[c] CPC, coil planet centrifuge; ACPC, angle rotor CPC; CDCCC, centrifugal droplet countercurrent chromatograph; CHCPC combined horizontal flow-through CPC; EC, elution centrifuge; HCPC, *horizontal flow-through CPC*; RC, rotating coil assembly; TCC, toroidal coil centrifuge; TCPC, toroidal CPC; VCPC (vertical) flow-through CPC.

Table 9
NONAQUEOUS SOLVENT SYSTEMS FOR CCC[68]

Solvent systems (by volume)[a]	Mobile phase	Apparatus	Substance
HEX:EtOAc:NO_2CH_3:MeOH; 560:125:125:190	Upper	DCCC	Essential oils
55:9:28:9	Upper	DCCC	Essential oils
54:13:13:20	Both	HFTCPC	Diaziquone
HEPT:acetone:MeOH; 48:376:576	Lower	DCCC	Oleanolic acid Hederagenin
HEPT:acetone:MeOH; 50:10:40	Lower	DCCC	Vulpinic acid
HEPT:CH_2Cl_2:CH_3CN; 50:15:35	Lower	DCCC	Triterpenes Steroids
HEPT:HOAc:MeOH;33:33:33	Upper	CDCCC	Saturated fatty acids
HEPT:HOAc:CH_3CN:MeOH; 57:14:14:14	Upper	CDCCC	Unsaturated fatty acids
Ethylene glycol: Et_2O	Upper	HFTCPC	Salicylates
Ethylene glycol: EtOAc	Upper	HFTCPC	Salicylates
Ethylene glycol: $CHCl_3$	Lower	HFTCPC	Diaziquone

[a] Abbreviations: HEX, hexane; EtOAc, ethyl acetate; MeOH, methanol; HEPT, heptane; DCE, 1,2-dichloroethane; HOAc, acetic acid; Et_2O, diethyl ether; DCCC, droplet countercurrent chromatography; HFTCPC, horizontal flow-through coil planet centrifuge; CDCCC, centrifugal DCCC.

Downloaded At: 15:26 17 January 2011

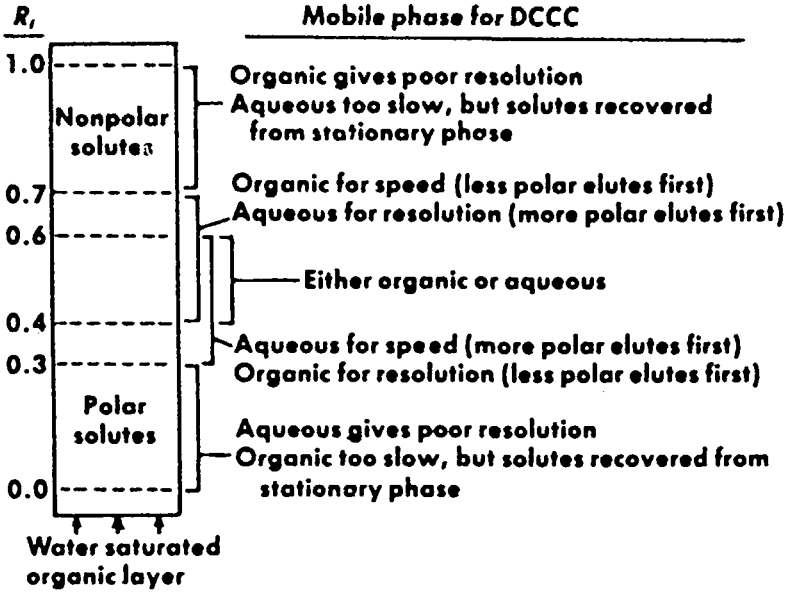

FIGURE 28. Choosing a CCC mobile phase using TLC on silica or cellulose layers.

of the stationary phase volume retained in the column. Sample volume also affects the partition efficiency as in other chromatographic methods.

A series of experiments have been carried out to study the effects of sample dose, sample volume, and choice of sample diluents on the stationary phase retention and peak resolution in high-speed CCC.[44] All data were obtained from a 400 mℓ capacity multilayer coil consisting of a 70 m long, 2.6 mm i.d. PTFE tube mounted on the coil planet centrifuge (Figure 20) at $\beta = 0.5$ to 0.8. The performance of the apparatus was evaluated on separation of a set of five DNP amino acid samples with a two-phase solvent system composed of chloroform, acetic acid, and 0.1 *N* hydrochloric acid (2:2:1). Both lower nonaqueous and upper

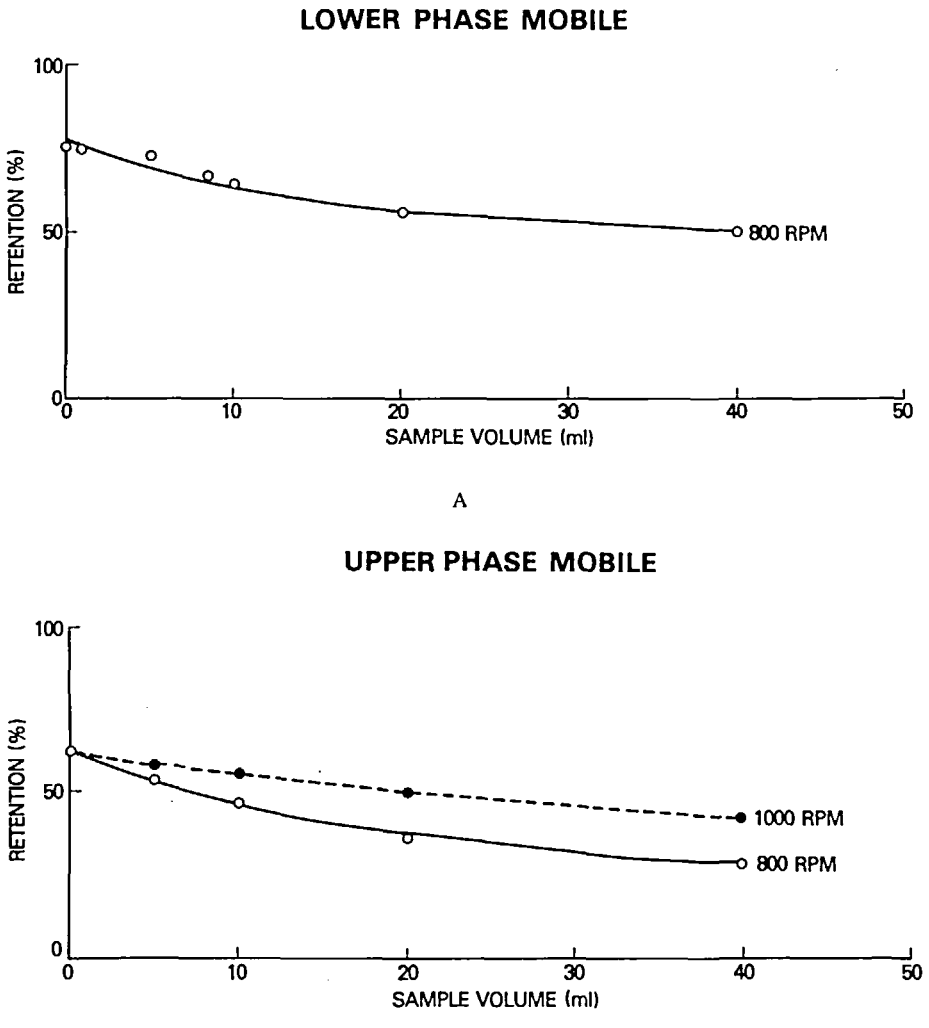

FIGURE 29. Effects of sample volume on retention level of the stationary phase. (A) Lower phase mobile and (B) upper phase mobile.

aqueous phases were used as the mobile phase at a flow rate of 500 mℓ/hr under a revolutional speed of 800 rpm.

a. Effects of Sample Dose

Figure 29 shows effects of the sample dose on the retention of the stationary phase where the retention volume expressed in percentages relative to the total column capacity is plotted against the applied sample volume. The results clearly indicate a general trend that the retention of the stationary phase decreases with the increased sample size for both mobile phase groups. The results also show that the retention level of the nonaqueous phase (B) is substantially lower than that of the aqueous phase (A). However, this low retention level of the nonaqueous phase is improved by applying a higher revolutional speed at 1000 rpm as indicated by the broken line (B).

Chromatograms obtained from these experiments are illustrated in Figure 30, where individual charts are arranged according to the sample dose and the mobile phase. Although

Downloaded At: 15:26 17 January 2011

Downloaded At: 15:26 17 January 2011

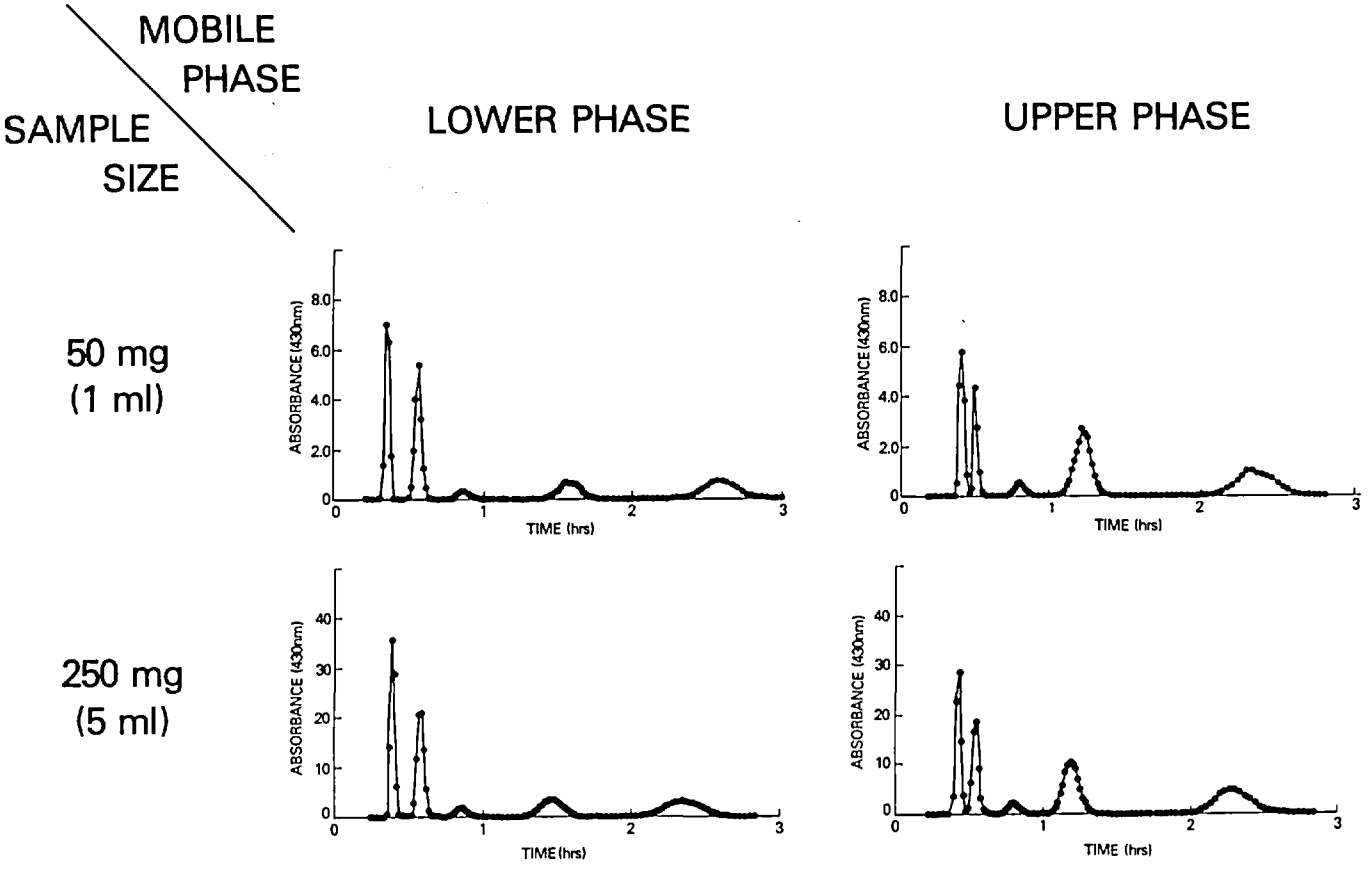

FIGURE 30. Effects of sample size on separation of a set of DNP amino acids. Order of elution: lower phase mobile (left column): DNP-valine, DNP-alanine, diDNP-cystine, DNP-glutamic acid, DNP-aspartic acid. Upper phase mobile (right column): DNP-aspartic acid, DNP-glutamic acid, diDNP-cystine, DNP-alanine, DNP-valine.

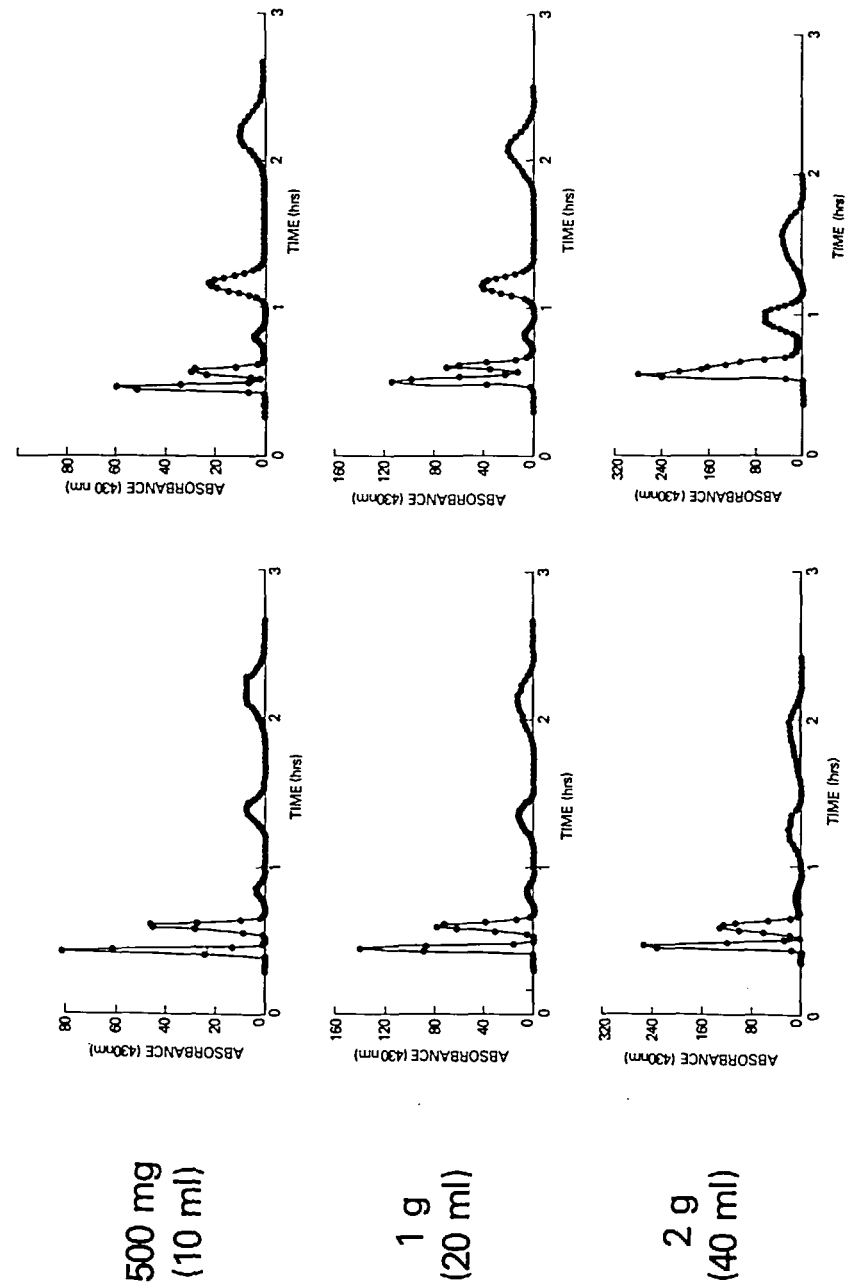

FIGURE 30B.

Downloaded At: 15:26 17 January 2011

the peak resolution gradually decreases with the increased sample dose, the integrity of the individual peaks is well preserved in all charts except for the 2 g run with the mobile upper phase. This lowest peak resolution coincides with the lowest retention level of the stationary phase at 28%. The results strongly suggest that the retention level of the stationary phase plays a critical role in partition efficiency in the present method.

b. Effects of Sample Volume and Choice of Diluents

Effects of the sample volume and the choice of the sample diluents on the peak resolution were studied on separations of 1 g quantity of the DNP amino acid mixture. The results are shown in Figure 31 where both the lower nonaqueous phase (A) and the upper aqueous phase (B) are used as the mobile phase.

These chromatograms clearly show that the choice of the sample diluent makes little difference in resolution for both early and late appearing peaks until the sample volume is increased to 40 mℓ. With a large sample volume a significant decrease in peak resolution is observed in early appearing peaks especially when the sample is dissolved entirely in the mobile phase (Figure 31, i and p). The loss of peak resolution becomes minimized if the sample is dissolved in the stationary phase (Figure 31, g and r). Further observation reveals that chromatograms i and p (Figure 31) with the lowest resolution in the early peaks show the best resolved late peaks among all 40 mℓ sample groups. This peculiar elution profile of the early and late peaks may be clearly understood on the basis of the two-phase interaction within the sample compartment at the beginning of the partition process.

Downloaded At: 15:26 17 January 2011

When the sample mixture is introduced with the stationary phase, the eluting mobile phase will pick up each individual component at a different rate according to the partition coefficient. The components which favor the partition in the mobile phase, hence producing the early appearing peaks, are quickly depleted from the sample compartment of the stationary phase and concentrated in a small volume of the mobile phase, resulting in a sharp sample band. Therefore, a large volume of sample can be injected into the column without causing significant peak broadening of early appearing peaks. Although the components favoring the partition in the stationary phase are not concentrated by the mobile phase, they are subjected to the partition process in the column for longer periods of time to produce broader but better resolved peaks. Therefore, the initial band width for these components becomes less significant for separation. The above effects become reversed when the sample mixture is introduced with a large volume of the mobile phase. In this case the components favoring the partition in the stationary phase, thus producing the late appearing peaks, are concentrated in the stationary phase at the beginning of the column, while other components tend to produce broader peaks affected by the sample volume. Because these early appearing peaks are eluted close together, the loss of resolution among those peaks becomes serious compared with the late eluted peaks. By dissolving the sample in equal volumes of the upper and lower phases, resolution can be relatively maintained for both early and late appearing peaks. There is a decrease in resolution when the sample is dissolved in a large volume of the upper and lower phase mixture but not to the degree seen when the sample is dissolved in a large quantity of the mobile phase.

As discussed above, in large-scale separations the best results are usually attained by dissolving the sample mixture entirely in the stationary phase. However, in some instances the sample mixture contains a component or components having low solubility in the stationary phase and, therefore, an enormously large volume of the stationary phase is required to dissolve the sample. In this situation the addition of the mobile phase to the sample solution will give beneficial effects in reducing the sample volume. The use of the two phases for the sample solution provides an additional advantage in that one can ensure formation of two phases in the sample solution. When the sample concentration exceeds the critical range, solvent system may form a single phase in the sample compartment at the

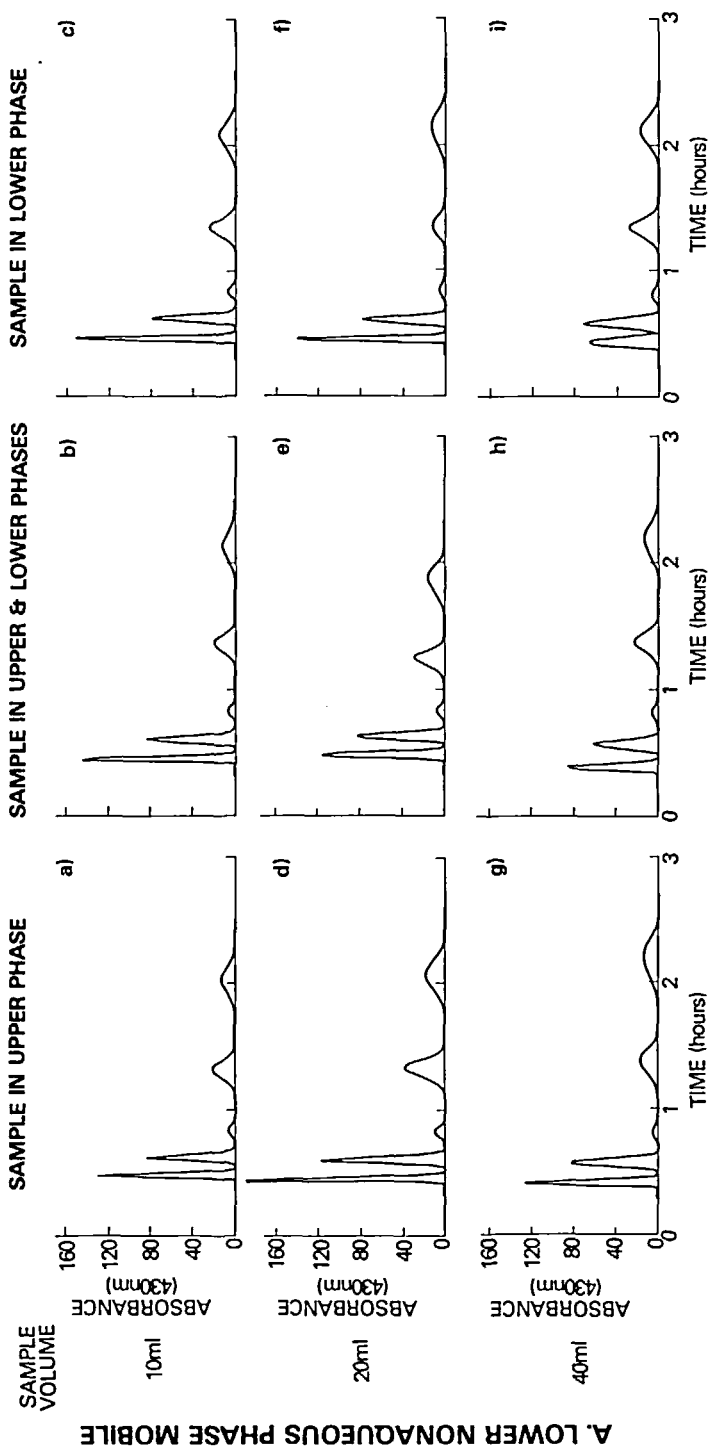

A

Downloaded At: 15:26 17 January 2011

Downloaded At: 15:26 17 January 2011

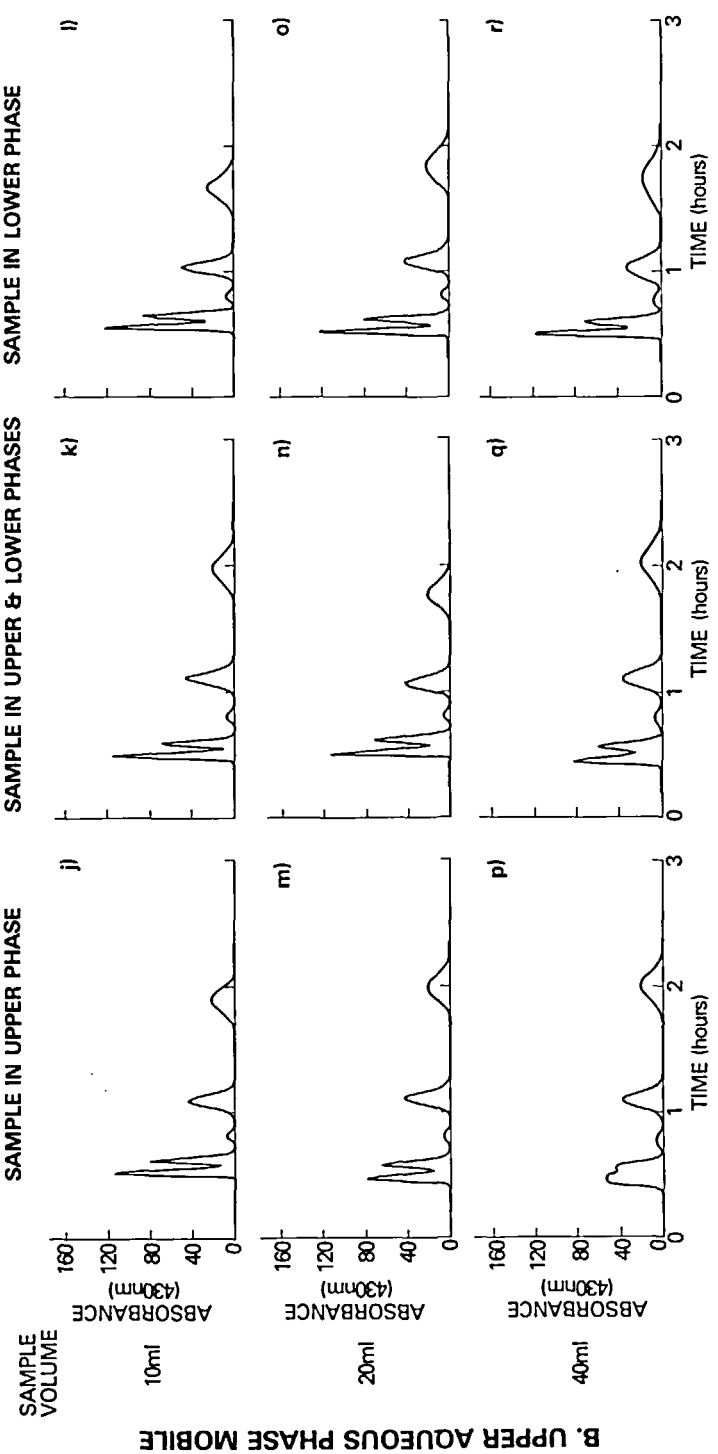

B

FIGURE 31. Effects of sample volume and sample diluent on separation of a set of DNP amino acids. Order of elution see Figure 30.

beginning of the column. Even though the sample solution forms the two layers, the excessive alteration of the phase composition may adversely affect the retention of the stationary phase. As described elsewhere, this can be predicted by measuring the settling time of the sample solution. When the settling time exceeds a critical range of 30 sec, it is most likely that the phase distribution mode in the sample compartment is reversed and in this situation the application of the normal elution mode may cause a large loss of the stationary phase. Because of these reasons, the use of two solvent phases for preparation of sample solution is strongly recommended.

c. Effects of Undissolved Material

Different from other chromatographic methods, the present method permits loading of sample solution containing undissolved small particles without detrimental effects. These solid materials are usually sedimented at the peripheral bed of the column by the centrifugal force and later recovered by flushing with solvents and N_2 gas. However, elimination of undissolved materials from the sample solution by either filter or centrifugation would be recommended.

3. Separation Procedure

a. General Procedure

As in many other CCC methods, high-speed CCC is performed in the following steps. The column is first entirely filled with the stationary phase; this is followed by sample injection through the sample port. Then, the apparatus is rotated at the desired rpm while the mobile phase is pumped into the column at the optimum flow rate. The effluent from the outlet of the column is continuously monitored with a UV monitor and fractionated into test tubes with a fraction collector. After the separation is completed, the apparatus is stopped and the column contents are collected by either eluting with solvents to fractionate into test tubes or flushing with pressured N_2 into a container. The column is then washed by introducing a small volume (20 to 30 mℓ) of intermediate solvent miscible with either phase such as methanol and flushing it with N_2. This process may be repeated until the washings become clean. Then the column is dried by passing N_2, if desired.

Downloaded At: 15:26 17 January 2011

b. Elution

The present system produces vigorous mixing of the solvents in the column and permits application of a high flow rate of the mobile phase without a loss in peak resolution provided that a satisfactory volume of the stationary phase (over 50% of the total column capacity) is retained in the column. Although the hydrodynamic behavior of the two solvent phases in the rotating coil is extremely complex, a simple settling test described earlier in Section III.D. may provide a useful guidance for optimizing the operational conditions to attain a satisfactory retention of the stationary phase.[42]

In a standard multilayer coiled column (β = 0.5 to 0.8, 10 cm revolutional radius),[33] a solvent system with a settling time less than 30 sec would display normal hydrodynamic behavior which distributes the upper phase toward the head and the lower phase toward the tail. Accordingly, the elution should be performed by pumping the upper phase from tail to head (broken curve in the phase distribution diagram, Figure 11A) or the lower phase from head to tail (solid curve in the phase distribution diagram Figure 11A). The flow rate of the mobile phase may also be judged from the settling times. For a 1.6 mm i.d. column, flow rates over 240 mℓ/hr may be applicable if the settling time is less than 10 sec, and a reduced flow rate should be used for solvent systems with longer settling times. When the settling time of the solvent system considerably exceeds 30 sec, it is most likely that the hydrodynamic behavior of the two phases is reversed, the upper phase now being distributed toward the tail and the lower phase toward the head. Accordingly, the upper phase should be pumped

from the head toward the tail (solid curve) and the lower phase pumped from the tail toward the head (broken curve) at the reduced flow rates; typically 60 mℓ/hr or less for the 1.6 mm i.d. column. For this type of solvent system, the best stationary phase retention is attained with a small β value around 0.25. A sufficient column capacity of the multilayer coil with this range of β values can be obtained from the apparatus with a wider hub of the holder and/or a greater radius of revolution.

Alternatively, the separation can be performed at an elevated temperature which permits the normal mode of elution for the viscous polar solvent systems.[42] Preliminary experiments have been successfully conducted at 45 to 50°C using a coil planet centrifuge equipped with a temperature control system.[52,53] In order to maintain the original two-phase composition in the column, the solvents were equilibrated and kept at the elevated temperature in a water bath. In many occasions, partition coefficient of the compound is sensitively altered with temperature and, therefore, the solvent system should provide a suitable partition coefficient of the aimed compound at the elevated temperature.

In addition to the isocratic elution described above, CCC enables stepwise and gradient elutions.[19,20,33,51] However, the successful application requires a particular choice of the solvent system as follows: the key element producing the gradient (such as acid, neutral salt, etc.) should be partitioned almost entirely into the mobile phase and at the same time should not significantly alter the volume ratio of the two solvent phases in the column. Solvent systems such as *n*-butanol/aqueous solution for the gradient of dichloroacetic acid or trifluoroacetic acid concentration and *n*-butanol/phosphate buffer for a pH gradient will suffice the above requirements if the lower aqueous phase is used as the mobile phase.

While the method permits a choice in the two elution modes, the head to tail elution usually gives superior results. In some solvent systems, the tail to head elution mode produces a steady carryover of the stationary phase, resulting in gradual loss of the stationary phase and reduced peak resolution. Even though quite often this carryover is minor and does not significantly affect the separation, presence of stationary phase droplets in the flow cell disturbs the absorbance monitoring of solute peaks by producing a large noise in recording. The tail to head elution mode also requires an additional consideration to maintain a uniform flow rate. Countercurrent flow of the two solvent phases through the rotating coil creates a pressure gradient along the length of the coil in such a way that the pressure on the head side becomes higher than that on the tail side. Consequently, introduction of the mobile phase through the tail may produce a negative pressure at the inlet of the column, resulting in an increased flow rate of the mobile phase by sucking an extra amount of solvent from the reservoir through the metering pump equipped with one-way check valves. This adverse phenomenon is enhanced by several factors such as a large density difference between the two solvent phases, application of high revolutional speed and slow flow rate, etc. However, this problem can be easily solved by restricting the flow through the column with a piece of narrow-bore tubing, typically 0.5 mm i.d. × 50 cm, inserted at the outlet of the column.[33] For monitoring the pressure, the use of a metering pump equipped with a pressure gauge is recommended.

c. Monitoring the Effluent

Equipment used for on-line monitoring in high-speed CCC are almost exclusively UV and/or visual spectrophotometers for recording absorbance of the effluent. An LKB Uvicord S and an ISCO model 1840 variable wavelength UV-VIS absorbance monitor are satisfactorily employed. The flow cells should be straight standard type, since the U-shape flow cell designed for the analytical HPLC has a tendency to trap droplets of the stationary phase producing extensive noise in recording. In order to avoid trapping the stationary phase in the flow cell, the lighter (mobile) phase should be introduced from the top of the flow cell downwards and the heavier (mobile) phase, from the bottom of the flow cell upwards.

Downloaded At: 15:26 17 January 2011

Different from other chromatographic methods, on-line monitoring in CCC creates some problems: the use of two solvent phases almost always produces carryover of the droplets of the stationary phase, causing the noise in recording. In addition, the mobile phase is in a subtle equilibrium with the stationary phase and a slight change in temperature may cause cloudiness of the effluent. In spite of these difficulties, careful monitoring will produce quite satisfactory recording of the elution peaks.

4. Applications

Table 6 summarizes the applications of high-speed CCC with a multilayer coil in separation and purification of natural and synthetic products. Although the limited number of published data is available for high-speed CCC, the method permits direct application of conventional two-phase solvent systems used in a variety of other CCC schemes. Table 7 shows the list of samples and two-phase solvent systems used in droplet CCC as reported by Hostettmann.[63] Similar data with various centrifugal CCC instruments other than high-speed CCC are summarized in Table 8. Table 9 lists various nonaqueous two-phase solvent systems successfully used for separation of hydrophobic compounds with CCC.[12]

Figures 32 to 36 show several examples of high-speed CCC separations obtained by isocratic elution at room temperature (Figures 32 to 35) and elevated temperature of 45 to 50°C (Figure 36). In Figure 32,[33] gramicidins were separated in major components and each component was further partially resolved into valine and isoleucine analogues. With the same solvent system separation of gramicidin C analogues can be improved by using the lower nonaqueous phase as the mobile phase. Figure 33 shows a chromatogram of indole auxins on a volatile solvent system of *n*-hexane/ethyl acetate/methanol/water (3:7:5:5).[33] As mentioned earlier, this solvent system provides suitable partition coefficients for a group of relatively nonpolar compounds by modifying the volume ratio between *n*-hexane and ethyl acetate. An example of antibiotics separation using a similar solvent system is shown in Figure 34. Two components, tirandamycin A and B, with a minor structural difference are completely separated, B being recovered from the column long after A is eluted out from the column.[57] Figure 35 shows chromatogram of tannins which exhibited poor peak resolution in HPLC columns.[61] Partition coefficient of tannins in *n*-butanol/aqueous systems was found to be insensitive to pH but conveniently adjusted by changing the ionic strength of neutral salts. A satisfactory separation was obtained with a solvent composition of *n*-butanol/0.1 *M* NaCl (1:1). High viscosity of the butanol solvent systems limits the applicable flow rate of the mobile phase. Performing CCC at an elevated temperature would reduce the viscosity of the solvent system and permit application of high flow rates to yield efficient separations in short periods of time. Chromatogram of bombesin in Figure 36A was obtained at 45 to 50°C with a solvent system composed of *n*-butanol/dichloroacetic acid/water (100:1:100).[53] The HPLC analysis of the original sample and the purified fraction are shown in Figures 36B and 36C, respectively. The results indicate that one step purification of crude synthetic peptides is possible with the present method. High-speed CCC also permits the use of gradient elution as applied in liquid chromatography. Figure 37[33] shows a chromatogram of seven dipeptides obtained by a gradient of dichloroacetic acid concentration in an *n*-butanol/0.1 *M* ammonium formate (1:1) as indicated in the figure. Two pairs of isomers, tyr-val vs. val-tyr and tyr-leu vs. leu-tyr, are well resolved.

As clearly demonstrated on the above examples of applications, high-speed CCC permits the use of a wide range of conventional two-phase solvent systems for separations of samples with various polarity. Although partition efficiency of the multilayer coil is limited to 1,000 theoretical plates, large retention of the stationary phase yields a high peak resolution as indicated in the separation of bombesin (Figure 36). Compared with other CCC schemes, separation times have been remarkably improved and most of the separations are completed within several hours. Because no solid support is used in the column, loaded samples are

Downloaded At: 15:26 17 January 2011

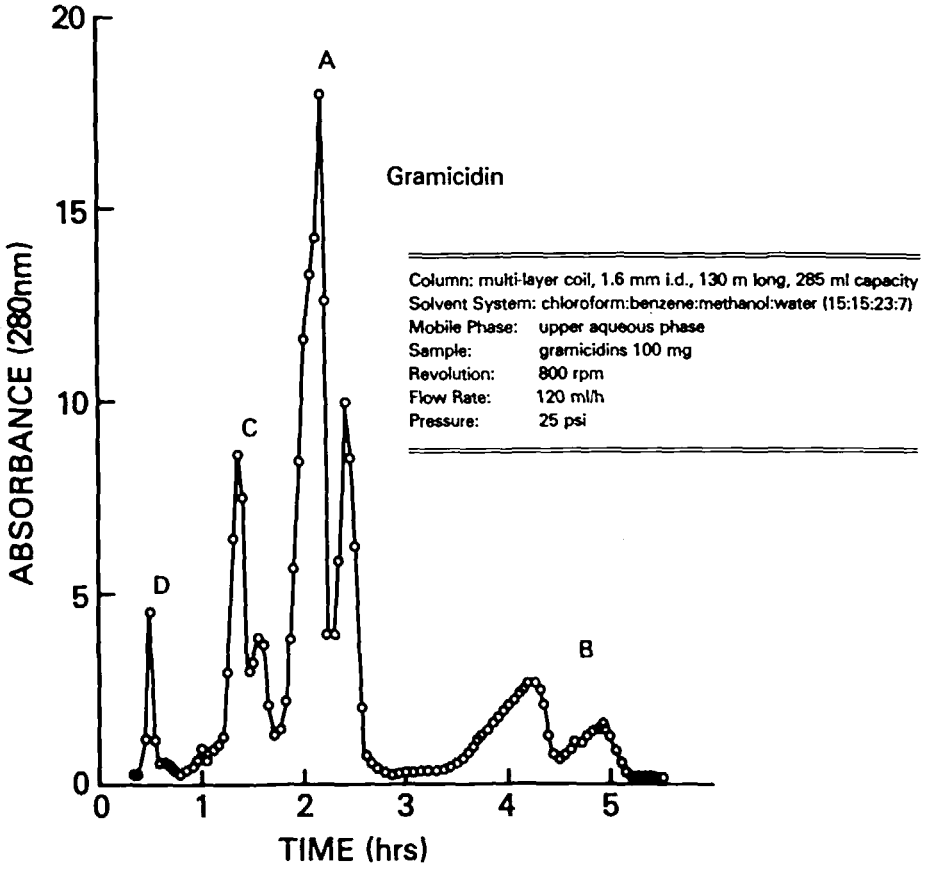

FIGURE 32. Chromatogram of gramicidins with high-speed CCC.

totally recovered without loss or inactivation caused by solid adsorbents. The column is easily cleaned after each run and reused for many times with high reproducibility and minimum risk of contamination. The solvent system suitable for the separation may be selected by means of a simple test tube measurement of the partition coefficient with which one can predict the retention volume of the solute peak.

D. Foam CCC Based on Dual Countercurrent System[34]

Foam separation method, which has been widely used in the past, covers a broad spectrum of samples ranging from small ions to macromolecules and particles. Despite the great potential capability, the method has remained rather primitive and inefficient, largely limiting the utility in research laboratories. Recently, the dual countercurrent system described in Section II has been successfully applied to foam separation to yield highly efficient separations in short periods of time. The preliminary studies strongly suggest that the present method may be applicable to macromolecules and cell particulates.

1. Principle of Foam CCC

As illustrated in Figure 2, the unilateral hydrodynamic equilibrium system enables dual countercurrent elution which is performed by simultaneous introduction of the two solvent phases each through the respective end of the coiled column. Foam CCC is a particular form of the dual countercurrent system in which one of the solvent phases is replaced with a gas phase to produce foams to collect the foam active materials. In this foam CCC, the

Downloaded At: 15:26 17 January 2011

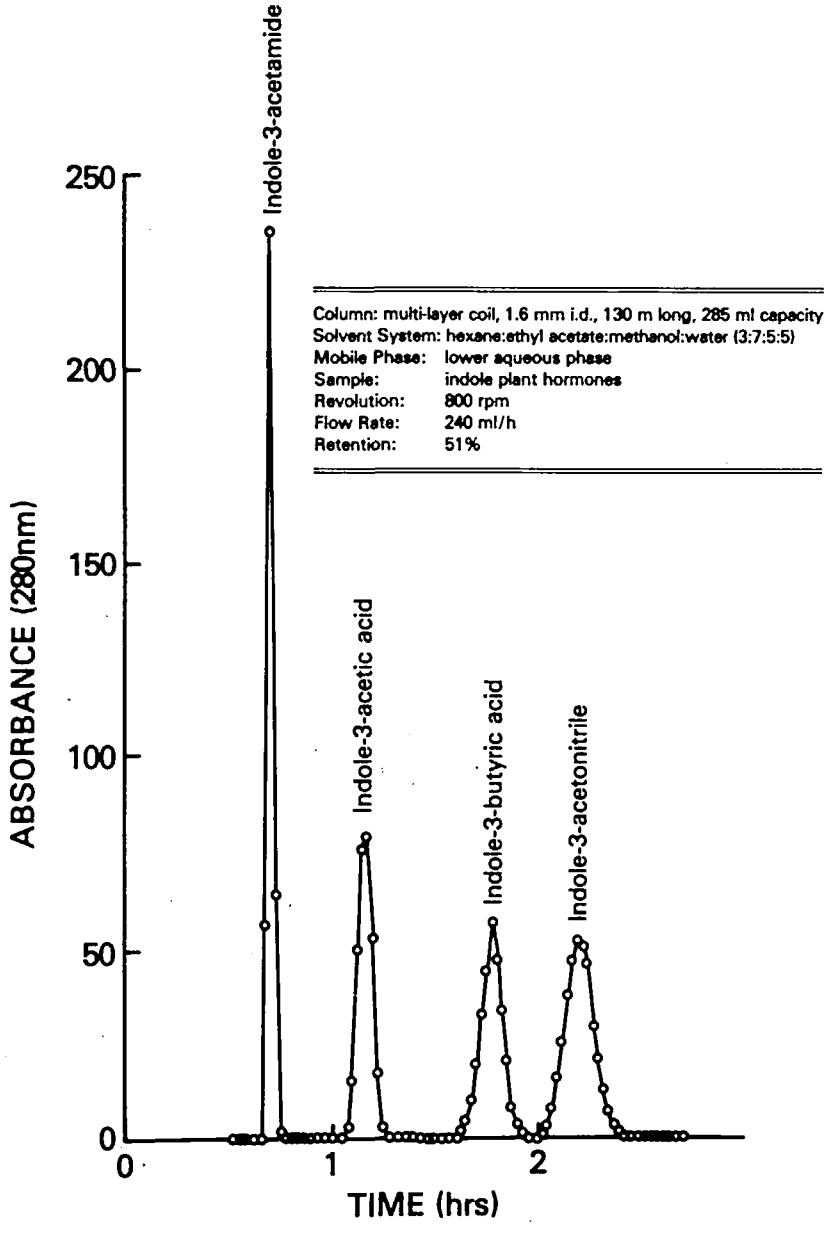

FIGURE 33. Chromatogram of indole plant hormones with high-speed CCC.

foaming stream moves from the head toward the tail, opposing to the liquid stream moving from the tail toward the head of the coil.

Figure 38 illustrates a schematic column design for foam CCC. The coiled column is equipped with five flow channels. The liquid phase is introduced through the liquid feed line located near the tail and drained through the liquid collection line at the head of the coil. The gas phase is similarly introduced through the gas feed line located near the head and the generated foams are harvested through the foam collection line at the tail of the coil. The sample solution may be introduced through the sample feed line opened at the middle portion of the coil.

In a typical operation mode the liquid phase containing surfactant and N_2 gas are simul-

Downloaded At: 15:26 17 January 2011

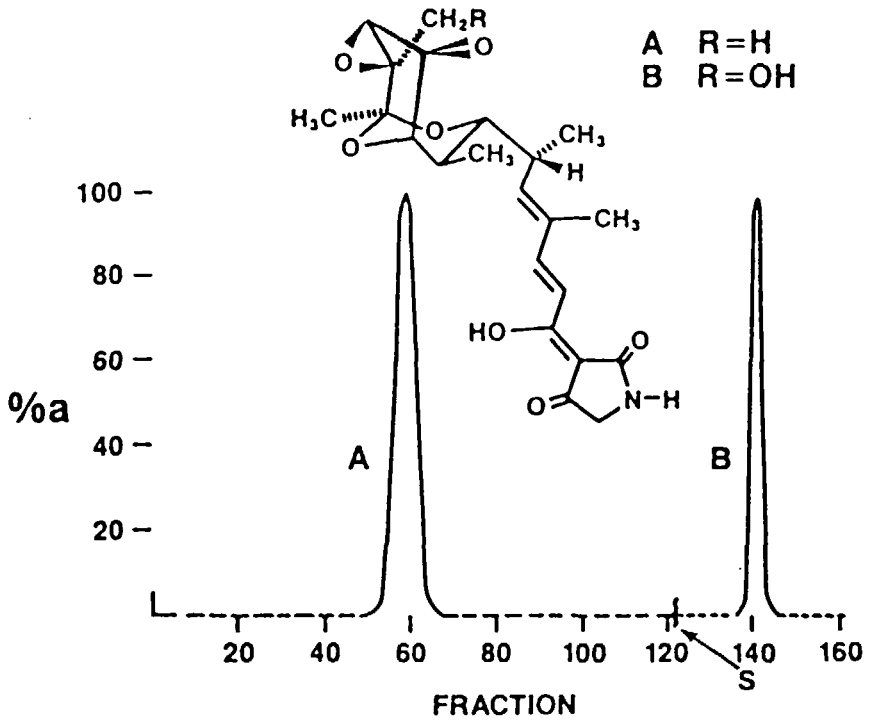

FIGURE 34. CCC separation of tirandamycin A and B with *n*-hexane/ethyl acetate/methanol/water (70:30:15:6).

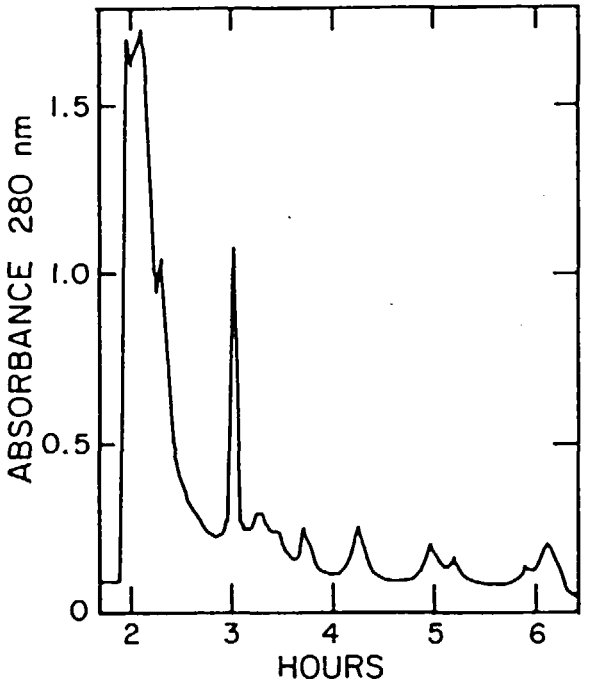

FIGURE 35. CCC of crude tannin extracted from 20 g of IS8768 sorghum. Sample volume: 8 mℓ (4 mℓ of each phase); solvent system: *n*-butanol/0.1 *M* sodium chloride (1:1); stationary phase: upper phase; flow rate: 38 mℓ/hr; retention of stationary phase: 78%.

Downloaded At: 15:26 17 January 2011

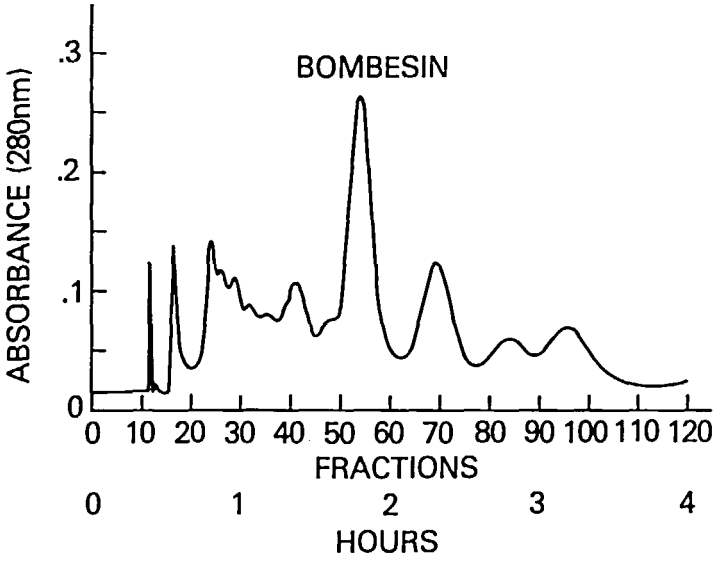

A

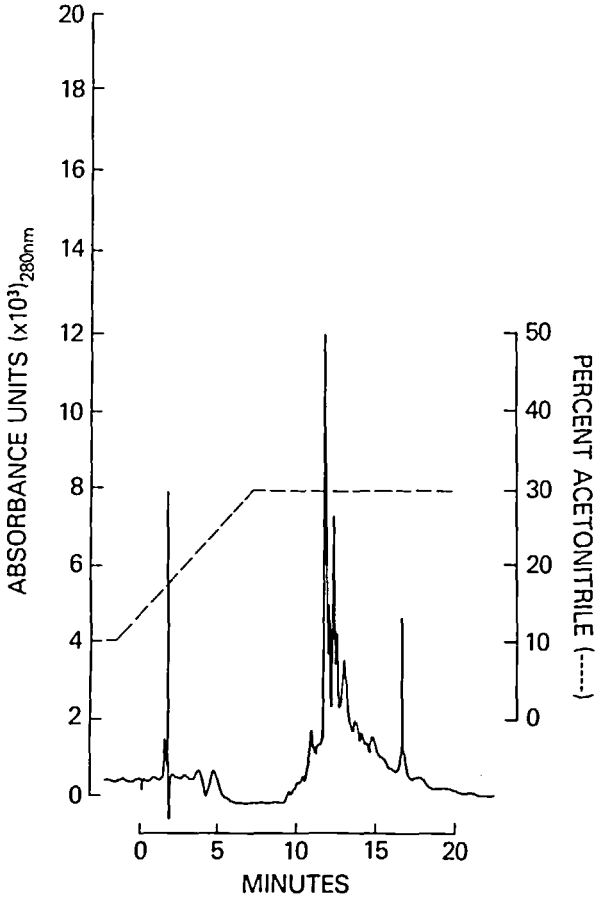

B

FIGURE 36. Purification of crude synthetic bombesin with high-speed CCC. (A) Chromatogram of bombesin with high-speed CCC. (B) HPLC analysis of the original sample. (C) HPLC analysis of the purified fraction.

Downloaded At: 15:26 17 January 2011

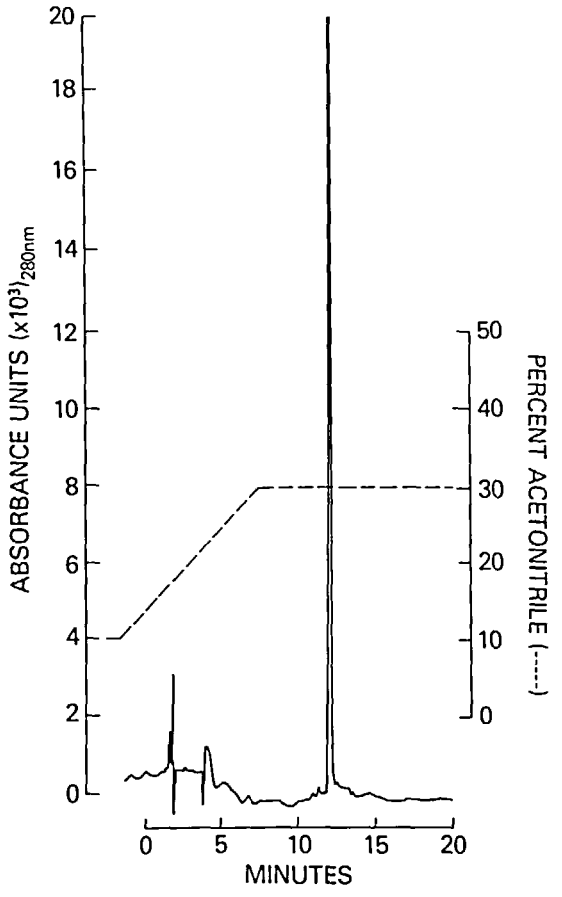

FIGURE 36C.

taneously introduced through the respective lines into the rotating column while the sample solution is continuously fed through the sample feed line. Consequently, the samples are separated according to their foam affinity. Solutes or particulates having an affinity to the foam are quickly carried with the foaming stream toward the tail and harvested through the foam collection line while other materials in the sample solution are carried with the liquid stream in the opposite direction toward the head and eluted out through the liquid collection line.

This foam CCC method can be applied to a broad spectrum of samples having a foam affinity which may be classified into the following two categories: (1) Direct affinity to the gas-liquid interface. Detergents and many other foam-producing materials can be harvested through the foam collection line without any special treatment. (2) Affinity to the foam-producing carrier or collector molecule. Samples which lack a direct affinity to the gas-liquid interface can be indirectly adsorbed to the foam if they have an affinity to the foam-producing agents lining the gas-liquid interface in the foams. This type of affinity effectively used for foam separation may vary in a wide range from a nonspecific form such as surface electric charges to a highly specific form such as enzyme-substrate or enzyme-inhibitor binding provided that one of the pair has either direct or indirect foam affinity.

2. Preliminary Studies

Series of preliminary experiments have been performed by using a combined horizontal flow-through coil planet centrifuge with a 20 cm revolutional radius (Figure 23). The coiled

Downloaded At: 15:26 17 January 2011

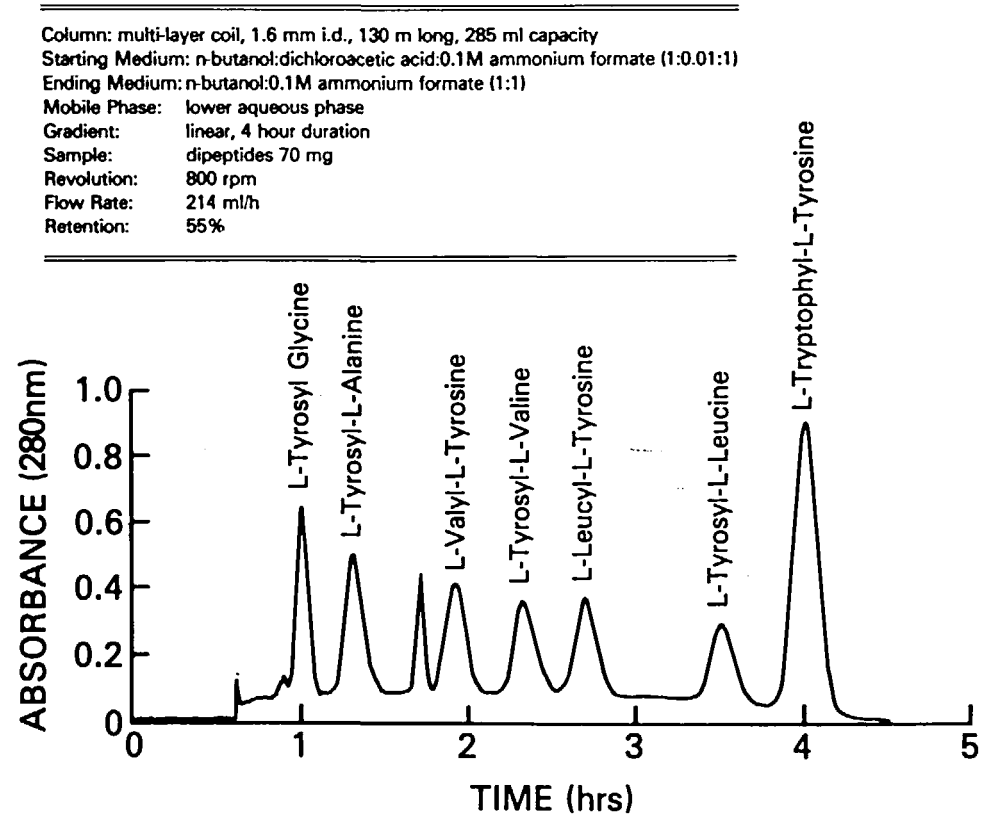

FIGURE 37. Chromatogram of dipeptides by gradient elution.

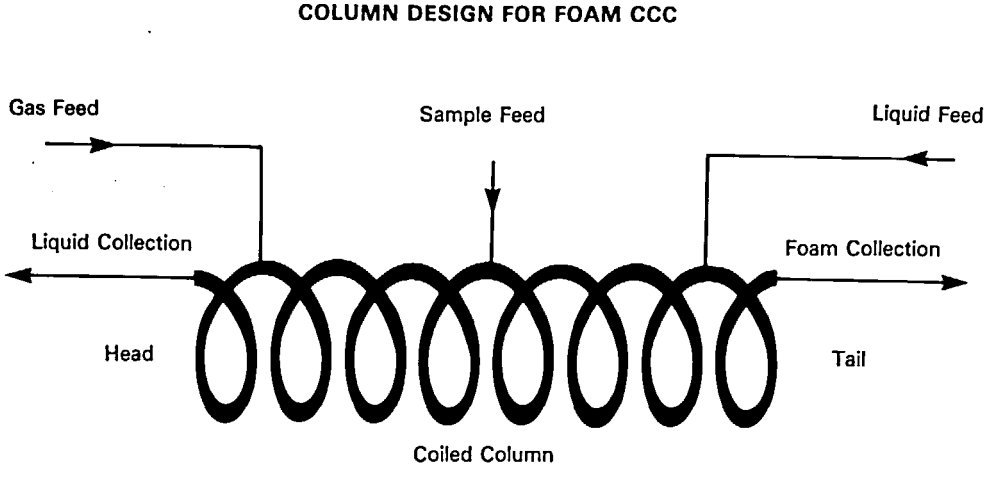

FIGURE 38. Column design for foam CCC.

column, consisting of a 10 m long, 2.6 mm i.d. PTFE tube with a total capacity of 50 mℓ, was mounted on the gear-driven holder of 12.5 cm diameter. The column was equipped with five flow channels as illustrated in Figure 38. The liquid feed line was connected to a Milton Roy Minipump (flow rate: 214 mℓ/hr) and the gas feed line to an N_2 cylinder pressured at 80 psi. Flow through the liquid collection line was regulated with a needle valve while

Downloaded At: 15:26 17 January 2011

the foam collection line was directly left open to the air. The sample solution was fed through the sample feed line either with a syringe (batch separation) or a metering pump (continuous separation). Effluents through each collection line were either manually fractionated into test tubes or pooled into a graduated cylinder. Preliminary studies were performed in three different elution modes using rhodamine B as a test sample and sodium dodecyl sulfate (SDS) as a collector.

a. Continuous Enrichment and Stripping

This experiment was performed to demonstrate the capability of the method to concentrate and/or eliminate a minute amount of material present in a large volume of sample solution. The sample solution containing rhodamine B at a 10^{-6} *M* concentration and SDS at 10^{-3} *M* as a collector was introduced through the liquid feed line at 214 mℓ/hr against N_2 flow through the gas feed line at 80 psi, while the apparatus was run at 500 rpm. The sample feed line was closed and not used in this experiment. The liquid collection rate was adjusted at a level slightly below the liquid feed rate so that the foam collection rate became as small as several hundred microliters per hour which yielded the foam highly enriched with rhodamine B. After 1 ℓ of the sample solution was eluted, the liquid collection line was closed to elute rhodamine B remaining in the column through the foam collection line. The stripped liquid collected through the liquid collection line was fluorometrically analyzed to determine the concentration of rhodamine B. The results showed that the dye concentration in the stripped solution was 1.3×10^{-9} *M* while over 99% of rhodamine B was recovered through the foam collection line within a 2 mℓ volume resulting in over 500-fold enrichment.

b. Batch Separation with Sample Injection through Sample Feed Line

This experiment was initiated by establishing a liquid-gas countercurrent flow equilibrium through the coiled column. At the revolutional speed of 500 rpm a surfactant solution containing SDS at 10^{-3} *M* was pumped through the liquid feed line while the N_2 gas flow was introduced through the gas feed line at 80 psi. After the hydrodynamic equilibrium was reached, 0.5 mℓ of sample solution containing rhodamine B and Evans blue each at 5×10^{-4} *M* was injected through the sample feed line. The needle valve on the liquid collection line was adjusted to make a 1:3 volume ratio between the foam and liquid fractions. Effluents from both collection lines were separately fractionated into a series of test tubes at 30 sec intervals. The concentration of each dye in the fractions was spectrophotometrically determined using 556 nm for rhodamine B and 620 nm for Evans blue. Figure 39 shows the typical experimental result obtained with the present method. The upper chromatogram obtained through the foam collection line shows a sharp single peak entirely consisting of rhodamine B with the peak maximum 1 min after sample injection. The lower chromatogram obtained through the liquid collection line shows a broad symmetrical peak of Evans blue with the peak maximum at 2.75 min after sample injection. These results are quite reproducible and injection of the single component produced the similar peak through the respected collection line. The volume of the liquid phase present in the column under a steady state hydrodynamic equilibrium in these experiments ranged between 4 and 5 mℓ which amounted to approximately 10% of the total column capacity.

c. Continuous Separation by Continuous Sample Feeding through Sample Feed Line

Rapid and clean separation of the two dyes in the batch separation method described above indicated the feasibility of continuous separation by steadily feeding the sample mixture at a proper rate. Under otherwise identical experimental conditions used in the batch separation, the sample solution was continuously introduced through the sample feed line at various flow rates. The satisfactory separations were obtained at sample feed rates of 0.36 mℓ/min or less, which separated each sample at the maximum rate of 1.8×10^{-7} mol/min.

Downloaded At: 15:26 17 January 2011

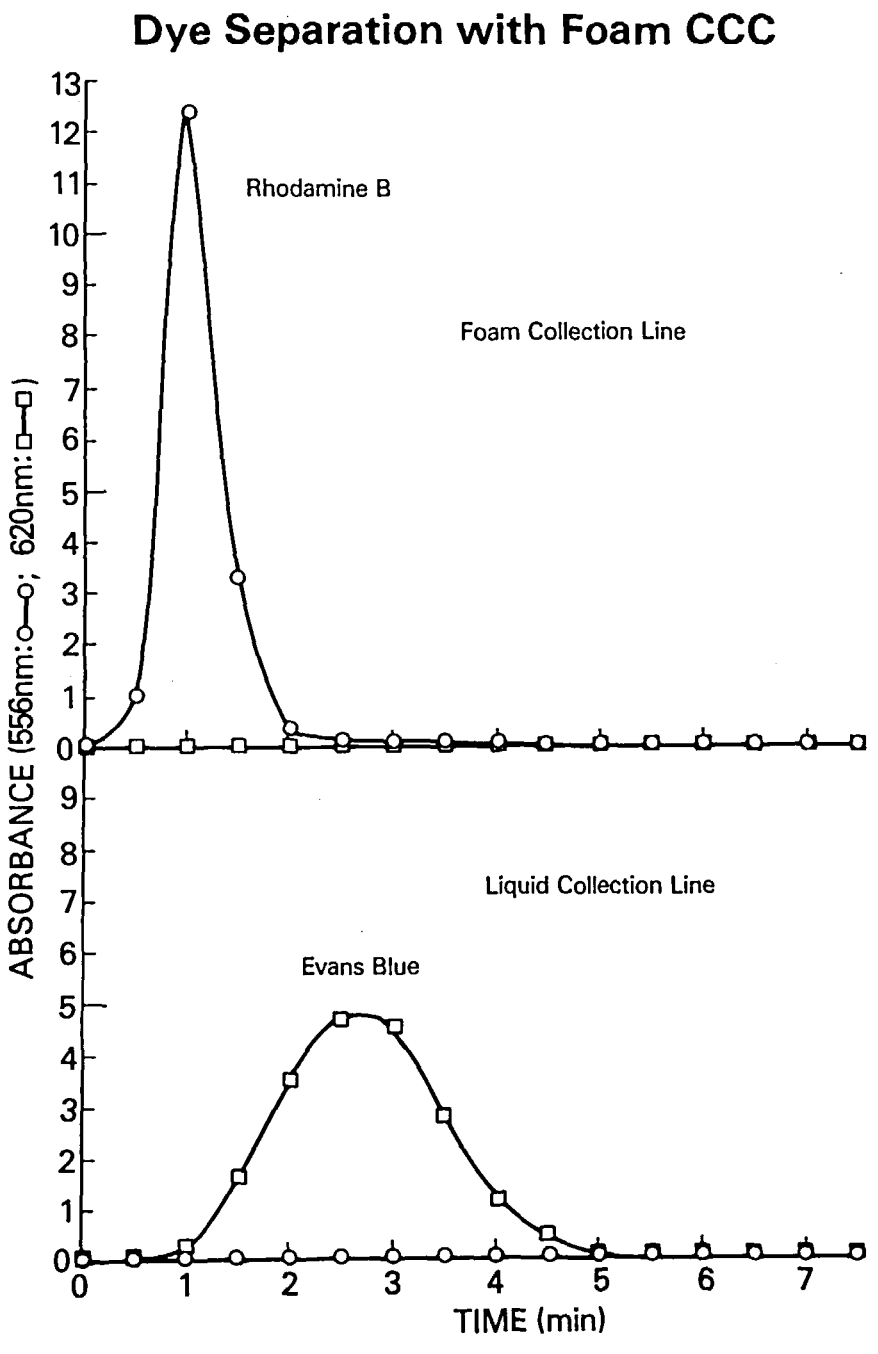

FIGURE 39. Dye separation with foam CCC with sodium dodecyl sulfate (SDS) solution. Rhodamine B having foam affinity was quickly eluted through the foam collection line (upper chromatogram) while Evans blue was carried with the liquid stream in the opposite direction and eluted through the liquid collection line (lower chromatogram).

Downloaded At: 15:26 17 January 2011

The application of higher flow rates resulted in initial accumulation of rhodamine B in the column which was later followed by elution of rhodamine B through the liquid collection line.

3. Feasibility Studies on Separation of Macromolecules

The present method has been applied to the separation of proteins without the use of a surfactant collector. As is well known, exposure of proteins such as BSA to a gas-liquid interface may cause denaturation which alters the physiological function of the molecule. The preliminary studies were conducted to test vulnerability and foam-producing capacity of proteins with the present system by injecting the sample solution into the running columnn through the sample feed line. Several kinds of proteins including BSA, human and sheep hemoglobin, and ovalbumin were examined. Among these only BSA showed an active foam-producing ability and was collected through the foam collection line whereas other proteins were mostly eluted through the liquid collection line without any visible evidence of denaturation. BSA fractions eluted through the foam collection line showed various degree of turbidity apparently due to denaturation of the molecule. Further experiments revealed that the intensity of turbidity highly depended upon the composition of the applied liquid phase. The use of salt-free distilled water or dilute acid solution caused most intensive turbidity. Addition of a surfactant to the liquid phase decreased the degree of turbidity but at the same time lowered the foam recovery rate of BSA. Sodium phosphate solution of slightly alkaline pH (7.2 to 8.9) at a relatively high ionic strength (0.2 to 0.5 *M*) produced minimum turbidity with a high BSA recovery of over 90% through the foam collection line.

Figure 40 illustrates a preliminary result of the batch separation of BSA and sheep hemoglobin obtained with a liquid phase composed of 0.2 *M* dibasic sodium phosphate solution (pH 8.9) under the standard experimental condition previously applied to the dye separation. BSA with a foam-producing capacity was quickly eluted through the foam collection line within 6 min while sheep hemoglobin was entirely recovered through the liquid collection line in about 10 min.

The preliminary studies on foam separation of proteins described above furnish a useful guidance for further development of the present method. Although simple adjustment of pH and ionic concentration of the liquid phase worked out well for separation of BSA, many other proteins lack an active foam-producing capability and therefore require the selective collectors to acquire the foam affinity. Hopefully, the use of such collectors would also prevent the protein molecules from direct contact with the gas-liquid interface, thus reducing the possibility of denaturation. One useful future application of the present method may be the separation of macromolecules or particulates with foam affinity CCC using highly specific collector molecules.

Downloaded At: 15:26 17 January 2011

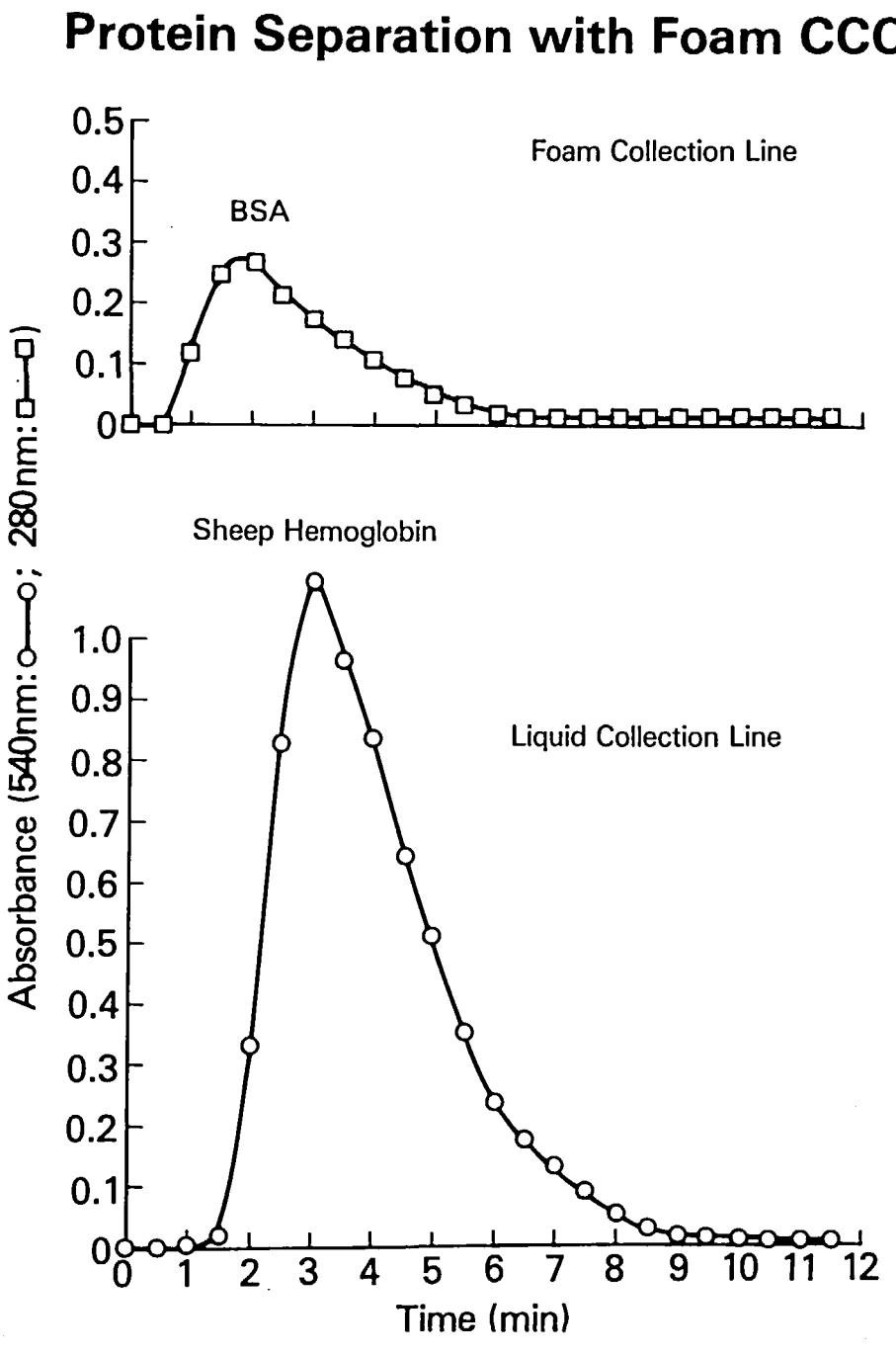

FIGURE 40. Preliminary separation of proteins with the foam CCC method. BSA having a foam-producing capacity was collected through the foam collection line (upper chromatogram) while sheep hemoglobin was entirely recovered through the liquid collection line (lower chromatogram).

Downloaded At: 15:26 17 January 2011

REFERENCES

1. **Ito, Y. and Bowman, R. L.,** Countercurrent chromatography: liquid-liquid partition chromatography without solid support, *Science*, 167, 281, 1970.
2. **Ito, Y. and Bowman, R. L.,** Countercurrent chromatography, *Anal. Chem.*, 43, 69A, 1971.
3. **Ito, Y., Hurst, R. E., Bowman, R. L., and Achter, E. K.,** Countercurrent chromatography, *Sep. Purif. Methods*, 3(1), 133, 1974.
4. **Ito, Y.,** Countercurrent chromatography: principle and application, *Protein, Nucleic Acid Enzyme*, 26(8), 1020, 1981.
5. **Ito, Y.,** Countercurrent chromatography (minireview), *J. Biochem. Biophys. Methods*, 5(2), 105, 1981.
6. **Ito, Y.,** Countercurrent chromatography, *Trends Biomed. Sci.*, 7(2), 47, 1982.
7. **Ito, Y.,** CCC: chromatography with a twist and no supports, *Ind. Res. Dev.*, 24(4), 108, 1982.
8. **Mandava, N. B., Ito, Y., and Conway, W. D.,** Countercurrent chromatography. I. Historical development and early instrumentation, *Am. Lab.*, 14(10), 62, 1982.
9. **Mandava, N. B., Ito, Y., and Conway, W. D.,** Countercurrent chromatography. II. Recent instrumentation and applications, *Am. Lab.* 14(11), 48, 1982.
10. **Ito, Y.,** Countercurrent chromatography, *Farumashia*, 19(10), 1054, 1983.
11. **Ito, Y. and Conway, W. D.,** Development of countercurrent chromatography, *Anal. Chem.*, 56(4), 534A, 1984.
12. **Conway, W. D. and Ito, Y.,** Recent applications of countercurrent chromatography, *LC Mag.*, 2, 368, 1984.
13. **Ito, Y.,** Development of high-speed countercurrent chromatography, *Advances in Chromatography*, Vol. 24, J. C. Giddings, E. Grushka, J. Cazes, and P. R. Brown, Eds., Marcel Dekker, New York, 1984, Chap. 6, 181.
14. **Ito, Y.,** Countercurrent chromatography: Development, application and future potentials, *Chromatogr. Int.*, 7, 4, 1985.
15. **Conway, W. D.,** Countercurrent chromatography, in *Handbook of Naturally Occurring Pesticides*, Vol. 1, Mandava, N. B., Ed., CRC Press, Inc., Boca Raton, Fla., 1983.
16. **Tanimura, T., Pisano, J. J., Ito, Y., and Bowman, R. L.,** Droplet countercurrent chromatography, *Science*, 169, 54, 1970.
17. **Ito, Y. and Bowman, R. L.,** Countercurrent chromatography: liquid-liquid partition chromatography without solid support, *J. Chromatogr. Sci.*, 8, 315, 1970.
18. **Ito, Y. and Bowman, R. L.,** Countercurrent chromatography with flow-through coil planet centrifuge, *Science*, 173, 420, 1971.
19. **Ito, Y. and Bowman, R. L.,** Countercurrent chromatography with the flow-through coil planet centrifuge, *J. Chromatogr. Sci.*, 11, 284, 1973.
20. **Ito, Y. and Bowman, R. L.,** Angle rotor countercurrent chromatography, *Anal. Biochem.*, 65, 310, 1975.
21. **Ito, Y., Bowman, R. L., and Noble, F. W.,** The elution centrifuge applied to countercurrent chromatography, *Anal. Biochem.*, 49, 1, 1972.
22. **Ito, Y. and Bowman, R. L.,** Horizontal flow-through coil planet centrifuge without rotating seals, *Anal. Biochem.*, 82, 63, 1977.
23. **Ito, Y. and Bowman, R. L.,** Preparative countercurrent chromatography with horizontal flow-through coil planet centrifuge, *J. Chromatogr.*, 147, 221, 1978.
24. **Ito, Y.,** A new horizontal flow-through coil planet centrifuge for countercurrent chromatography. I. Principle of design and analysis of acceleration, *J. Chromatogr.*, 188, 33, 1980.
25. **Ito, Y.,** A new horizontal flow-through coil planet centrifuge for countercurrent chromatography. II. The apparatus and its partition capabilities, *J. Chromatogr.*, 188, 43, 1980.
26. **Ito, Y. and Putterman, G. J.,** New horizontal flow-through coil planet centrifuge for countercurrent chromatography. III. Separation and purification of dinitrophenyl amino acids and peptides, *J. Chromatogr.*, 193(1), 37, 1980.
27. **Ito, Y.,** The toroidal coil planet centrifuge for countercurrent chromatography, *Anal. Biochem.*, 102, 150, 1980.
28. **Ito Y.,** The toroidal coil planet centrifuge for countercurrent chromatography, *J. Chromatogr.*, 192(1), 75, 1980.
29. **Ito, Y., Carmeci, P., and Sutherland, I. A.,** Nonsynchronous flow-through coil planet centrifuge applied to cell separation with physiological solution, *Anal. Biochm.*, 94, 249, 1979.
30. **Ito, Y., Carmeci, P., Bhatnagar, R., Leighton, S., and Seldon, R.,** The non-synchronous flow-through coil planet centrifuge without rotating seals applied to cell separation, *Sep. Sci. Tech.*, 15(9), 1589, 1980.
31. **Ito, Y., Bramblett, G. T., Bhatnagar, R., Huberman, M., Leive, L., Cullinane, L. M., and Groves, W.,** Improved non-synchronous flow-through coil planet centrifuge without rotating seals: principle and application, *Sep. Sci. Tech.*, 18(1), 33, 1981.

Downloaded At: 15:26 17 January 2011

32. **Ito, Y.,** Efficient preparative countercurrent chromatography with a coil planet centrifuge, *J. Chromatogr.*, 214, 122, 1981.
33. **Ito, Y., Sandlin, J., and Bowers, W. G.,** High-speed preparative countercurrent chromatography (CCC) with a coil planet centrifuge, *J. Chromatogr.*, 244, 247, 1982.
34. **Ito, Y.,** Foam countercurrent chromatography based on dual countercurrent system, *J. Liq. Chromatogr.*, 8, 2131, 1985.
35. **Ito, Y.,** New continuous extraction method with a coil planet centrifuge, *J. Chromatogr.*, 207, 161, 1981.
36. **Nakazawa, H., Riggs, C. E., Jr., Egorin, M. J., Redwood, S. M., Bachur, N. R., Bhatnagar, R., and Ito, Y.,** Extraction of urinary anthracycline antitumor antibiotics with the coil planet centrifuge, *J. Chromatogr.*, 307, 323, 1984.
37. **Ito Y. and Bhatnagar, R.,** Improved scheme for preparative countercurrent chromatography (CCC) with a rotating coil assembly, *J. Liq. Chromatogr.*, 7(2), 257, 1984.
38. **Conway, W. D. and Ito, Y.,** Phase distribution of liquid-liquid systems in spiral and multi-layer helical coils in a centrifugal countercurrent chromatography, paper presented at the Pittsburgh Conf. Expo. Anal. Chem. Appl. Spectrosc., 1984, 472.
39. **Sutherland, I. A. and Heywood-Waddington, D.,** Hydrodynamics of liquid-liquid systems in a spiral section of the multi-layer coil planet centrifuge, abstract of the Pittsburgh Conf. Expo. Anal. Chem. Appl. Spectrosc., 1985, 302.
40. **Ito, Y.,** Experimental observations of the hydrodynamic behavior of solvent systems in high-speed countercurrent chromatography. Part I. Hydrodynamic distribution of two solvent phases in a helical column subjected to two types of synchronous planetary motion, *J. Chromatogr.*, 301, 377, 1984.
41. **Ito, Y.,** Experimental observations of the hydrodynamic behavior of solvent systems in high-speed countercurrent chromatography. Part II. Phase distribution diagrams for helical and spiral columns, *J. Chromatogr.*, 301, 387, 1984.
42. **Ito, Y. and Conway, W. D.,** Experimental observations of the hydrodynamic behavior of solvent systems in high-speed countercurrent chromatography. Part III. Effects of physical properties of the solvent systems and operating temperature on the distribution of two-phase solvent systems, *J. Chromatogr.*, 301, 405, 1984.
43. **Sandlin, J. L. and Ito, Y.,** Large preparative-scale countercurrent chromatography with a coil planet centrifuge, *J. Liq. chromatogr.*, 8, 2153, 1985.
44. **Sandlin, J. L. and Ito, Y.,** Gram quantity separation of DNP (dinitrophenyl) amino acids with multi-layer coil countercurrent chromatography (CCC), *J. Liq. Chromatogr.*, 7(2), 323, 1984.
45. **Ito, Y.,** Countercurrent chromatography with a new horizontal flow-through coil planet centrifuge, *Anal. Biochem.*, 100, 271, 1979.
46. **Conway, W. D. and Ito, Y.,** Solvent selection for countercurrent chromatography by rapid estimation of partition coefficients and application to polar conjugates of p-nitrophenol, *J. Liq. Chromatogr.*, 7(2), 275, 1984.
47. **Conway, W. D. and Ito, Y.,** Evaluation of nonaqueous solvent systems for countercurrent chromatography using an HPLC assay to determine partition coefficients of a mixture of compounds, *J. Liq. Chromatogr.*, 7(2), 291, 1984.
48. **Conway, W. D. and Ito, Y.,** Resolution in countercurrent chromatography, *J. Liq. Chromatogr.*, 8, 2195, 1985.
49. **Brown, E. A. B. and Ito, Y.,** Separation of prostaglandins using the new horizontal flow-through coil planet centrifuge, *J. Biochem. Biophys. Methods*, 3, 77, 1980.
50. **Knight, M., Kask, A. M., and Tamminga, C. A.,** Purification of solid-phase synthesized peptides on the coil planet centrifuge, *J. Liq. Chromatogr.*, 7, 351, 1984.
51. **Ito, Y. and Bowman, R. L.,** Application of the elution centrifuge to separation of polynucleotides with the use of polymer phase systems, *Science*, 182, 391, 1973.
52. **Knight, M., Ito, Y., Kask, A. M., Tamminga, C. A., and Chase, T. N.,** Chromatography of AC-ASP-TYR-MET-GLY-TRP-MET-ASP-NH_2 on the horizontal flow-through coil planet centrifuge and the high-speed multi-layer coil planet centrifuge, *J. Liq. Chromatogr.*, 7(13), 2525, 1984.
53. **Knight, M., Ito, Y., Peters, P., and diBello, C.,** Rapid purification of synthetic bombesin by countercurrent chromatography in the multi-layer coil planet centrifuge, *J. Liq. Chromatogr.*, 8, 2281, 1985.
54. **Lee, Y. W. and Cook, C. E.,** Preparative separation of demeton isomers with Ito multi-layer coil countercurrent chromatography, *J. Liq. Chromatogr.*, 8, 2253, 1985.
55. **Mandava, N. B., Ito, Y., and Ruth, J. M.,** Separation of s-triazine herbicides by countercurrent chromatography, *J. Liq. Chromatogr.*, 8, 2221, 1985.
56. **Mandava, N. B. and Ito, Y.,** Plant hormone analysis by countercurrent chromatography, *J. Liq. Chromatogr.*, 7(2), 303, 1984.
57. **Brill, G. M., McAlpine, J. B., and Hochlowski, J. E.,** Use of the coil planet centrifuge in the isolation of antibiotics, *J. Liq. Chromatogr.*, 8, 2259, 1985.

Downloaded At: 15:26 17 January 2011

58. **Williams, R. G.,** Countercurrent chromatography of cortical steroids on the multilayer coil planet centrifuge, paper presented at the Pittsburgh Conf. Expo. Anal. Chem. Appl. Spectrosc., New Orleans, 1985, 300.
59. **Romanach, R. J., deHaseth, J. A., and Ito, Y.,** Preliminary studies for countercurrent chromatography (CCC) with Fourier transform infrared (FT-IR) spectrometry, *J. Liq. Chromatogr.*, 8, 2209, 1985.
60. **Fales, H. M., Pannell, L. K., Sokoloski, E. A., and Carmeci, P.,** Separation of methyl violet 2B by high-speed countercurrent chromatography and identification by californium-252 plasma desorption mass spectrometry, *Anal. Chem.*, 57, 376, 1985.
61. **Putman, L. J. and Butler, L. G.,,** Fractionation of condensed tannins by counter-current chromatography, *J. Chromatogr.*, 318, 85, 1985.
62. **Sandlin, J. L. and Ito, Y.,** unpublished data, 1985.
63. **Hostettmann, K,** Droplet counter-current chromatography, in *Advances in Chromatography*, Vol. 21, Giddings, J. E., Grushka, E., Cazes, J., and Brown, P. R., Eds., Marcel Dekker, New York, 1983, 165.
64. **Hurst, R. E. and Ito, Y.,** Countercurrent chromatographic separation of catecholamine metabolites from urine, *Clin. Chem.*, 18 (8), 814, 1972.
65. **Zhang, T. Y.,** Horizontal flow-through coil planet centrifuge: some practical applications of countercurrent chromatography, *J. Chromatogr.*, 315, 287, 1984.
66. **Mandava, N. B. and Ito, Y.,** Separation of plant hormones by countercurrent chromatography, *J. Chromatogr.*, 247, 315, 1982.
67. **Nakazawa, H., Andrews, P. A., Bachur, N. R., and Ito, Y.,** Isolation of daunorubicin derivatives by counter-current chromatography with the horizontal flow-through coil planet centrifuge, *J. Chromatogr.*, 205, 482, 1981.
68. **Friedman, R. D., Nakazawa, H., Chou, F. E., Bachur, N. R., and Ito, Y.,** Counter-current chromatography of diaziquone by a horizontal flow-through coil planet centrifuge, *J. Chromatogr.*, 252, 283, 1982.
69. **Lightbown, J. W., Newland, P., Sutherland, I. A., and Dymond, J. W. A.,** Analysis of candicidin and related polyene antibiotics by means of the coil planet centrifuge, *Proc. Analyst. Div. Chem. Soc.*, 14, 34, 1977.
70. **Sutherland, I. A., Lee, J. S., and Gauvreau, D. J.,** Separation of quinozaline antibiotics by coil planet centrifugation, *Anal. Biochem.*, 89, 213, 1978.
71. **Murayama, W., Kobayashi, T., Kosuge, Y., Yano, H., Nunogaki, Y., and Nunogaki, K.,** A new centrifugal counter-current chromatograph and its application, *J. Chromatogr.*, 239, 643, 1982.
72. **Hurst, R. E., Sheng, Y. P. J., and Ito, Y.,** Countercurrent chromatography: a new method for the fractionation of glycosaminoglycans, *Anal. Biochem.*, 85, 230, 1978.
73. **Ito, Y., Aoki, I., Kimura, E., Nu gaki, K., and Nunogaki, Y.,** New micro liquid-liquid partition techniques with the coil planet centrifuge, *Anal. Chem.*, 41, 1579, 1969.
74. **Ito, Y. and Bowman, R. L.,** Preparative countercurrent chromatography with a slowly rotating helical tube, *Anal. Biochem.*, 78, 506, 1977.
75. **Ito, Y. and Bowman, R. L.,** Preparative countercurrent chromatography with a slowly rotating helical tube, *J. Chromatogr.*, 136, 189, 1977.
76. **Ito, Y.,** Preparative countercurrent chromatography with a slowly rotating glass coil, *J. Chromatogr.*, 196, 295, 1980.
77. **Putterman, G. J., Perini, F., White, E. L., and Ito, Y.,** Purification of synthetic peptides by means of countercurrent chromatography with the horizontal flow-through coil planet centrifuge, in *Proc. Sixth American Peptide Symp.*, Pierce Chemical Co., 1979, 113.
78. **Ito, Y.,** Countercurrent chromatography, in *Method in Enzymology, Enzyme Structure, Part I, Vol. 91*, Hirs, C. H. W. and Timasheff, S. N., Eds., Academic Press, New York, 1983, 335.
79. **Ito, Y. and Bowman, R. L.,** Countercurrent chromatography with flow-through centrifuge without rotating seals, *Anal. Biochem.*, 85, 614, 1978.
80. **Putterman, G. J., Spare, M. B., and Perini, F.,** Synergistic use of countercurrent chromatography for the purification of synthetic peptides, *J. Liq. Chromatogr.*, 7, 341, 1984.
81. **Knight, M., Ito, Y., and Chase, T. N.,** Preparative purification of the peptide des-enkephalin γ-endorphin. Comparison of high-performance liquid chromatography and countercurrent chromatography, *J. Chromatogr.*, 212, 456, 1981.
82. **Somasundaran, P.,** Foam separation methods, *Sep. Purif. Methods*, 1, 117, 1972.

Downloaded At: 15:26 17 January 2011